Synthetic lethality concepts for colon cancer cell lines in the background of mutations in the SWI/SNF complex

Inaugural-Dissertation

zur

Erlangung des Doktorgrades

Dr. rer. nat.

der Fakultät für Biologie

an der

Universität Duisburg-Essen

vorgelegt von

Shan Xu

aus Mian Yang, Sichuan Province, China

Die der vorliegenden Arbeit zugrunde liegenden Experimente wurden am Institut für Medizinische Strahlenbiologie an der Universität Duisburg-Essen, Standort Essen, durchgeführt.

1. Gutachter: Prof. Dr. Martin Stuschke
2. Gutachter: Prof. Dr. Verena Jendrossek

Vorsitzender des Prüfungsausschusses: Prof. Dr. Stefan Westermann

Tag der mündlichen Prüfung: September 6th 2023

DOI: 10.17185/duepublico/79035
URN: urn:nbn:de:hbz:465-20230926-073144-0

Table of Contents

List of Abbreviations III

List of Figures VII

1. Introduction 1

1.1 Current situation of Colon cancer Treatment 4

1.2 Mating Type Switching/Sucrose Non-Fermentable (SWI/SNF) complex 6

1.3 SWI/SNF complex in Cancer 11

1.4 Frequent mutation of the SWI/SNF chromatin remodeling complex in colon cancer 14

1.5 Synthetic lethal in SWI/SNF complex 15

1.6 ARID1A directed synthetic lethal in SWI/SNF complex 18

2. Aims of the present study 23

3. Materials and Methods 25

3.1 Materials 25

3.1.1 Biological and chemical substances 25

3.1.2 Solutions and Buffers 26

3.1.3 Primary antibodies and dyes 27

3.1.4 Secondary antibodies 28

3.1.5 siRNAs und inhibitors 28

3.1.6 Softwares 29

3.1.7 Technical devices 29

3.2 Methods 30

3.2.1 Cell lines 30

3.2.2 Transfection with siRNA 30

3.2.3 Immunoblotting 31

3.2.4 Clonogenic survival assay 31

3.2.5 Immunofluorescence (IF) assay 32

3.2.6 Analysis of digital images 33

3.2.7 Quantitative image-based cytometry (QIBC) conducted to evaluate DSB repair foci dependent on cell cycle 33

3.2.8 HRR functional analysis on the I-SceI-induced DSBs based on GFP reporter cells 34

3.2.9 Ethics statement 35
3.2.10 Patient information and tissue specimens 35
3.2.11 IHC and scoring 36
3.2.12 ATP-TCA 37
3.2.13 Statistical analysis 38
4. Results 39
4.1 ARID1B knockdown and its effect on radiosensitivity 39
4.2 ARID1A-directed synthetic lethality on radiosensitivity 42
4.2.1 Impact of ARID1A/ PARPi synthetic lethality on radiosensitivity 43
4.2.2 Impact of ARID1A/ AURKAi synthetic lethality on radiosensitivity 50
4.2.3 Impact of ARID1A/ ATRi synthetic lethality on radiosensitivity 55
4.3 Cell cycle specific radiosensitization of CRC cell lines by ATRi 70
4.4 Impact of ATRi /ARID1A mt on DSB repair 78
4.5 ARID1A expression and characteristics in CRC primary tumors 91
4.6 ATRi /ARID1A interaction in primary tumors of CRC patients 93
5. Discussion 95
5.1 ARID1A directed synthetic lethal in SWI/SNF complex 95
5.2 Effect ATRi/ ARID1A synthetic lethality on colon cancer cell lines 96
5.3 ATRi/ ARID1A impact on DNA damage repair in colon cancer 98
5.4 ATRi/ ARID1A significantly decreased maintenance of radiation induced G2 checkpoint in colon cancer 100
5.5 ATRi/ ARID1A synthetic lethality in clinical colon cancer patients. 101
6. Summary 104
7. Zusammenfassung 107
8. Acknowledgements 113
9. References 114
10. Declaration 123
11. Curriculum Vitae 125

List of Abbreviations

<	“Less-than” sign
~	“Approximately” sign
°C	Degree Celsius
%	Percent
ãH2AX	Phosphorylated form of the histone H2AX
53BP1	P53 Binding Protein 1
aa	Amino acid
ATM	Ataxia telangiectasia mutated
ATP	Adenosine triphosphate
ATP–TCA	ATP-based tumor chemosensitivity assay
ATR	Ataxia telangiectasia and Rad3-related
ATRi	Ataxia telangiectasia and Rad3-related inhibitor
ARID1A	AT-rich interaction domain 1A
ARID1B	AT-rich interaction domain 1B
AURKA	Aurora Kinase A
AURKAi	Aurora Kinase A inhibitor
B-NHEJ	Backup nonhomologous end joining
bp	Base pair
BRCA1	Breast cancer susceptibility protein 1
BRCA2	Breast cancer susceptibility protein 2
BRCT	BRCA1 C-terminal domain
BSA	Bovine serum albumin
CDK1	Cyclin-dependent protein kinase 1
CHK1	Checkpoint kinase 1
CHK2	Checkpoint kinase 2
cm^2	Square centimeter
CO^2	Carbon dioxide
CTIP	C-terminal binding protein interacting protein

CSR	Class switch recombination
DAPI	4',6-diamidino-2-phenylindole
dH_2O	Distilled water
DDR	DNA damage response
DMEM	Dulbecco's modified eagle medium
DMSO	Dimethyl sulfoxide
DNA	Deoxyribonucleic acid
DSB	DNA double strand break
EDTA	Ethylene diamine tetraacetic acid
e.g.	Latin abbreviation for “exempli gratia”
et al.	Latin abbreviation for “et alii”
etc.	Latin abbreviation for “et cetera”
eV	Electronvolt
EZH2	Enhancer of zeste homolog 2
FACS	Fluorescence activated cell sorting
FBS	Fetal bovine serum
FHA	Forkhead-associated domain
g	Gravity
GFP	Green fluorescent protein
Gy	Gray - SI unit of absorbed radiation dose of ionizing radiation, and is defined as the absorption of one joule of ionizing radiation by one kilogram of matter
h	Hour
H1	Histone 1 – linker histone that binds to the DNA where it exits from nucleosome
H2AX	Histone H2AX variant
H_2O	Water
H_2O_2	Hydrogen peroxide
HR	Homologous recombination

HRR	Homologous recombination repair
IC50	Respective half maximal inhibitory concentrations
i.e.	Latin abbreviation for “id est”
IF	Immunofluorescence
IR	Ionizing radiation
kDa	Kilodalton
Ku	Protein that binds to DNA double-strand break ends
LET	Linear energy transfer
M	Molar (mol/l)
MEM	Minimum essential medium
min	Minute
MMR	Mismatch Repair
MRN	MRE11-RAD50-NBS1 complex
Mrx	Mre11-Rad50-Xrs2 complex
ms	Milisecond
mt	mutant
μm	Micrometer
NBS	Nijmegen breakage syndrome
NBS1	Nibrin
NLS	N-lauryl sarcosine
NHEJ	Non-homologous end-joining
p53	Tumor protein 53
PARP1	Poly [ADP-ribose] polymerase 1
PARP2	Poly [ADP-ribose] polymerase 2
PARPi	Poly [ADP-ribose] polymerase inhibitor
PBS	Phosphate-buffered saline
PE	Plating Efficiency
PFA	Paraformaldehyde
PFGE	Pulsed field gel electrophoresis

Prof.	Professor
Rad51	Radiation protein 51
RNA	Ribonucleic acid
RNase	Ribonuclease
ROS	Reactive oxygen species
RPA	Replication protein A
RPMI	Roswell park memorial institute medium
rpm	Revolutions per minute
RT	Room temperature
s.d	Standard deviation
SEM	Standard error of mean
siRNA	Small interfering RNA
SSB	Single strand break
SF	Surviving Fraction
TBS	Tris-buffered saline
Tris	Tris-(hydroxymetheyl)-aminomethane
UV	Ultraviolet Light
WB	Western Blotting
wt	Wild-Typ

List of Figures

Figure 1.1 The number of new CRC cases in top 10 countries with highest incident cases in 2020 and projections for 2040. 1

Figure1.2: Age-standardised incidence rates of malignant neoplasms of the colon and rectum by localisation and sex, ICD-10 C18–C20, Germany 2

Figure1.3: Pathways offering potential sites for targeted therapy 5

Figure1.4: Overview of mammalian SWI/SNF complexes 8

Figure 1.5 Schematic representation of synthetic lethality 16

Figure 1.6 Synthetic lethal interactions in SWI/SNF- mutant cancers with chemical tools for targeted cancer therapy. 19

Figure 4.1 Western blot results of ARID1A+ and ARID1A- CRC cell lines 39

Figure 4.2 ARID1A/ARID1B synthetic lethality on radiosensitivity 41

Figure 4.3 The IC50 of ARID1A+ and ARID1A- CRC cell lines to PARPi were calculated using the colony formation assay. 44

Figure 4.4 ARID1A/ PARPi synthetic lethality with 2Gy radiation; 47

Figure 4.5 The IC50 of ARID1A+ and ARID1A- CRC cell lines to AURKAi were calculated using the colony formation assay 51

Figure 4.6 ARID1A/ AURKAi synthetic lethality with 2Gy radiation 53

Figure 4.7 The IC50 of ARID1A+ and ARID1A- CRC cell lines to ATRi were calculated using the colony formation assay 56

Figure 4.8: ARID1A/ ATRi synthetic lethality with 2Gy radiation. 59

Figure 4.9: Effect of ATRi on radiosensitivity 63

Figure 4.10: Effect of ATR inhibitor (VE822) in ARID1A+ cell 65

Figure 4.11: Effect of ARID1B/ARID1A on radiosensitivity. 67

Figure 4.12: Effect of ARID1A knockdown in ARID1A+ cell plus ATR inhibitor (VE822) on radiosensitivity 69

Figure 4.13: Cell cycle synchronization by Aphdicoline 71

Figure 4.14 : Cell cycle effect of ATRi/ARID1A 73

Figure 4.15: Cell cycle redistribution of ATRi/ARID1A 76

Figure 4.16: ATRi/ARID1A synthetic lethality on phospho-Histone H3 expression. 78

Figure 4.17: Foci formation in the G2-phase based on EdU staining 79

Figure 4.18: Effect of ATRi on γH2AX foci formation in G2-phase CRC cell lines 81

Figure 4.19: Kinetics of γH2AX foci formation and decay in G2-cells in ARID1A+ and ARID1A- CRC cells exposed to 0 Gy, 0.5 Gy, 1.0 Gy and 2.0 Gy. 82

Figure 4.20: Effect of ATRi on γH2AX foci formation in G2-phase CRC cell lines 83

Figure 4.21: Effect of ATRi on RAD51 foci formation in G2-phase CRC cells... 85

Figure 4.22: Kinetics of RAD51 foci formation and decay in G2-cells in ARID1A+ and ARID1A- CRC cells exposed to 0 Gy, 0.5 Gy, 1.0 Gy and 2.0 Gy 86

Figure 4.23: Effect of ATRi on RAD51 foci formation in G2-phase CRC cell lines 87

Figure 4.24: Knockdown of ARID1A decreases HRR in U2OS/DR-GFP and A549/DR-GFP reporter cells 89

Figure 4.25: ATRi effect on HRR in ARID1A+ U2OS/DR-GFP reporter cells and ARID1AKD U2OS/DR-GFP reporter cells. 90

Figure 4.26: Effect of ATRi on ex vivo explants from CRC patients 94

1. Introduction

Colorectal cancer (CRC) is considered as the third most common type of cancer [1]. It is currently the most common malignant cancer of the gastrointestinal tract, accounting for 13% of all malignancies [2]. In addition, it is considered the second most common cause of death affecting men and women alike worldwide. Approximately one in eight cancers in Germany affects the large intestine (colon) or rectum (Figure 1.1).

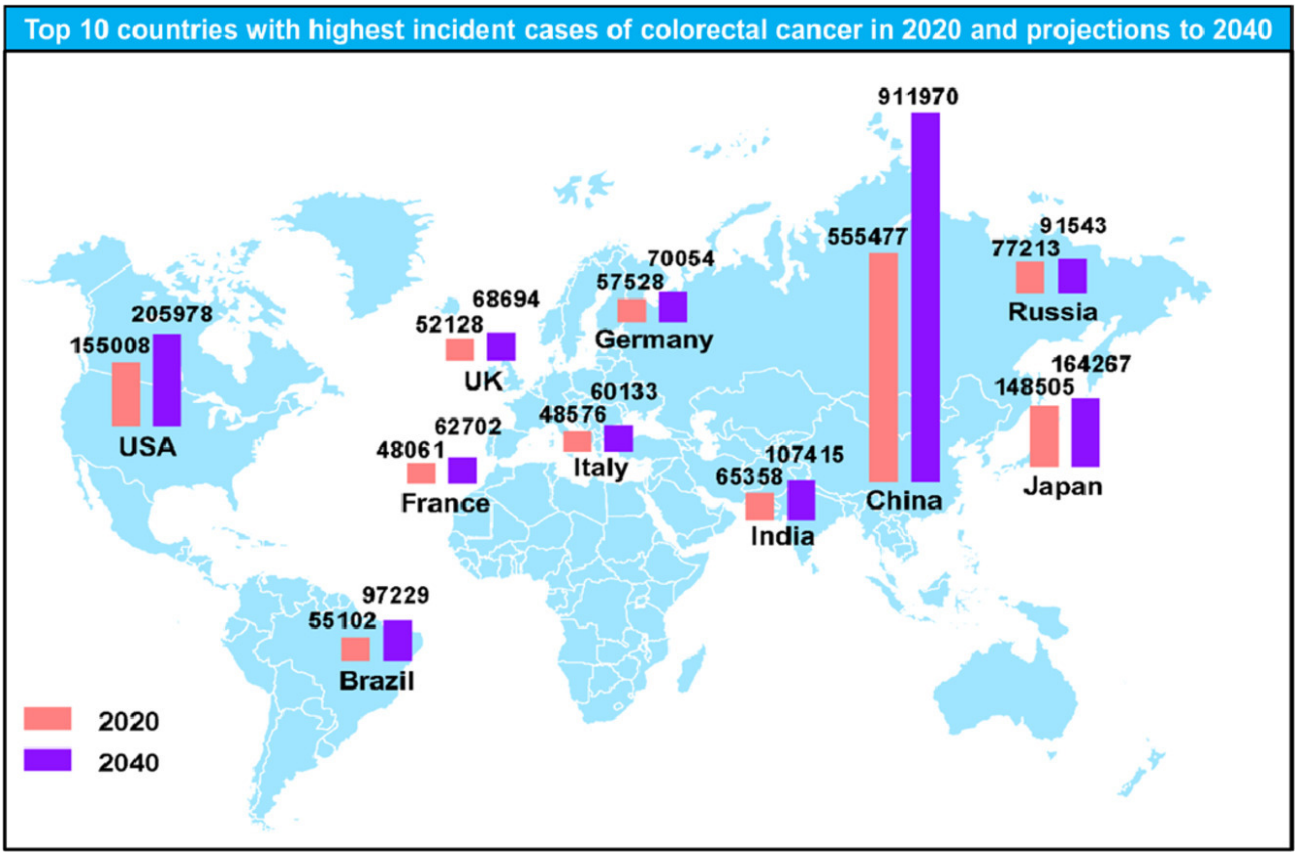

Figure1.1: The number of new CRC cases in top 10 countries with highest incident cases in 2020 and projections for 2040. (Xi Y et al. 2021)

no data on prevalence in this paper [3]. Approximately 2/3 of such patients are diagnosed with cancer of the colon and the risk increases with age (Figure 1.2). The diagnosis of half of the cases is made after 70 years, while only approximately 10% of cases of CRC occur before the age of 55; thus, the diagnosis is made at an average age of 72 years in males and 76 in females.

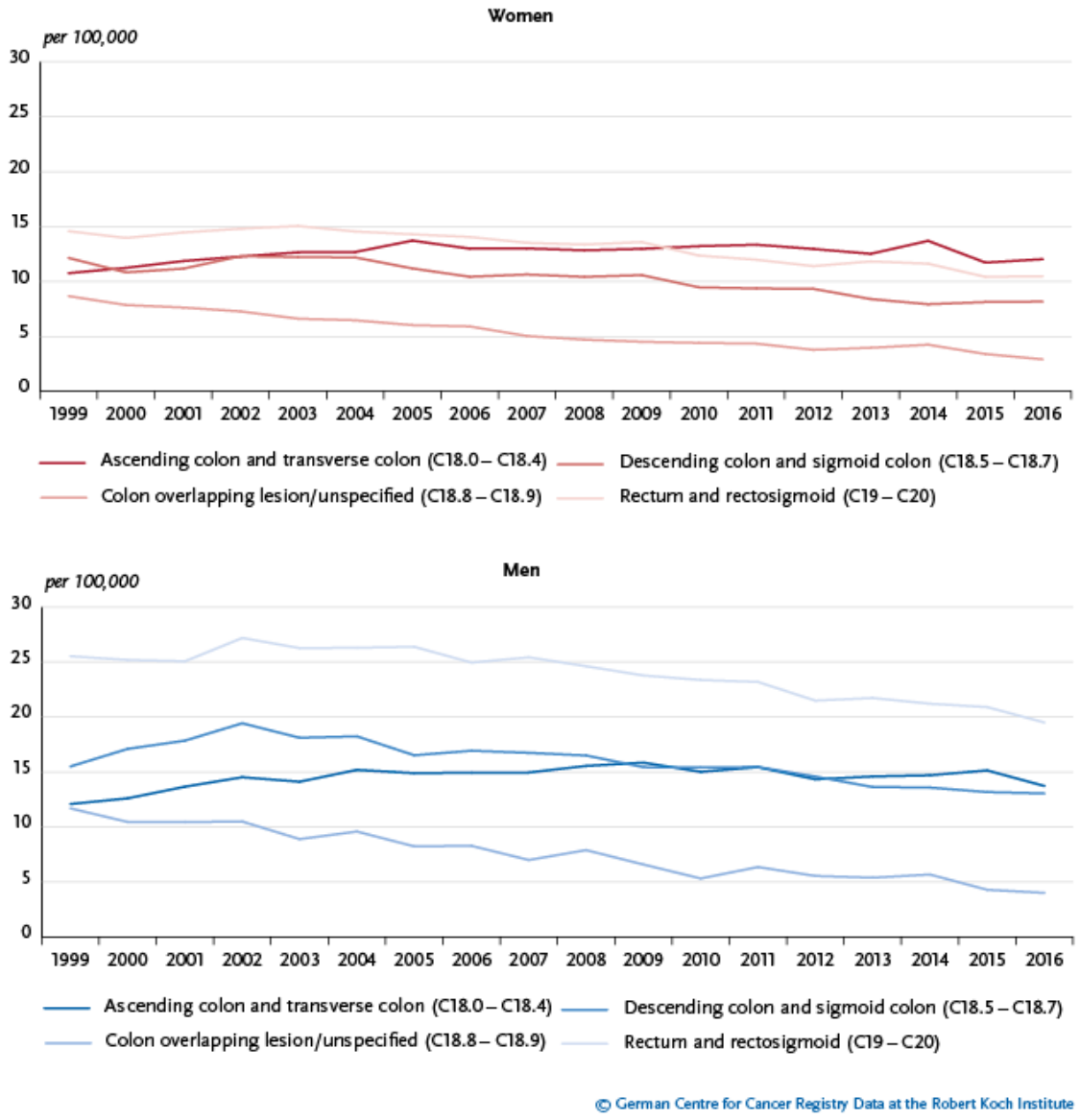

Figure1.2: Age standardised incidence rates of malignant neoplasms of the colon and rectum by localisation and sex, ICD-10 C18–C20, Germany.

CRC is usually diagnosed among young adults, meaning that it may be associated with risk factors such as sedentary lifestyle, obesity, smoking, unfavorable eating habits (high protein/fat diet), as well as aging[4]. The clinical manifestations of CRC depend on the tumor size, location, presence or absence of metastatic lesions, and include abdominal distension, stomachache, changes in bowel movement/chronic bowel habits, vomiting, nausea, involuntary weight loss, anorexia, and malaise [5]. Two main carcinogenic pathways have been identified: the suppressor or chromosome instability pathway and the mutator or microsatellite instability pathway [6]. The former is due to a chromosomal instability that determined the progression of the adenoma observed in 80% of sporadic CRC cases, while the latter is due to a microsatellite instability, including diverse gene mutations in 80% of the hereditary CRC and 20% of sporadic CRC cases, which mostly include p53 70%, DCC 70%, APC 60%, BAX 50% and KRAS 40%[7]. CRC generally develops from an intestinal mucosal polyp, but it may also start as benign adenoma that converts to malignancy according to the size and histological presentation. Approximately 40% and 60% of patients have multiple adenoma and single adenoma, respectively, while the lesions in 24% of cases progress into cancer if left untreated[8].

1.1 Current situation of Colon cancer Treatment

CRC treatments currently in use include surgical therapy, neoadjuvant radiotherapy and chemotherapy, postoperative chemotherapy, targeted therapy, maintenance therapy, and immunotherapy[9]. So far, the survival time of CRC patents has greatly improved thanks to advances in primary and adjuvant therapies. To be specific, an appropriate treatment for CRC is to completely remove the tumor and metastasis using surgery as the main treatment. Nonetheless, although many screening programs have been developed to reduce CRC incidence, the diagnosis of about 1/4 of CRC cases is made at the late stage when metastatic lesions occur, whereas the 20% rest patients have metachronous metastatic lesions, making radical surgical treatment difficult, resulting in cancer-associated mortality[9].

Recent years, the identification of molecular biomarkers for the diagnosis and treatment of CRC gives us hope. In early 1900s, the idea of a chemical compound specifically targeting one microorganism was initially proposed, theory that expanded to tumor therapy in 1988[9]. The idea of targeted therapy has been well developed over the past 2 decades. Targeted therapy is effective on tumor cells through the direct inhibition of cell growth, migration, and differentiation (Figure1.3).

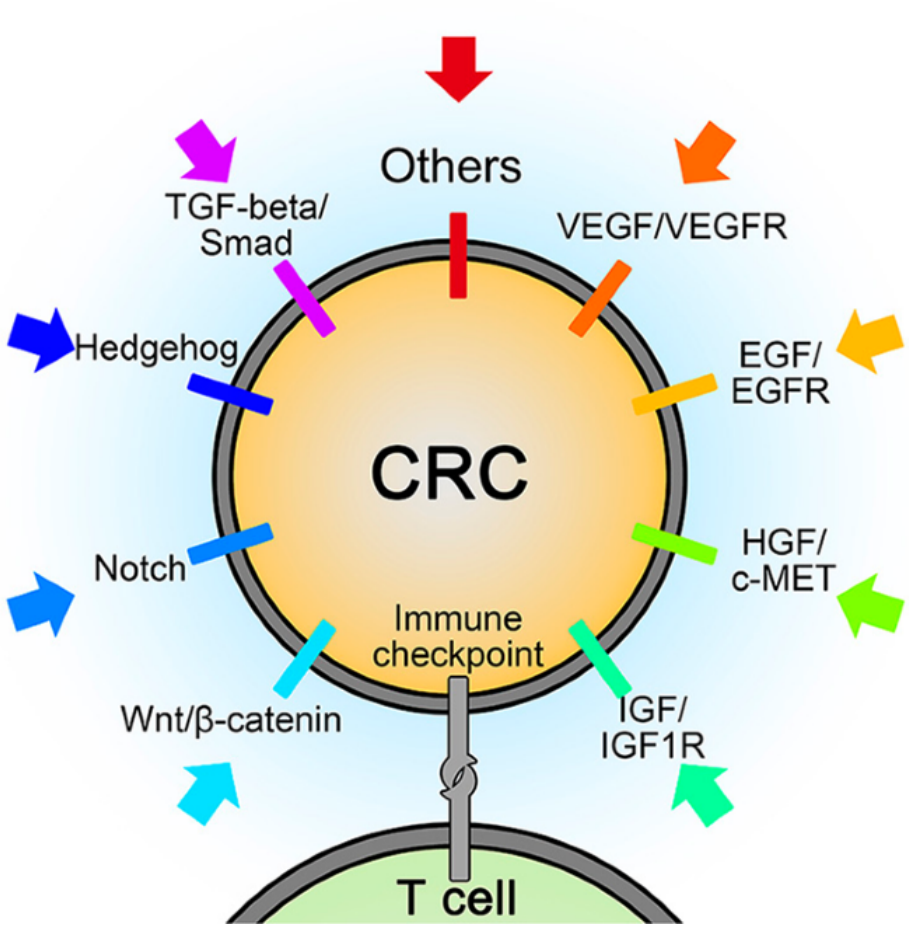

Figure 1.3 Pathways offering potential sites for targeted therapy. CRC: colorectal cancer; VEGF/VEGFR: vascular endothelial growth factor/vascular endothelial growth factor receptor; EGF/EGFR: epidermal growth factor/epidermal growth factor receptor; HGF: hepatocyte growth factor; c-MET: mesenchymal–epithelial transition factor; IGF/IGF-1R: insulin-like growth factor/ insulin-like growth factor 1 receptor; TGF: transforming growth factor. (Xie Y H, et al. 2021

Targeted drugs can alter tumor microenvironment (TME), which includes immune cells and local blood vessels, to inhibit cancer development and perform an enhanced immune attack and surveillance[9]. Micromolecules like monoclonal antibodies have a molecular weight lower than 900 Da and exert important effects on targeted therapy. These molecules enter cells and usually work by inactivating selective target proteins, inducing apoptosis and thus blocking

cancer development [10]. Currently, numerous clinical trials demonstrated that the use of such targeted therapies using cetuximab and bevacizumab improves the survival of patients with metastatic CRC by targeting epidermal growth factor receptor (EGFR)/HER1 and vascular endothelial growth factor (VEGF). In addition, prognostic markers contribute to decision-making; for instance, mutations of the KRAS gene predict the benefits that can be obtained from anti-EGFR antibodies. Nevertheless, regardless of these advances, specific diagnostic and prognostic markers and therapeutic targets for CRC cases are lacking. Therefore, it is necessary to identify trustable markers for CRC.

1.2 Mating Type Switching/Sucrose Non-Fermentable (SWI/SNF) complex

The human genome contains 3 billion base pairs, corresponding to approximately 2 meters of DNA condensed to form chromatin, in order to adapt to the nucleus whose diameter is just 5 μm[11]. The nucleosome is the core particle that consists of 147 base pairs of DNA wrapped in helical turns surrounding the histone octamer consisting of 4 core histones (H2A, H2B, H3, and H4), thus creating the compact chromatin structure[12]. The heterochromatin, which is the highly condensed chromatin DNA, is transcriptional silent [12]. Epigenetic mechanisms, such as histone acetylation and DNA demethylation, change the chromatin structure to a more open euchromatin state. Thus, chromatin remodelers, along with the related enzymes, change the composition of nucleosomes to which transacting factors bind, resulting in the initiation of gene expression and activation of biological pathways and signaling cascades[12].

Four evolutionarily conserved ATP-dependent chromatin remodeling complexes exist in mammalians: ISWI, CHD, INO80 and SWI/SNF [13]. The multiprotein complexes (approximately 2 MDa in size) have the same central Snf2-like ATPase domain, whereas different compositions in the interaction of subunit or recruited protein decide their biological functions. Specifically, SWI/SNF complexes contain the combinatorial product of a minimum of 29 proteins[14]. The detailed description of the discovery and evolutionary history of SWI/SNF chromatin remodelers is available. SWI/SNF complexes are important in regulating the proliferation and differentiation of the cells. However, the mechanism used by remodelers to perform these functions is still unclear. Multiple nucleosome-binding domains contain DNA-binding domains, like AT-rich interactive domains (ARIDs), zinc-finger domains or high-mobility group box domains (HMGs), as well as histone-binding domains, like bromodomains (BRDs), plant homeodomains (PHDs) or chromodomains in most of the SWI/SNF subunits (Figure 1.4)[14] .

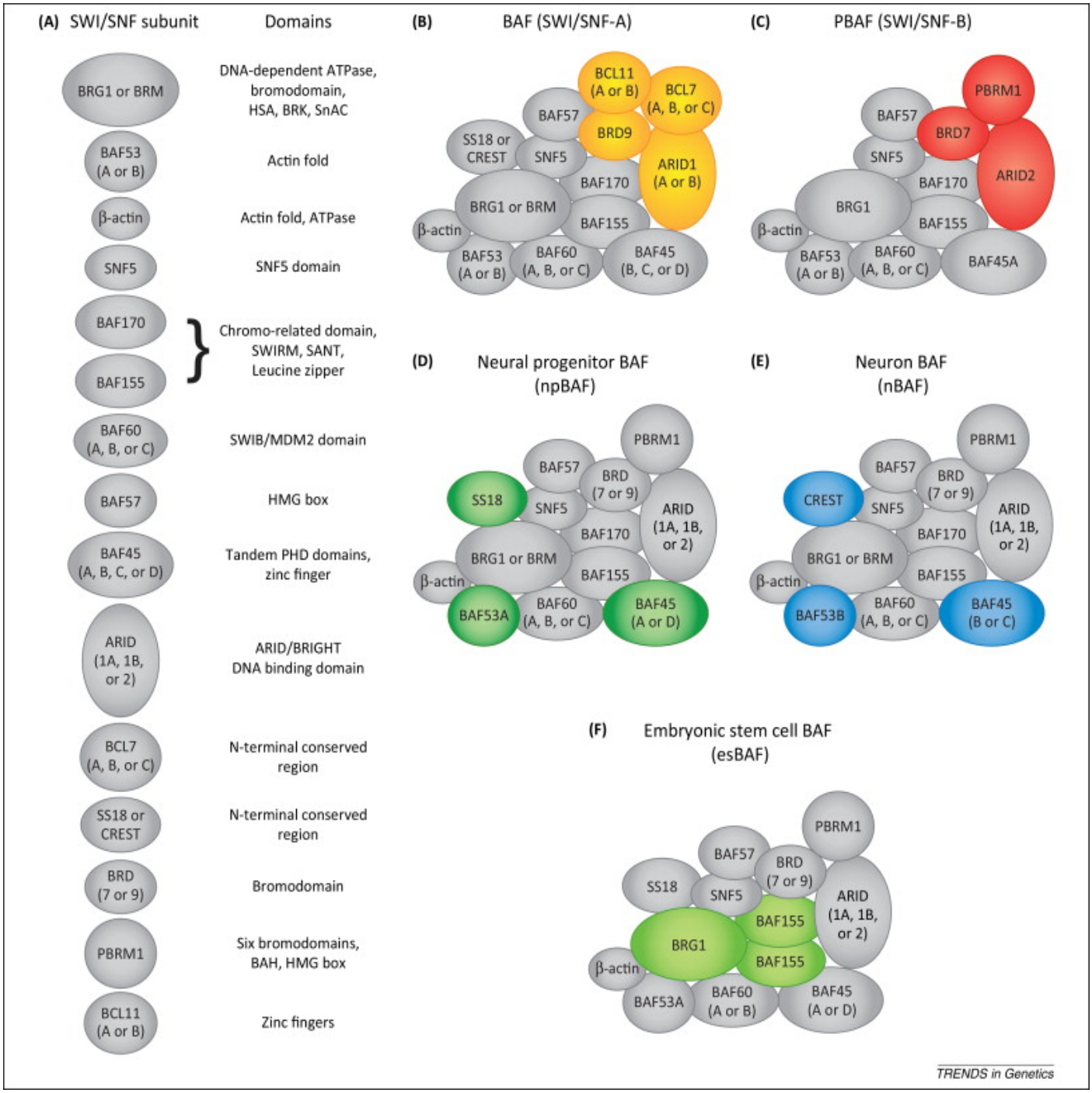

Figure 1.4 Overview of mammalian SWI/SNF complexes. (A) Subunits that comprise the mammalian SWI/SNF complex. Protein domains present in each subunit are listed on the right. (B–F) Examples of known SWI/SNF subunit configurations. (B,C) BAF and PBAF represent two alternative subunit arrangements for SWI/SNF that can exist in the same cell type. (D–F) Examples of cell type-specific SWI/SNF subunit configurations. (Hohmann A F, et al. 2014)

Three mammalian SWI/SNF complexes are known, such as BRG1/BRM-associated factor (BAF), polybromo-associated BAF (PBAF) and the recently discovered non-canonical BAF (ncBAF or GBAF) domain [14]. All of them include one mutually exclusive catalytic ATPase subunit, SMARCA2 or SMARCA4, sharing some relevant proteins. BAF and PBAF include one ARID and one SMARCB1 subunit. Besides, the newly reported cryo electron microscopy (EM) structures in recombinant and endogenous human BAF complexes offer encouraging novel perspectives to better understand the overall complex assembly and mechanism regulating the interaction between nucleosomes and BAF complexes [15]. The structures show the modular organization in the complex, in agreement with former data on the complex assembly pathway, and in the meantime allow a deeper understanding on the mechanism of histone eviction caused by ATP-driven rearrangements [15]. ARID1A represents the structural core in the base module, in which SMARCC1/2 serves as a scaffolding protein and SMARCE1/D1 as a supporting complex formation. In addition, the nucleosome is located between SMARCB1 and the ATPase module SMARCA4, and they have interactions with the acidic patch regions of the nucleosome H2A/H2B. ATP-driven bind of nucleosome to SMARCA4 finally causes nucleosome eviction, such as the elongation of the nucleosome-free DNA that is used as transcription factor.

PBAF is the second major human SWI/SNF chromatin remodeler highly homologous with BAF, although they are very different in the composition of subunits. ARID1A, the structural core of the base module of the BAF complex, is replaced by the paralogue ARID2

of PBAF[16]. Additionally, PBAF includes the bromodomain-containing protein 7 (BRD7). With an especially entertaining property, The subunit polybromo-1 (PBRM1) is a subunit of PBAF, and contains six tandem-acting bromodomains (PBs 1-6). the central ARID1A subunit in smaller ncBAF is replaced by the glioma tumor suppressor candidate region gene 1 (GLTSCR1) subunit[17]. ncBAF is short compare to other base module BAF subunits, such as SMARCC2, SMARCE1 as well as nucleosome-recognition unit SMARCB1, and contains the bromodomain-containing BRD9 subunit unavailable in the other two complexes, according to the latest systematic research on SWI/SNF complex assembly[18].

The three human SWI/SNF chromatin remodelers have interactions with different enhancers and promoters in a cell-type-specific manner due to the diversity in combination and structure [19]. Similarly, BAF complex subunits are subjected to different transitions during development, causing different transcriptional signatures. BAF is often related to the bind to enhancers, while PBAF or ncBAF enrichment often occurs in promoter regions. SMARCA4 co-localizes with H3K27ac in the enhancers, which regulate lineage-specific developmental programs [16; 20]. Besides, two recently published articles provide interesting perspectives on how the expression of the key subunit SMARCB1, exclusive to BAF and PBAF, changes the balance between canonical and non-canonical SWI/SNF complexes, which in turn change transcriptional signatures. SMARCB1 loss leads to an extensive damage of the representative enhancer activity, excluding the super-enhancer activity[21]. On the contrary, SMARCB1 reversely regulates super-enhancers of all cell types, indicating that the high expression of SMARCB1 prevents ncBAF formation[22].

1.3 SWI/SNF complex in cancer

The SWI/SNF complex exerts significant effects on the maintenance and regulation of the transcription factor access, thus characterizing its strong tumor-suppressive activity[23]. Thus, SWI/SNF perturbation may cause the reprogramming of cellular processes, including the oncogenic ones. Loss-of-function mutations of genes that encode the SWI/SNF subunits occur in over 20% human cancers, and the frequency of point mutations is approximately twice than that of deletions [23; 24; 25].

According to the latest study on cryo EM structures in human BAF complex, most oncogenic mutations map to intra-complex subunit–subunit interfaces, and the exposed surfaces can have potential interactions with regulatory proteins or interaction sites with nucleosome to alter the complex chromatin remodeling activity[26]. SWI/SNF genes also undergo amplifications in numerous cancer types. The occurrence of common amplifications is largely determined by cancer types, mostly lung squamous cell carcinoma, ovarian cancer or sarcoma[23]. Particularly, BRD9 and ACTL6A show a high propensity for amplification in many tumors, which highlights their oncogenic capacity[23].

SWI/SNF chromatin remodelers on cancer development were first studied over 20 years ago, at which time biallelic loss-of-function mutations in the SMARCB1 gene were reported as driving tumorigenesis of malignant rhabdoid tumors (MRTs)[27]. Additionally, SMARCB1 rescue trials in MRTs restored enhancer-based activation, demonstrating the role of wild-type BAF in antagonizing gene repression mediated by polycomb repressive

complexes [28]. The results are in agreement with those in a former report which shows that SMARCB1 loss contributes to the enhanced expression pf the polycomb subunit EZH2 (enhancer for zeste 2) and increased H3K27me3 gene silencing transforms MRT[29]. In addition, the loss of SMARCB1 activity is the main factor for the development of synovial sarcoma[30]. Indeed, the loss of SMARCB1 is associated with the development of malignant tumors and the activation of some oncogenic signaling pathways[31].

According to previous findings, SMARCA4, as the most common mutated Snf2-like ATPase, is inactivated in multiple types of cancers, such as lung cancer[32; 33]. Indeed, BAF's ARID1 subunit and PBAF's PBRM1 subunit have the highest prevalence of mutations. However, SMARCA4-mutant cancer tends to be more aggressive and is associated to a relatively poor prognosis[32]. At present, the ATPase subdomain of SMARCA4 is considered a hotspot. It is noteworthy that mutations of this subdomain lead to impaired ATPase activity and damage the competition of BAF with the polycomb repressive complex[34]. However, SMARCA2 mutation in cancer is less frequent. Nevertheless, it tends to be silenced, which is confirmed by restoring SMARCA2 functions in cancers with deficient SMARCA2[35].

ARID1A, which connects DNA through its AT-abundant DNA-binding domain, is the one mutating most frequently among the subunits of BAF [36]. ARID1A works as a tumor suppressor, and the loss of function is related to the development of breast cancer [37] and pancreatic cancer [38]. It is interesting that cancer mutation is spread across nearly all areas

of the ARID1A genes and does not gather in the DNA binding domain [36]. This is because ARID1A participates in many contacts that stabilize the base modules of the complexes. Apart from that, the loss of the suppressive function of ARID1A leads to the development of cancers through the interference of DNA-damaging response pathways [36]. According to some studies, the loss of ARID1A is associated to the activation of PIK3CA together with a loss of PTEN expressions, which triggers the PI3K/AKT/mTOR cell-cycle pathway [39; 40].

Cancer related to ARID1B is less common [41]. Nevertheless, the mutation of this gene is associated to the disability of development [42]. ARID2 also works as a tumor suppressor. Apart from that, ARID2 is usually mutated in hepatocellular carcinoma [43]. According to studies on the mechanism associated to the function of ARID2 in lung cancer and hepatocellular carcinoma [44], ARID2 loss not only triggers transcriptional reprogramming but also damages the DNA-damage response pathway [45].

1.4 Frequent mutation of the SWI/SNF chromatin remodeling complex in colon cancer

Over decades, research has provided insights into how mutations in classical oncogenes and colon cancer tumor suppressor genes (TSGs) such as APC, TP53, KRAS, CDKN2A and PIK3CA drive tumor development[46; 47]. Importantly, recent reports from large-scale cancer genome landscape studies such as the Cancer Genome Atlas (TCGA) as well as others firmly establish the frequent occurrence of these pathogenic mutations in colon cancer[48; 49; 50]. For example, TP53 carries the 70% of somatic coding mutations, APC in 60% and KRAS in 49%[46; 51; 52]. However, one unexpected finding from these studies is the pathogenic mutations in components of the SWI/SNF chromatin remodeling complex in nearly 15% of colon cancers[53]. The SWI/SNF complex, first discovered in *S. cerevisiae*, is an evolutionarily conserved multi-subunit complex that utilizes the energy of ATP hydrolysis to mobilize nucleosomes and remodel chromatin. Since the complex consists of 12–15 subunits, multiple complex configurations can appear, depending on the subunit composition. All complexes include a catalytic ATPase subunit (mutually exclusive SMARCA4/BRG1 or SMARCA2/BRM) and core subunits including BAF155 and SMARCB1. Three broad sub-families of SWI/SNF complexes have been identified: BRG1 associated factors (BAF), polybromo-associated BAF (PBAF) and the recently-described ncBAF, each defined by signature subunits including ARID1A or ARID1B (BAF), PBRM1 and ARID2 (PBAF) and GLTSCR1 (ncBAF). SWI/SNF complex subfamilies also contain variant subunits, often encoded by multi-gene families. Multiple reports showed the role of the complex in the regulation of a broad range of normal

functions such as gene transcription, RNA processing, cell cycle, apoptosis, development, differentiation of the tumor and DNA replication and repair. Thus, this pivotal role in regulating these diverse pathways may predict an association of altered SWI/SNF function with diseases. Therefore, the identification of cancer vulnerability associated with the mutation of the SWI/SNF chromatin remodeling complex has a high clinical significance in colon cancer, because it promotes more effective applications of the combination of radiotherapy with chromatin-targeted therapy.

1.5 Synthetic lethal in SWI/SNF complex

The term of synthetic lethality, which was introduced by the geneticist Calvin Bridges[54], was named in 1946 by Theodor Dobzhansky[55]. Synthetic lethality refers to the condition in an organism, in which mutations in two genes together result in cell death or death of an organism, while a mutation in either gene alone exerts little or no effect [56] (Figure 1.5).

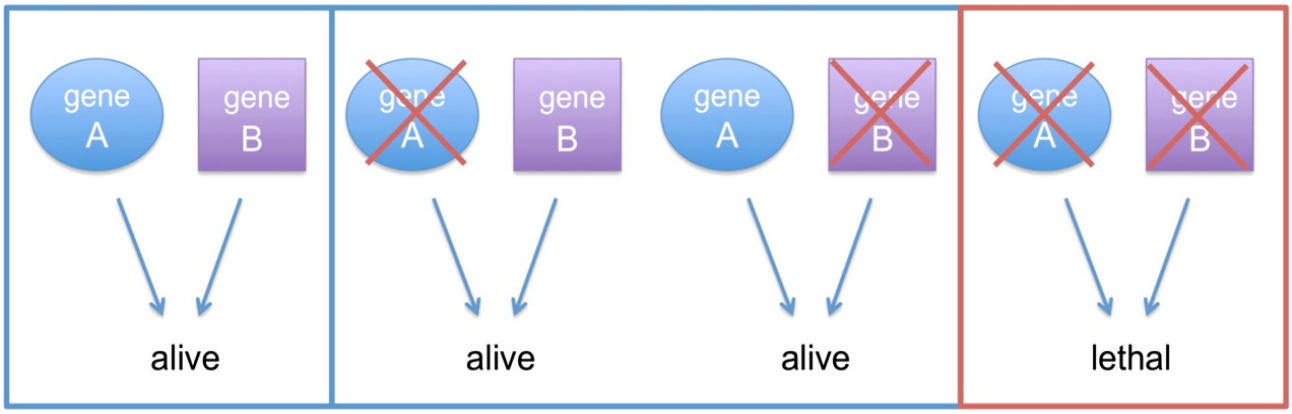

Figure 1.5 Schematic representation of synthetic lethality. Two genes are synthetic lethal only when their simultaneous inactivation results in cellular or organismal death. In this example, deletion of either gene A or gene B does not affect viability whereas inactivation of both at the same time is lethal. (Sebastian M.B, et al. 2011)

Many developmental biologists and geneticists investigated this paradigm. Notably, the research by Hartwell et al[57] shows the application of the synthetic lethality concept to develop cancer therapeutics. The synthetic lethal interaction is also a context-dependent form, since the alteration of a given gene makes the second gene important for the survival of cells[58]. Furthermore, the pharmacological inhibition of the product of these synthetic lethal genes can be detrimental to tumor cells, but most of the non-malignant cells are not affected[59]. Hence, synthetic lethality may represent an approach to target tumor cells without affecting the healthy cells of the patients. Moreover, the application of the principle of synthetic lethality improves the possibility to accurately target subgroup of cancers,

enabling individual therapeutic approaches. Indeed, the synthetic lethal connection increases the chance to target the residual SWI/SNF complex for treating cancers with mutations in the SWI/SNF. Experiments on SWI/SNF-regulating proteins or SWI/SNF subunits were performed in the project of Achilles (http://www.broadinstitute.org/achilles) [16; 60]. Some genes for the therapy of SWI/SNF-mutant cancers have been identified [61; 62]. Some SWI/SNF mutations have been associated with synthetic lethal phenotypes in SWI/SNF deficient tumors (Figure 1.9). In some cases, the two mutually exclusive paralogues' concomitant knockout leads to synthetic lethality [63]. For example, the SMARCA4-deficient tumors are quite sensitive to the depletion of SMARCA2[25], and ARID1B is needed for the survival of ARID1A-mutant cancers [64].

The vulnerability of SWI/SNF-mutant cancer is discovered in the interactome of SWI/SNF chromatin remodelers. Indeed, not all protein kinases can be targeted, but there are many inhibitors for each kinome family that can offer excellent starting points for targeted therapies. As a result, targeting particular SWI/SNF vulnerable proteins with small molecule is a good strategy for cancer treatment. Nonetheless, this method needs the validation and identification of targets as well as the development of high-quality probes to demonstrate the biological function of the targets [65]. Apart from that, such kind of probe needs to meet multiple specific criteria, such as potency and selectivity. Besides, their action mode should be well characterized[66; 67].

1.6 ARID1A directed synthetic lethal in SWI/SNF complex

ARID1A, also called BAF250a as well, belongs to the SWI/SNF complex subunit[36]. Besides, it is the most frequently mutated gene of the SWI/SNF subunit genes. In addition, ARID1A is characterized by the greatest frequency of mutations in malignancies because associated with tumor activity and poor prognosis [68]. The mutation frequency of ARID1A in CRC increases in cancer showing microsatellite instability (MSI) [69; 70; 71]. Since the mutation frequency of ARID1A is high in CRC, it is important to develop drugs for selectively targeting ARID1A-deficient cancer cells to promote the development of novel treatment options to combat CRC.

Since the high mutation frequency and loss of expression of ARID1A in cancer were discovered, ARID1A deficiency has been used to treat cancer based on synthetic lethality (Figure 1.6).

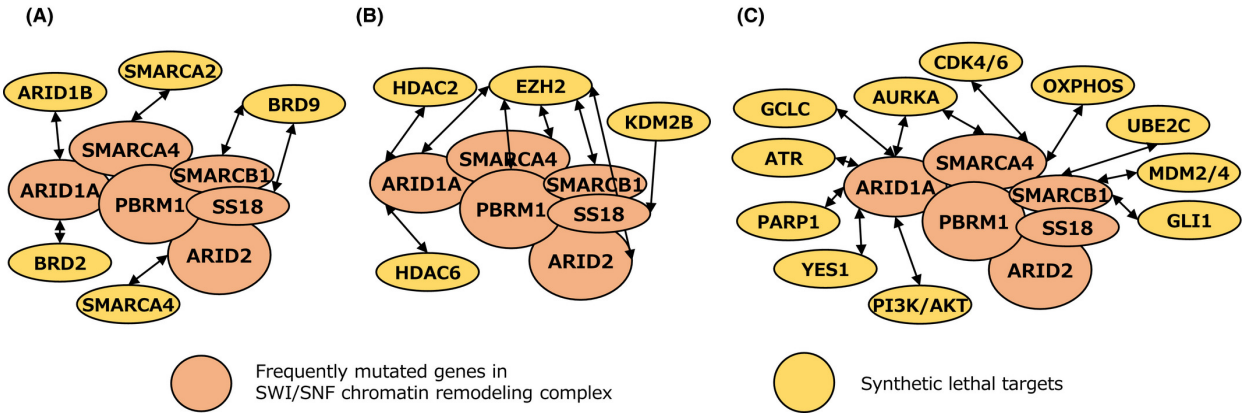

Figure 1.6 Synthetic lethal interactions in SWI/SNF- mutant cancers with chemical tools for targeted cancer therapy. (Sasaki M, et al. 2020)

ARID1A and ARID1B, which form a synthetic lethal pair, are mutually exclusive elements of BAF complexes [72]. It is worth mentioning that the loss of ARID1B and ARID1A not only leads to the collapse of the BAF complex, but also results in the loss of functional activities of the BAF complexes [72]. Hence, the inhibition of ARID1B function is a prospective strategy to treat cancers with deficient ARID1A. Nonetheless, the development of an inhibitor against ARID1B can result very challenging because ARID1B has no functional domain (e.g. catalytic domain) [73]. However, the ARID1A-guided synthetic lethality can be obtained through several types of molecular mechanisms[74]. The

synthetic lethal interactions with mutations of ARID1A are not only associated ARID1B direct targeting.

In addition to the regulatory function in SWI/SNF complexes that bind to DNA, ARID1A is involved in the repair of DNA double-strand break (DSB) as well [75]. SMARCA2 and SMARCA4 interact with the DSB once formed, suggesting a function of SWI/SNF in the DNA damage response (DDR). Furthermore, ARID1A and ARID1B are localized in the DSBs and promote the activity of the NHEJ pathway [76]. ARID1A also plays a function in Homologous recombination (HR) [77]. NHEJ is a more error-prone DSB repair mechanism than HR. Apart from that, ARID1A and ARID1B recruit the NHEJ proteins KU70 and KU80 to the DNA damaging sites, thus participating in the early phase of DSB repair [78].

The synthetic lethality concept was explored by targeting DDR proteins in ARID1A mutant cancers [77; 79]. Shen et al. [77] confirmed that ARID1A plays a role in DSB repair as ATR binding partner. They discovered that ARID1A is increased in chromatin areas approaching DSBs, as revealed by the chromatin immunoprecipitation assay. The inactivation of ARID1A by introducing a stop codon in the colorectal carcinoma cell line HCT116 leads to impaired G2/M checkpoint control after DSB induction. Cells lacking ARID1A re-enter the cell cycle more frequently after irradiation than control cells. Besides, the phosphorylation of ATR and CHK1 is decreased in ARID1A mutant cells. Thus, ARID1A seems to actively control G2/M progression. In addition, loss of ARID1A

decreases the localization of the DDR adaptor proteins at the DSBs sites. In short, these results indicate a significant function of ARID1A in the ATR-mediated DDR signaling. However, it is still unclear whether ARID1A localizes to DSBs and activates ATR as well as subsequent DDR. Based on the participation of ARID1A in the DSB repairing, Shen et al[77] examined the synthetic lethality of PARP inhibitors in ARID1A mutant cells, since these types of inhibitors are lethal in the DSB repair deficient cells. Beyond that, many inhibitors of PARP are toxic in isogenic pairs of breast epithelial carcinoma and colorectal carcinoma cells, which show more than three times less colony formation in ARID1A-depleted cell lines. Moreover, the efficacy of PARP treatment increases in ARID1A-depleted xenograft cancer models [77]. Williamson et al. discovered that ARID1A loss is a dominant factor for the sensitivity to ATR inhibition in breast cancer cell line HCC1143[79]. Besides, ATR inhibition by VX-970 in ARID1A deficient cell lines is three times more effective in multiple cancer types [80; 81]. Moreover, increased sensitivity to the inhibition of ATR is observed in ARID1A mutated HCT116 cells in xenograft models as well as in models of ARID1A mutant TOV21G OCCC cells.

Recently, an epigenetics drug screen showed that inhibitors of aurora kinase A (AURKA) work as a synthetic lethality partner of ARID1A [82]. AURKA belongs to a member of the mitotic serine protein family, and it plays many roles in mitosis and non-mitotic biologic processes [83]. AURKA activates the nuclear localization of CDC25C [84], consequently phosphorylating some substrates to drive the entry into mitosis from the G2-phase [85]. In addition, the over-expression of AURKA is involved in tumorigenesis and

genetic instability in multiple types of cancers, such as lung, pancreas, and CRC [86; 87; 88]. High expression of AURKA is related to poor outcome in patients with lung and colon cancer. This evidence makes it a significant therapeutic target to develop anti-cancer drugs. As pointed out by Wu [82], ARID1A has an interaction with the AURKA in CRC cells. In addition, genetic and pharmacological perturbations of AURKA hinder the growth of ARID1A-deficient CRC cells. Indeed, ARID1A occupies the promoter of AURKA gene and regulates its transcription in a negative way. Cells that lack ARID1A show an increased AURKA transcription, leading to the constant activation of CDC25C. Moreover, the inhibition of AURKA activities in ARID1A-deficient cells not only greatly leads to G2/M arrest but also triggers cellular multinucleation and apoptosis [82].

The present work investigated the role of ARID1B silencing in the radiosensitivity of CRC cells through the detection of the clonogenic survival after the exposure to irradiation in the presence/absence of ARID1A mutation. Subsequently, the synthetic lethality concept was performed to identify drugs affecting DNA repair with potential synergistic effect with irradiation on ARID1A-depeleted cancer cells. Our results demonstrated that ATR was the most potent synthetic lethal interactor.

2. Aims of the present study

ARID1A as a member of the SWI/SNF complex is frequently mutated in colorectal cancer. Thus, it is of fundamental clinical importance to understand its molecular functions and determine whether this specificity can be exploited therapeutically by combined treatment modalities. Usually, loss of ARID1A compromises DNA damage repair, and induced DNA damage burdens may increase the reliance on PARP or ATR-dependent DNA repair pathways of cancer cells to maintain genome integrity and renders cell susceptible to ATR or PARP inhibitor therapy. In the present study, the effect of ionizing radiation (IR) in combination with ATR was tested in colon carcinoma cell lines with wild type (wt) and mutant (mt) ARID1A. Besides, our recent studies showed that loss of its homolog ARID1B is synthetically lethal with ARID1A mutation. Here, the effect of radiation in combination with small molecules inhibiting repair factors on the sensitivity was tested in wild type and mutant ARID1A in colon carcinoma cell lines.

For this, colon carcinoma cell lines with wild-type (HCT15, HCT116, Colon320) and mutant ARID1A (RKO, SW48, LS180) were treated with inhibitors of ATR, PARP and AURKA and its consequences for radiation sensitivity was measured by clonogenic survival. In addition, the effect of ARID1B knock-down with siRNA in combination with ATRi on radiation sensitivity was further tested. Mechanistically, the effect on double strand break (DSB) repair markers measured by immunofluorescence staining of ɣ-H2AX and Rad51-foci was investigated. In addition, the homologous recombination (HR) direct-repeat green fluorescent protein (DR)-GFP) system was used to confirm the effect of ATRi

on DSB repair in ARID1A depleted cells. Lastly, the effect of ATRi in the background of ARID1A deficiency was tested in an ex-vivo model. For this, cells from CRC patients with and without ARID1A expression were tested for the efficacy of ATRi by using a ATP-tumor chemosensitivity assay (ATP-TCA).

3. Materials and Methods

3.1Materials

Description	Supplier
6-Well Cell Culture Plates	TPP
4-8-Well Culture Slides	Falcon
15-50 mL Tubes	Greiner Bio-One
Coverslips	Roth
flexiPERM® slide reusable 8-Well	SARSTEDT
SuperFrost® Plus GOLD Culture Slides	Thermo Scientific

3.1.1 Biological and chemical substances

Description	Supplier
Antibiotic-Antimycotic (100X)	Gibco™
BSA	Calbiochem
Click-iT™ Plus EdU Assay Kit	Invitrogen™
DC Protein Assay Reagent A & B	Bio-Rad
DMSO	Sigma-Aldrich
ECL Prime Blocking Agent	GE Healthcare
EDTA	Sigma-Aldrich
Ethanol	Honeywell
FBS	Gibco™
Fibroblast Basal Medium	ATCC®
Formaldehyd 37%	Roth
HBSS	Gibco™
Immu Mount™	Thermo Scientific™
Kristallviolett	Merck
Lipofectamine® RNAiMAX	Invitrogen™
LowCross Buffer	Candor
MEM	Gibco™

NEAA, Nicht essentielle Aminosäuren	Gibco™
Methanol	J.T.Baker
NuPAGE Transfer Buffer 20x	Invitrogen™
NuPAGE 7% Tris-Acetat Gel 12 Well	Invitrogen™
OptiMEM	Gibco™
PBS (20x)	Gibco™
Phosphatase & Protease Cocktail 100x	Thermo Scientific™
Pierce® RIPA Buffer	Thermo Scientific™
Roti®-Histofix 4%	Roth
RPMI	Gibco™
Super Signal Stable Peroxide Puffer	Thermo Scientific™
Super Signal Luminol/ Enhancer Solution	Thermo Scientific™
Tris-Acetat SDS Running Buffer 20x	Invitrogen™
Triton 100	Sigma-Aldrich
Trypan Blue Stain 0,4%	Logos Biosystems
0,05 % Trypsin-EDTA	Gibco™
Tween20	Sigma-Aldrich

3.1.2 Solutions and Buffers

Cristallviolett	3,75g Kristallviolett 1,75g NaCl 162,5ml Ethanol 43,2ml Formaldehyd 37% ad 500ml dH_2O
P1 Puffer (Permeabilisierung)	100mM Tris-Cl pH 7,4 50nM EDTA 0,5% Triton 100
Block Puffer (IF)	3% BSA

	7,7 mM NaN_3 4x SSC 0,1%Tween20 in dH_2O
Block Puffer (WB)	5 % ECL Prime Blocking Agent 0,5 % TWEEN20 in TBS
TBS	10mM Tris-Cl pH 7,4 150mM NaCl in dH_2O

3.1.3 Primary antibodies and dyes

Antibody	**Company**	**Cat. No.**	**Host**	**Dilution**
ARID1B	GeneTex	GTX130708	Mouse	1:500 (WB)
ARID1B	LSBio	LS-C382223	Rabbit	1:500 (WB)
ARID1B	Abcam	Ab57461	Mouse	1:500 (WB)
ARID1A	CellSignalling	12354P	Rabbit	1:1000 (WB)
GAPDH	Abcam	ab8245	Mouse	1:2000 (WB)
γH2A.X	EMD Millipore	05-636	Mouse	1:500 (IF)
Rad51	Calbiochem®	PC130-100UL	Rabbit	1:500 (IF)
Histone H3 (pS10)	EMD Millipore	05-373	Mouse	1:500 (IF)

3.1.4 Secondary antibodies

Antibody	**Company**	**Cat. No.**	**Host**	**Dilution**
Anti-Mouse, Alexa Fluor 488	Invitrogen™	A11029	Goat	1:2000 (WB)

Anti-Mouse, Alexa Fluor 488	Invitrogen™	A11017	Goat	1:500 (IF)
Anti-Mouse, HRP linked	GE Healthcare	NA931V	Sheep	1:10000 (WB)
Anti-Rabbit, HRP linked	GE Healthcare	NA934V	Donkey	1:100000 (WB)
Anti-Rabbit, Cyanine Cy™3	Jackson	111-165-008	Goat	1:500 (IF)
DAPI	Invitrogen™	D1306		1γg/ml (Flow Cytometry) 20γg/ml (IF)

3.1.5 siRNAs und inhibitors

	Company	**ID**
siARID1B a	Ambion®	s199170
siARID1B b	Ambion®	s199168
si Negative Control No. 1	Ambion®	Cat# 4390843
VE-821 (ATR Inhibitor)	Selleckchem	S8007
VE-822 (ATR Inhibitor)		S7102
AZD2461 (PARP Inhibitor)	Selleckchem	S7029
Olaparib (PARP Inhibitor)	Selleckchem	S1060
Alisertib (AURKAi Inhibitor)	Selleckchem	MLN8237

3.1.6 Softwares

Software	**Version**	**Provider**
Prism	6	Graphpad Software, Inc.
FloMax	2.4	Partec GmbH
Imagelab	4.1	Bio Rad
Multicycle für Windows	3	Washington Universität, USA

Axiovision	8.4.2	Zeiss
EndNote	X7	Thomson Reuters, USA
ImarisXT® 7.0	7.0	Bitplane Scientific Solutions, Switzerland

3.1.7 Technical devices

Description	**Supplier**
CO_2 Incubator	Thermo scientific
Centrifuge	Universal 32R, Hettich zentrifugen Rotina 380R, Hettich zentrifugen Mikro 200, Hettich zentrifugen
ChemiDOC, Imaging System	Bio RAD
FluorImager	Typhoon 9400, Molecular Dynamics, Germany
Light Microscopy	LEITZ DM IL, Leica, Germany
Florescence Microscopy	Imager.Z1, Zeizz, Germany
Confocal Microscopy	TCS SP5 Leica Microsystems, Wetzlar, Germany
Flow cytometry system, Galaxy	DAKO
iBlot® Dry Blotting System	Introgen, Life Technologies, Germany
Spectrophotometer, Multiskan Ascent	Thermo Electron Corporation
X-ray machine, Isovolt 320 HS	General Electric, Pantak/Seifert
SDS-PAGE equipment	Bio-Rad, USA
pH meter	WTW GmbH, Germany
Imaging scanner	GE Healthcare, USA
Laminar flow cabinet	Heraeus, Germany

3.2Methods

3.2.1 Cell lines

The human CRC cell lines LS180, RKO, SW48, HCT15, HCT116 and Colo320DM were obtained from ATCC (LGC Standards, Wesel, Germany). LS180, RKO and SW48 were kept in MEM (Invitrogen) supplemented with 15% FBS, 1% essential amino acids and antibiotics. HCT15, HCT116 and Colo320DM were kept in RPMI (Invitrogen) supplemented with 10% FBS plus antibiotics. U2OS and A549 cells harboring DSB repair reporter substrates (DR-GFP) were grown as a monolayer in McCoy's 5A medium supplemented with 10% fetal bovine serum (FBS) and antibiotics. Cells were cultivated at 37 °C in 5% CO2. Irradiation was done usig the RS320 X-Ray machine by XStrahl Ltd. at 300 kV, 10 mA, dose rate 0,9 Gy/min.

3.2.2 Transfection with siRNA

Cells were seeded in 6-well plates and incubated for 24 hours, obtaining a 70–80% confluent monolayer. Cells were then washed in HBSS and OptiMEM (both Gibco), and subsequently incubated with transfection reagent for 4 hours. We used 500 ul OptiMEM with 40 nM siRNA and 6 ul Lipofectamine RNAiMAX (Invitrogen) as a transfection reagent. To downregulate ARID1B, we established a mix of two siRNAs (Ambion s199170, Ambion s199168,) at 40 nM each for optimal efficiency. To downregulate ARID1A, we ues siRNAs (Ambion s15786) at 40 nM for optimal efficiency. As controls, we used non-targeting siRNA (Ambion 4390843) as well as lipofectamin alone. After 4 hours of incubation with the transfection reagent, 500 µl of culture medium with double FBS was

added and cells incubated for 48 hours until harvesting for further experiments. Expression of targeted proteins was regularly checked by western blot.

3.2.3 Immunoblotting

Western blots were performed with anti-ARID1A (CellSignalling, 12354P), anti-ARID1B (LS-Bio, LS-C382223) and anti-GAPDH (Abcam, ab8245). The secondary antibodies were HRP-linked antibodies raised against mouse or rabbit IgG (GE Healthcare, NA931V and NA934V) and Alexa Fluor 488-linked antibodies against mouse (Invitrogen A11029).

3.2.4 Clonogenic survival assay

48 hours after transfection, cells were harvested and plated in triplicates in 9,6 cm2 6-well culture dishes. After 4–6 hours in culture, cells were irradiated and subsequently incubated for 10–14 days at 37 °C in 5% CO2. Cells were fixed and stained with 96% ethanol, 15% Giemsa and destained with distilled water. Colonies consisting of at least 50 cells were counted. Surviving fractions after the indicated treatments are presented as a fraction of colony formation of irradiated to non-irradiated cells.

SF = number of colonies after IR/number of colonies in non-irradiated cells

3.2.5 Immunofluorescence (IF) assay.

In IF assay, we cultured cells directly onto coverslips. To specifically rate the scores of IR-mediated repair foci at G2-phase, cells at exponential growth phase were subject to 30-min

pulse-labeling using EdU (10 uM) immediately prior to irradiation. Subsequently, cells were subject to 15-min 2% paraformaldehyde (PFA) fixation at specific time points and PBS (0.01 M phosphate buffer, 0.14 M NaCl, pH 7.0) washing. Later, we processed cells by 5-min permeabilization within the solution containing 0.5% Triton X-100, 50 mM EDTA and 100 mM Tris–HCl. After PBS washing, we blocked cells with PBG buffer (consisting of 0.5% BSA fraction V and 0.2% Gelatin dissolved within PBS) under 4◦C overnight. To detect RAD51, we adopted the mouse anti-RAD51 monoclonal antibody (mab, clone 14B4, GeneTex; diluted with PBG at 1/400). To detect y-H2AX, we adopted the mouse anti- y-H2AX mab (clone 3F2, Abcam; diluted at 1/400). Cells were subject to 1.5-h incubation with primary antibodies, followed by PBS rinsing for 5 min thrice. Later, secondary antibody including anti-rabbit Alexa Fluor 568-labeled IgG or anti-mouse Alexa Fluor 488-labeled IgG (ThermoFisher Scientific) was added to further incubate cells for another 1 h. Thereafter, we treated slides using Click-IT staining kit (ThermoFisher Scientific) in line with specific protocols with EdU. At last, we rinsed coverslips by PBS, followed by 15-min incubation with DAPI solution (0.1 ug/ml) as well as embedding into the Prolong Gold Antifade mounting medium (ThermoFisher Scientific). For detecting the repair foci, we used the Leica TCS SP5 confocal microscope to scan those processed slides. Spillover out of diverse channels was eliminated by sequential scanning. To compare different experiments, we maintained the constant detector settings in identical antibody batch.

3.2.6 Analysis of digital images

To analyze those 3D image stacks obtained, we utilized Spots and Split Spots module in Imaris 8.0 software (Bitplane) or Cell module in Imaris 8.0-9.3 software for determining the number of foci. We maintained the constant threshold of grayscale value to separate background from signal within diverse experiments using identical antibody batch, for the sake of ensuring that the two datasets were comparable. We deemed objects that had the lowest diameter of 0.5 um following thresholding to be the foci. We calculated about 150 cells at each time point and dose. To analyze the cell cycle of DSB repair foci within G2-phase EdU- cells, we acquired data by Imaris software and analyzed them using the Orange graphic software.

3.2.7 Quantitative image-based cytometry (QIBC) conducted to evaluate DSB repair foci dependent on cell cycle

RAD51 and H2AX foci were evaluated depending on cell cycle phase, following the aforementioned IF processing through high-throughput slide-scanning analysis using AxioScan.Z1 platform (Zeiss). EdU (10 uM) was used to label cells for a 30-min period, followed by irradiation at increasing X-ray doses. Following irradiation, cells were fixed at specific time points, placed them onto coverslips and scanned the areas of 4 × 4 mm. We obtained 10 000–20 000 cells according to the cell density of the screened area. Thereafter, we analyzed cell fragmentation on the images (Imaris), so as to offer nuclear fluorescence intensity information for EdU and DAPI staining, and for RAD51- and H2AX focus number. We transformed the Imaris software-produced data into the format for flow

cytometric analysis (Kaluza, Beckman Coulter); besides, we also generated data in relevant figures. Only cells in the G2/M-phase during irradiation and post-irradiation incubation were analyzed.

3.2.8 HRR functional analysis on the I-SceI-induced DSBs based on GFP reporter cells

For experiments, 2×10^6 A549 DR-GFP and U2OS DR-GFP cells were firstly knockdown ARID1A expression by siRNA and then transfection by nucleofection (Lonza) with 2 ug of the I- SceI expressing plasmid, pCMV3xNLS-I-SceI. After 24 of transfection, we harvested cells through trypsinization and then conducted flow cytometry (Gallios, Beckman Coulter) to analyze GFP level with the 488-nm argon laser. The 510BP filter was utilized to collect GFP emission at FL1. Besides, we determined repair event frequency as GFP-positive cell frequency. Replicate cultures containing GFP-expressing pEGFP-N1 construct (1 ug/1 × 106 cells) were adopted to determine transfection efficiency in every assay. We just analyzed experiments whose transfection efficiency was more than 80%.

3.2.9 Ethics statement

All patients provided written informed consent for their information to be stored and used in the MianYang Fulin hospital database. Study approval was obtained from the independent ethics committee at the MianYang Fulin hospital, China (IRB ID: TJ-C20210701). The study was undertaken in accordance with the ethical standards of the World Medical Association Declaration of Helsinki. All excised samples were obtained

from tumor tissues within 1 h after surgery. For each specimen, half sent to lab for ATP-TCA Test, and the remainder was fixed with formalin for immunohistochemistry (IHC).

3.2.10 Patient information and tissue specimens

This study was conducted using a total of 41 archived paraffin-embedded primary CRC samples. All patients underwent resection of primary tumors between July 2021 and January 2022 at MianYang Fulin hospital, China. All procedures performed with these biopsies were performed at the Mian Yang Fulin hospital, China. None of the patients had preoperative chemotherapy or preoperative radiotherapy. The staging of tumors was determined according to the American Joint Committee on Cancer (AJCC) TNM staging system. Each tumor was pathologically classified according to the World Health Organization classification criteria.

3.2.11 IHC and scoring

We analyzed ARID1A expression within 41 primary CRC tissues by means of IHC according to previous description. In brief, we processed each tissue section by deparaffinage, rehydration, blocking of endogenous peroxide and antigen retrieval, followed by overnight incubation using ARID1A (PSG3):sc-32761 antibody (Santa Cruz Biotechnology, Inc., CA, United States) under 4℃. Later, sections were rinsed by PBS contained within Tween-20, followed by 30-min incubation using anti-mouse secondary antibody and subsequently incubation using the streptavidin-HRP complex. Afterwards, diaminobenzidine tetrahydrochloride was adopted for color developing of sections,

followed by hematoxylin counterstaining. All immunostained sections were examined and scored by 2 reviewers blinded to pathological and clinical data of patients. We examined 1000 or more cancer cells in every slide upon the thresholds of staining degree and stained cell percentage. We scored positive cell percentages below, 0, ≤10%; 1, 10%-25%; 2, 25%-50%; 3, 50%-75%; and 4, >75%. We deemed nuclear immunoreactivity to be positive expression. Besides, we rated staining degree below, 0, 1, 2 and 3 indicating negative, weak, moderate, and strong staining, separately. We classified those immunostained sections as 2 groups, positive (overall score≥1) and negative (overall score=0) ARID1A expression groups.

3.2.12 ATP-TCA

We conducted ATP-TCA according as previously described[89]. We cut solid tumor tissues into pieces before overnight collagenase digestion (1.5 mg/ml, Sigma, Poole, UK; C8051). Later, Ficoll-Hypaque (Sigma; 1077-1) was adopted to purify samples for removing excessive debris as well as red blood cells, followed by resuspension within the complete medium without serum (CAM; DCS Innovative Diagnostik Systeme, Hamburg, Germany) that contained gentamicin (Sigma), penicillin–streptomycin (Sigma), metronidazole (Rhône Poulenc Rorer, Eastbourne, UK) along with amphotericin B (Sigma). Thereafter, we determined cell number and evaluated cell viability through the Trypan blue exclusion approach. The final cell suspension was made up to a concentration of 200000

cells/ml for solid tumors and 100000 cells/ml for malignant effusions. Round-bottomed polypropylene 96-well plates (Corning-Costar, High Wycombe, UK) were prepared with CAM and cytotoxic drugs at six dilutions (6.25–200%) of the test drug concentration (TDC) in triplicate. The TDC for each drug has previously been calculated from pharmacokinetic and response data. The drugs were stored appropriately and made up according to the manufacturer's instructions. Dilutions were prepared in the plates from freshly made up 800% TDC drug solutions. Combinations of drugs were made by adding both drugs each at their 800% TDC. Two endogenous reference rows were prepared in every plate, including the medium only (MO) of CAM with no drug, and the maximum inhibitor (MI) killing the whole cells that gave the zero ATP count. At 6-day post-incubation under 37°C, 5% CO2 and 100% humidity conditions, we used the detergent-based Tumor Cell Extraction Reagent (DCS Innovative Diagnostik Systeme) to lyse cells, and determined ATP level in every well with the microplate luminometer by luciferin–luciferase system (MPLX; Berthold, Pforzheim, Germany).

3.2.13 Statistical analysis

All statistical analyses were performed using SPSS 14.0 statistical software, or SAS software version 9.4, SAS/STAT 15.1 (SAS-Institute, Cary, NC). A p value < 0.05 was considered statistically significant in all cases. The association between ARID1A expression and the clinicopathological characteristics was analyzed by χ 2 test or Kruskal-

Wallis H test based on the type of data. The interaction between ARID1B knock down and the radiation dose response or ATRi with $ARID1A^{+}$/ $ARID1A^{-}$ and the radiation dose response was described as a slope modifying effect of the linear term of the linear-quadratic model. ANOVA was used to calculate the statistical significance between two groups at certain radiation dose.

4. Results

4.1 ARID1B knockdown and its effect on radiosensitivity

CRC cell lines with wild type ARID1A (HCT15, HCT116, and Colo320) and mutant ARID1A (LS180, RKO, and SW48) were used in the present study. The expression of ARID1A was examined in all cell lines by immunoblotting (Figure 4.1). The results clearly show that cells with mutant ARID1A, in comparison to CRC with wild-type ARID1A have no detectable expression of ARID1A protein and thus considered as ARID1A deficient ($ARID1A^-$) and proficient ($ARID1A^+$).

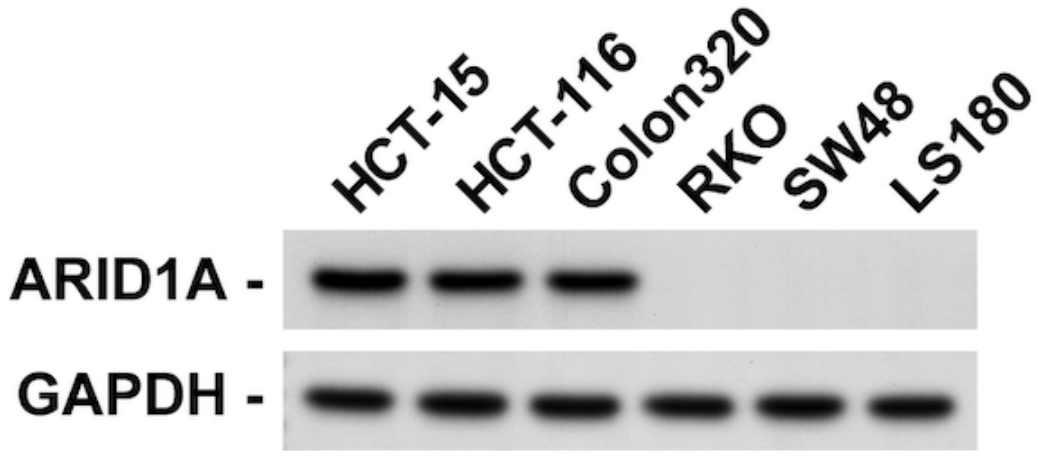

Figure 4.1 Western blot results of $ARID1A^+$ and $ARID1A^-$ CRC cell lines

The radiosensitivity was evaluated in all cell lines by measuring the clonogenic survival fraction after irradiation with 2 Gy (SF2). Slightly lower SF2 values were found

in ARID1A$^-$ CRC cells compared with ARID1A$^+$ CRC cells (P>0.05), as shown in Table 1.

Table 1: The radiosensitivity of ARID1A$^+$/ ARID1A$^-$ colon cancer cell lines.

	ARID1A +			ARID1A -			
	HCT15	HCT116	Colon320	RKO	SW48	LS180	P_1
SF2	0.39 ± 0.019	0.38 ± 0.021	0.4±0.042	0.36 ± 0.018	0.35 ± 0.019	0.35 ± 0.058	>0.05

SF2: survival fraction in 2Gy. P_1: ANOVA was used to calculate the statistical significance between groups, N=3.

In addition, the effect of siRNA targeting ARID1B, a mutually exclusive homolog of ARID1A in the SWI/SNF complex, on cell viability was evaluated in ARID1A$^+$ and ARID1A$^-$ cells by colony formation assay. For this purpose, cells were transfected for 48 h, seeded for colony formation and irradiated 4 h later with doses from 0 to 6 Gy. Transfection of the cells with siRNA targeting ARID1B significantly reduced the expression of ARID1B to 55 ± 9.1% compared to the non-transfected cells (Figure 4.1A). As a result, ARID1B knockdown led to a selective and significant reduction of the viability after irradiation of CRC cells harboring ARID1A mutation (P<0.05) (Figure 4.1B) (Table 2), but not of ARID1A$^+$ cell lines.

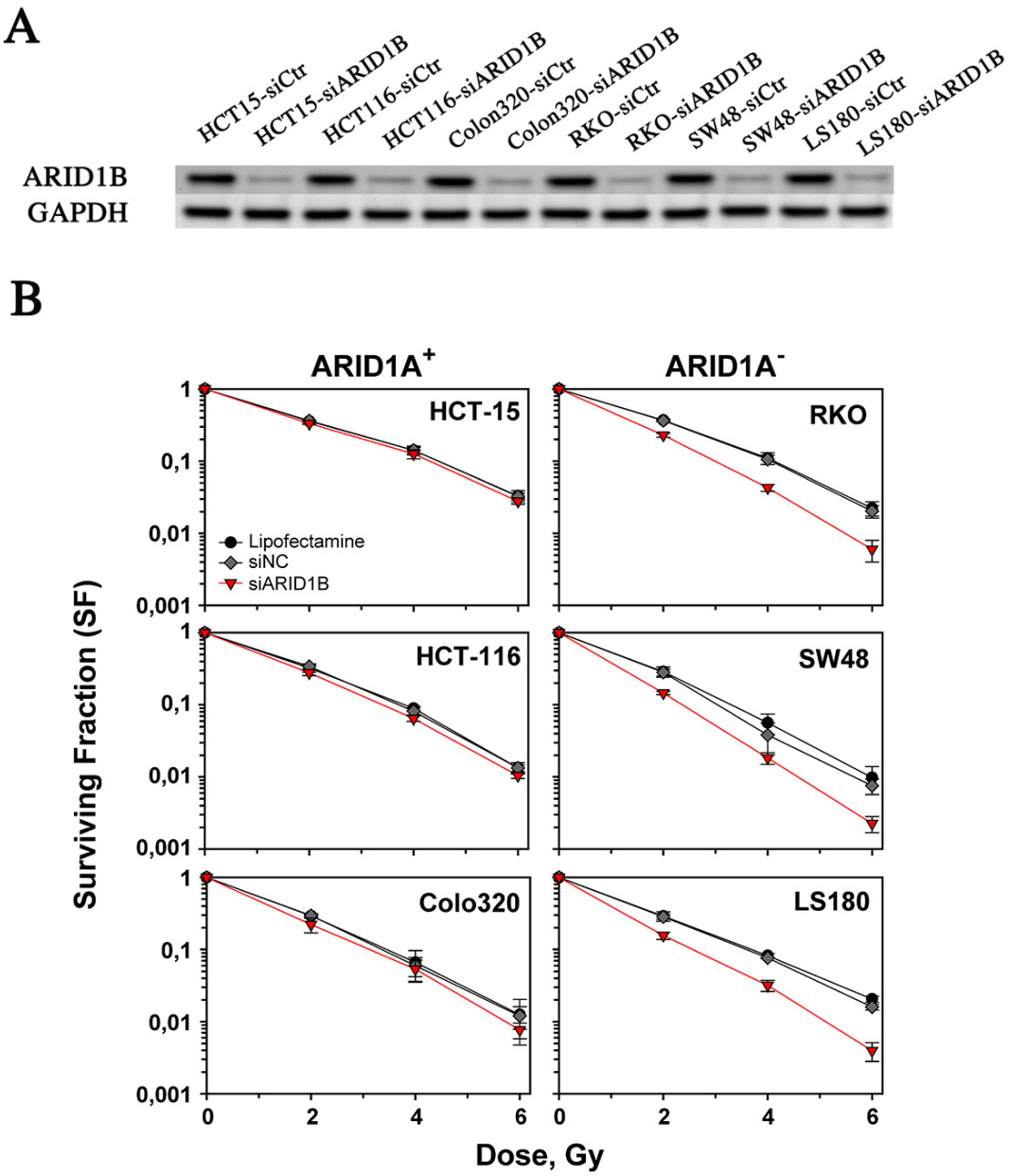

Figure 4.2 ARID1A/ARID1B synthetic lethality on radiosensitivity A: Western blot results of ARID1A^{+} and ARID1A^{-} CRC cell lines, ARID1B knockdown and ARID1A knockdown of our CRC cell lines; B: Effect of ARID1B knockdown on radiosensitivity. Representative results of 4 independent experiments are shown. Statistically significant differences compared with corresponding control cells. P values indicate the results from the ANOVA F-test.

Table 2: The radiosensitivity of ARID1B knock down on ARID1A^{+}/ ARID1A^{-} colon cancer cell lines.

	ARID1A +			ARID1A -			
	HCT15	HCT116	Colon320	RKO	SW48	LS180	P[1]
Control SF2	0.39 ± 0.019	0.38±0.021	0.4±0.042	0.36 ±0.018	0.35±0.019	0.35±0.058	>0.05
ARID1B KD SF2	0.36 ± 0.027	0.36±0.03	0.37±0.045	0.30 ±0.016	0.26±0.013	0.30±0.011	<0.05

SF2: survival fraction in 2Gy. P[1]: ANOVA was used to calculate the statistical significance between groups, N=3.

4.2 ARID1A-directed synthetic lethality concepts on radiosensitivity

Although ARID1B knockdown increased the radiation sensitivity of ARID1A^{-} CRC cells, currently no ARID1B inhibitors are available. Thus, the translation of these results into clinical practice is limited. However, several studies showed that ARID1A-dependent synthetic lethality can be obtained through diverse molecular mechanisms [79; 90; 91]. Some studies suggested that PARP, AURKA and ATR and inhibitors can also be synthetic lethal partner for ARID1A deficient cancer cells [79; 82; 92].

4.2.1 Impact of ARID1A/ PARPi synthetic lethality on radiosensitivity

Usually, loss of ARID1A compromises DNA damage repair, and the induced DNA damage burdens may increase the dependence on PARP dependent DNA repair pathways in cancer cells to maintain genome integrity which render cells susceptible to PARP inhibitor therapy [93]. Therefore, two PARP inhibitors, Olaparib and AZD2461, were used to evaluate the effect on the synthetic lethality of PARP inhibition and ARID1A deficiency in ARID1A^{+} and ARID1A^{-} colon cancer cell lines. ARID1A^{+} and ARID1A^{-} CRC cells were treated with different concentrations of PARP inhibitors (0-5 μM for Olaparib and 0-5 nM for AZD2461) and the respective concentration for half maximal reduction of the viability (IC50) was measured in all cell lines and PARP inhibitors (Figure 4.3) (Table 3). IC50 values defined as the concentration resulting in 50% inhibition of colony formation were estimated from nonlinear regression analysis of concentration–response curves obtained. Curve fitting was performed using the GraphPad Prism computer program (version 9.0). As a result, ARID1A^{-}cell lines were more sensitive to both PARP inhibitors, compared with ARID1A^{+} cell lines.

A

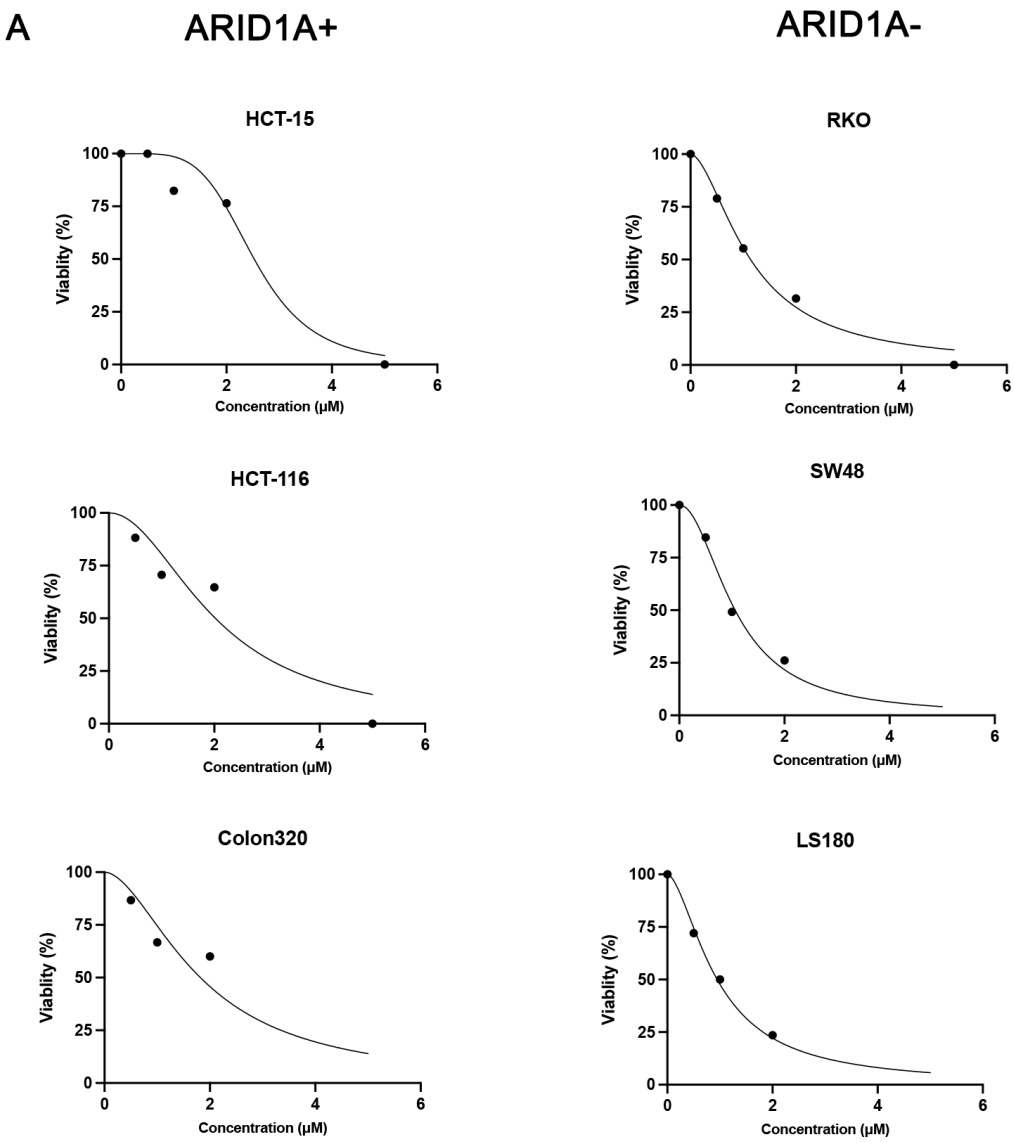
ARID1A+
ARID1A-
HCT-15
RKO
HCT-116
SW48
Colon320
LS180
Viablity (%)
Concentration (μM)
0
25
50
75
100
0
2
4
6

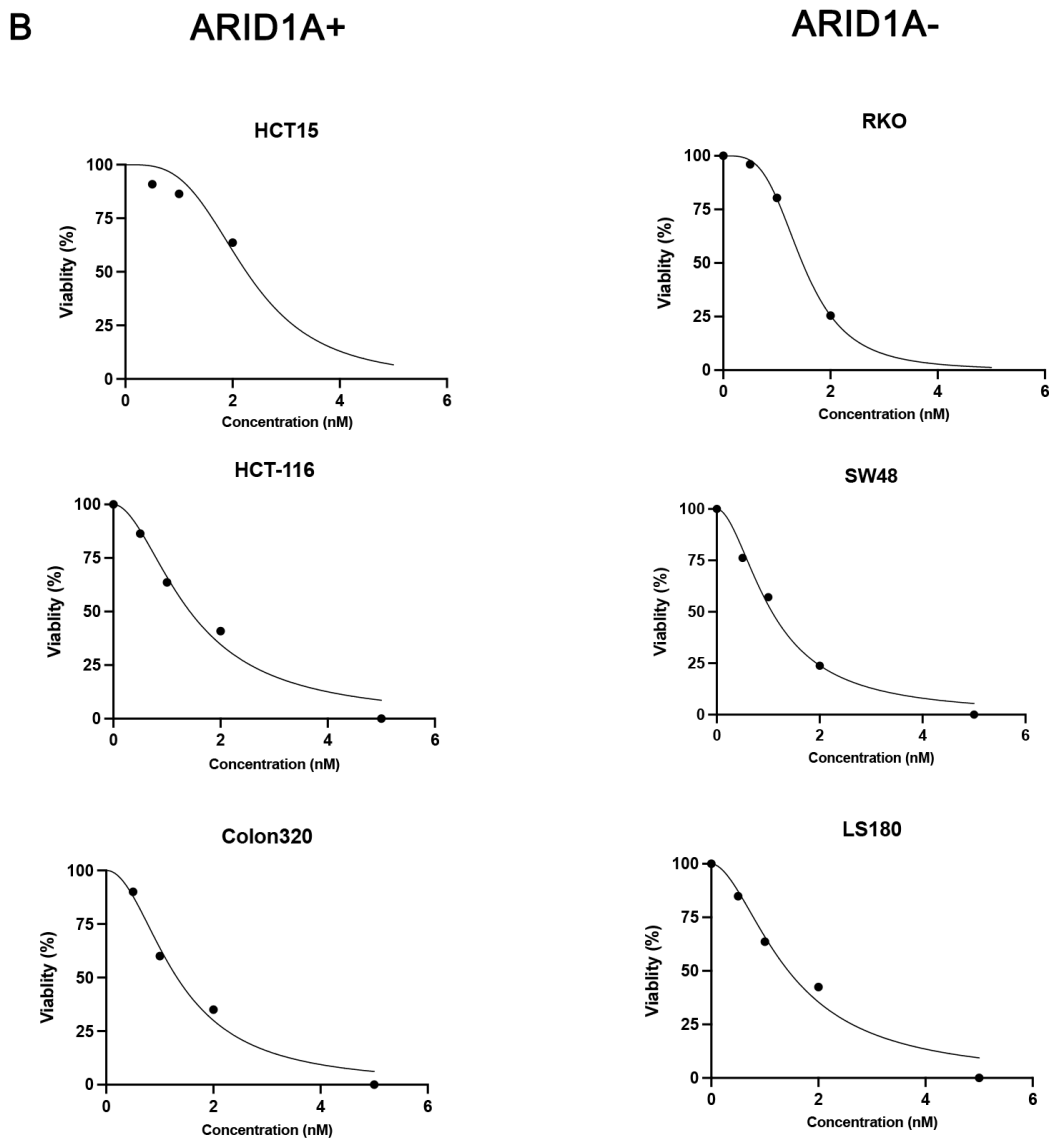

Figure 4.3 The IC50 of ARID1A$^+$ and ARID1A$^-$ CRC cell lines to PARPi were calculated using the colony formation assay. A: IC50 of PARPi (Olaprib) in ARID1A$^+$ and ARID1A$^-$ CRC cell lines; B A: IC50 of PARPi (AZD2461) in ARID1A$^+$ and ARID1A$^-$ CRC cell lines; Dose-response curves and IC50 were calculated with GraphPad Prism software; Representative results of 3 independent experiments are shown.

Table 3: IC50 values of PARP inhibitors in ARID1A+and ARID1A- colon cancer cell lines.

	ARID1A +			ARID1A -			P[1]
	HCT15	HCT116	Colon320	SW48	RKO	LS180	
AZD2461 (nM)	2±0.73	1.5±1.1	1.4±0.54	1.3±0.3	1.1±0.51	1.0±0.4	<0.05
Olaparib (μM)	2.9±1.4	2.0±1.09	1.8±0.83	1.0±0.9	1.2±0.67	1.0±0.57	<0.05

P[1]: ANOVA was used to calculate the statistical significance between groups, N=3.

For the evaluation of the radiosensitization effect, cells were irradiated with 2 Gy after pre-treatment with PARPi for 1 h and its effect on viability was measured by colony formation assay. Both PARP inhibitors led to a slight but not significant reduction of the viability after the irradiation of $ARID1A^{+}$ CRC cells. In comparison, a significant decrease in the viability of $ARID1A^{-}$ CRC cells were evident (Figure 4.4A and 4.2B).

A

ARID1A+

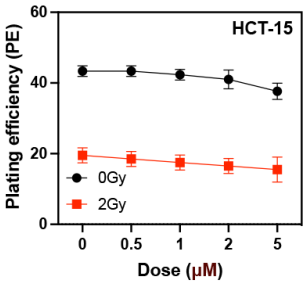

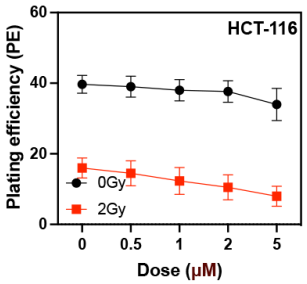

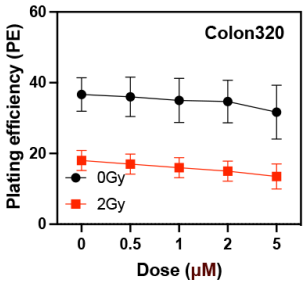

ARID1A-

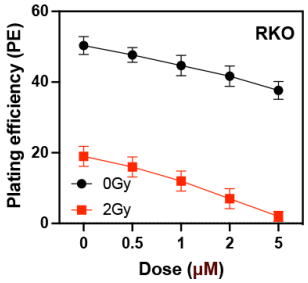

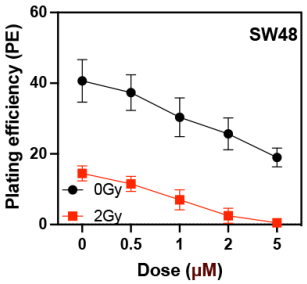

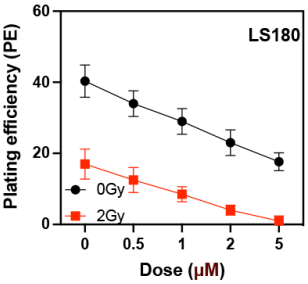

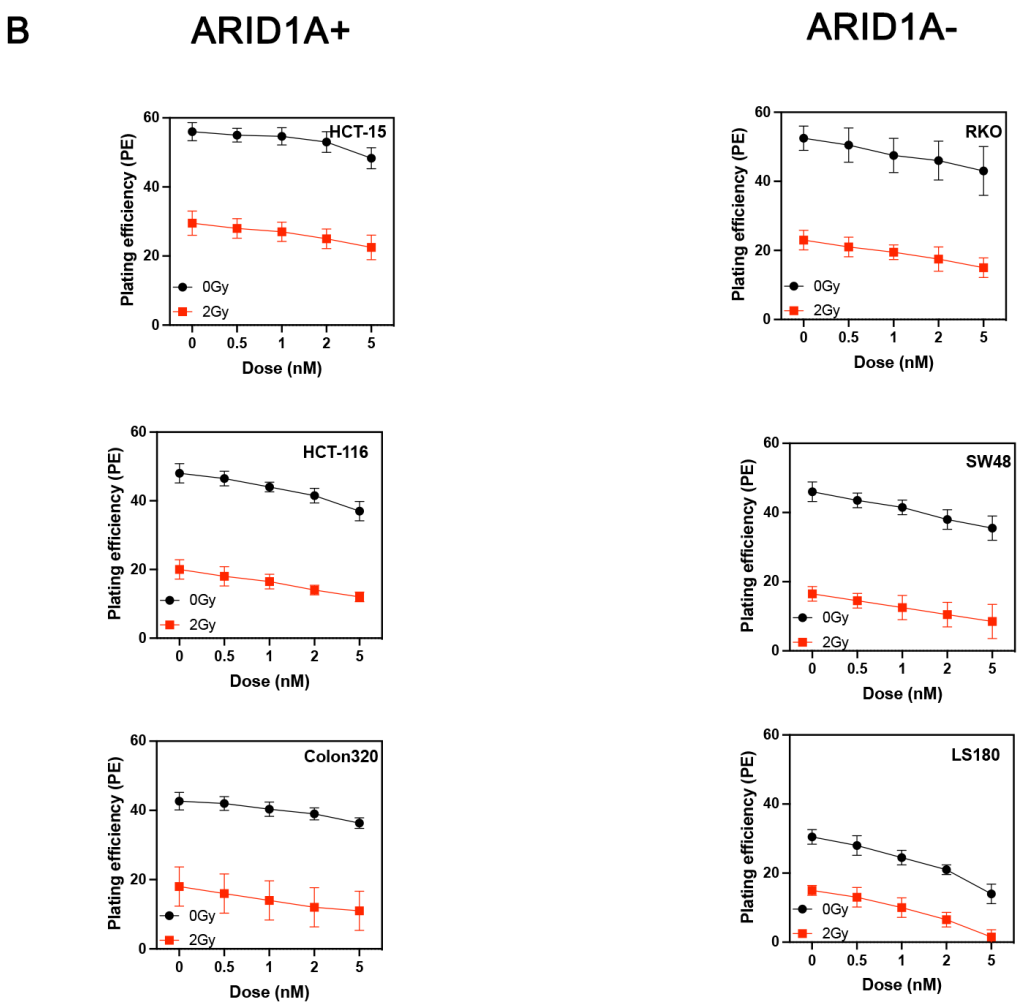

Figure 4.4 ARID1A/ PARPi synthetic lethality with 2Gy radiation; A: PARPi (Olaprib) results of ARID1A^{+} and ARID1A^{-} CRC cell lines; B: PARPi (AZD2461) results of ARID1A^{+} and ARID1A^{-} CRC cell lines. Representative results of 3 independent experiments are shown.

In order to better explore the synthetic lethal effect of ARID1A$^-$ and PARP inhibitors, we selected the IC50 concentration of ARID1A$^-$ cells for calculation of the survival fraction (1 μM for Olaprib and 1 nM for AZD2561). As a result, the effect of both PARP inhibitors was significantly higher in ARID1A$^-$ cell lines compared to wild type cells ($P<0.05$) (Table 4).

Table 4: The radiosensitivity of PARP inhibitors on ARID1A$^+$ and ARID1A$^-$ CRC lines.

		ARID1A +			ARID1A -			
		HCT15	HCT116	Colon320	RKO	SW48	LS180	P[1]
Control	SF2	0.39 ± 0.019	0.38±0.021	0.40±0.042	0.36 ±0.018	0.35±0.019	0.35±0.058	>0.05
Olaprib (1 μM)	SF2	0.37±0.018	0.35±0.02	0.41±0.017	0.27±0.011	0.25±0.033	0.28±0.031	<0.05
AZD2561 (1 nM)	SF2	0.38±0.022	0.35±0.09	0.31±0.038	0.26±0.032	0.24±0.018	0.27±0.022	<0.05

SF2: survival fraction in 2Gy. P[1]: ANOVA was used to calculate the statistical significance between groups, N=3.

4.2.2 Impact of ARID1A/ AURKAi synthetic lethality on radiosensitivity

Aurora kinases (Aurora A, B, and C) are a family of serine/threonine kinases that play critical roles during mitotic initiation and progression[94]. Overexpression and/or amplification of Aurora A in CRC have been associated with poor prognosis. Recently, the screening of epigenetic drugs revealed that Aurora kinase A (AURKA) inhibitors showed synthetic lethality interaction with ARID1A$^-$, especially in CRC cells [82]. Therefore, the effect of the AURKA inhibitor Alisertib on the viability of ARID1A$^-$ and ARID1A$^+$ CRC cell lines was evaluated. Cells were treated with Alisertib at different concentrations (from 0 to 100 nM) and IC50 values were determined. IC50 values defined as the concentration resulting in 50% inhibition of colony formation were estimated from nonlinear regression analysis of concentration–response curves obtained. Curve fitting was performed using the GraphPad Prism computer program (version 9.0). The IC50 values were significantly lower in ARID1A$^-$ compared with ARID1A$^+$ cell lines (Figure 4.5) (Table 5).

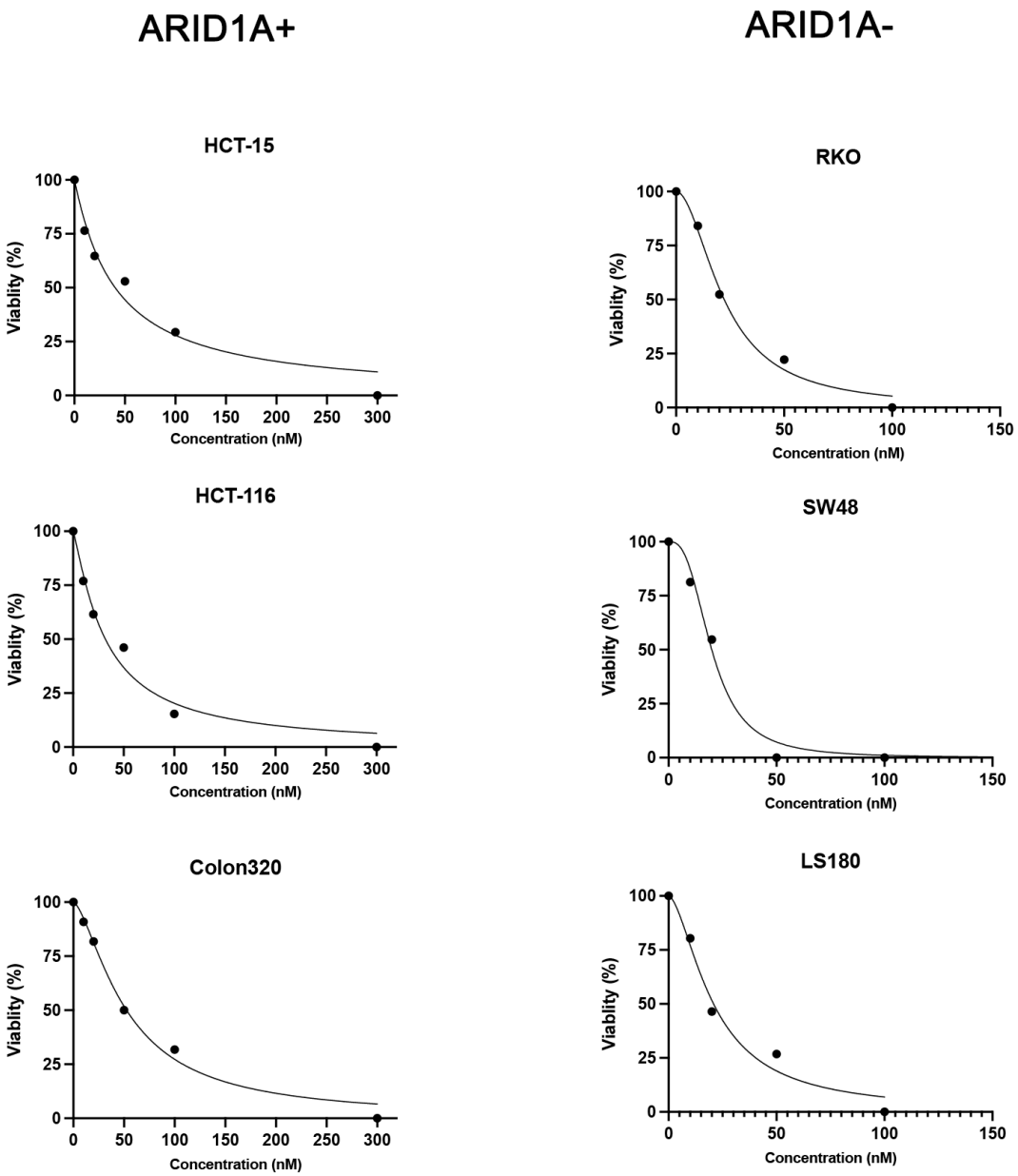

Figure 4.5 The IC50 of ARID1A^{+} and ARID1A^{-} CRC cell lines to AURKAi were calculated using the colony formation assay. Dose-response curves and IC50 were calculated with GraphPad Prism software; Representative results of 3 independent experiments are shown.

Table 5: IC50 values of AURKA inhibitor in ARID1A+ and ARID1A- CRC cell lines.

P1: ANOVA was used to calculate the statistical significance between groups. N=3

	ARID1A +			ARID1A -			P1
	HCT15	HCT116	Colon320	SW48	RKO	LS180	
Alisertib (nM)	40±5.73	30.5±8.13	52±8.21	19±1.6	20±1.2	22±2.2	<0.05

In addition, the effect of AURKAi on radiation induced cell death was determined after the irradiation with 2 Gy. AURKA inhibitor decreased the radiation sensitivity, especially in in ARID1A$^-$ CRC cells (Figure 4.6).

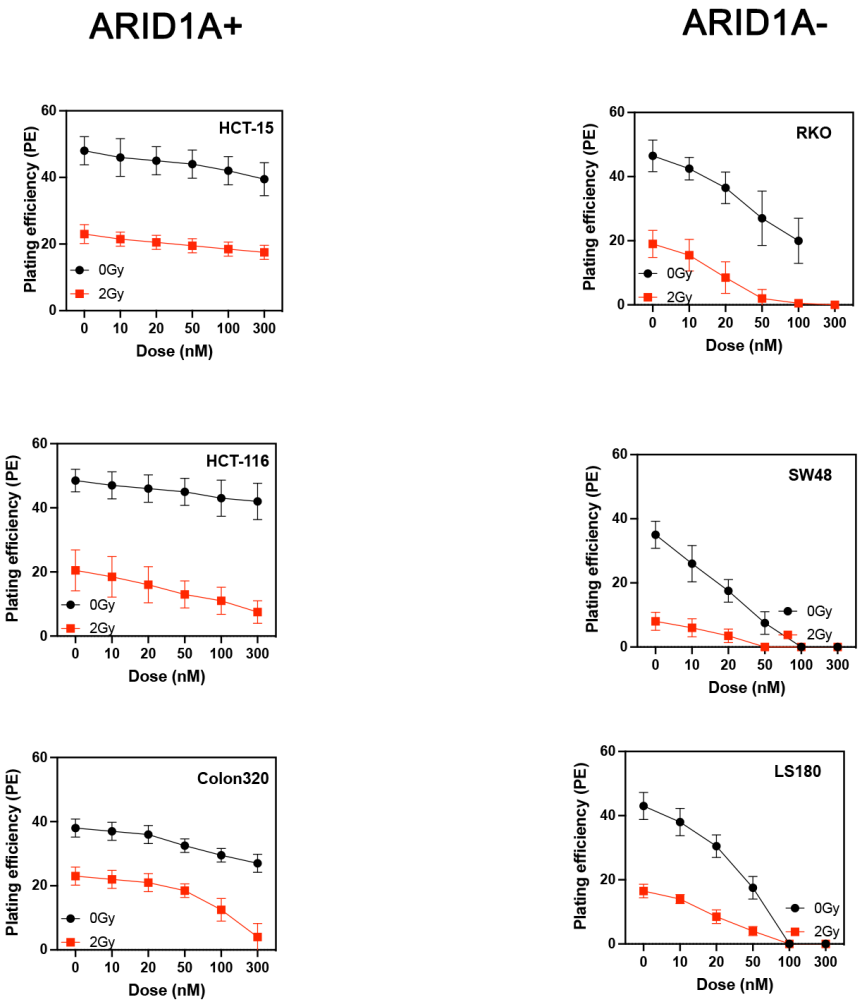

Figure 4.6 ARID1A/ AURKAi synthetic lethality with 2Gy radiation. Representative results of 3 independent experiments are shown.

The IC50 concentration of Alisertib obtained in ARID1A$^-$ cells (20 nM) was chosen for the calculation of the viability to better compare the synthetic lethal effect of the AURKA inhibitor and ARID1A$^-$. The radiosensitization effect of the AURKA inhibitor was significantly higher in ARID1A$^-$ compared to the wild type cell lines (P<0.05) (Table 6) (Figure 4.6).

Table 6: The radiosensitivity of AURKA inhibitor on ARID1A+/ ARID1A- colon cancer cell lines.

		ARID1A +			ARID1A -			
		HCT15	HCT116	Colon320	RKO	SW48	LS180	P[1]
Control	SF2	0.39 ± 0.019	0.38±0.021	0.4±0.042	0.36 ±0.018	0.35±0.019	0.35±0.058	>0.05
Alisertib (20 nM)	SF2	0.38±0.031	0.32±0.02	0.31±0.034	0.26±0.02	0.22±0.013	0.25±0.07	<0.05

SF2: survival fraction in 2Gy. P[1]: ANOVA was used to calculate the statistical significance between groups, N=3.

4.2.3 Impact of ARID1A/ ATRi synthetic lethality on radiosensitivity

Recent studies showed that defects in ARID1A sensitize tumor cells to clinical inhibitors of the DNA damage checkpoint kinase ATR [79]. Therefore, two ATR inhibitors VE821 and VE822 were used to evaluate the synthetic lethality of ATR inhibition and $ARID1A^-$ on CRC cell lines. $ARID1A^+$ and $ARID1A^-$ CRC cell lines were treated with different concentrations of VE821 (0-10 μM) and VE822 (0-100 nM) and the respective IC50 values were determined (Figure 4.7) (Table 7). IC50 values defined as the concentration resulting in 50% inhibition of colony formation were estimated from nonlinear regression analysis of concentration–response curves obtained. Curve fitting was performed using the GraphPad Prism computer program (version 9.0).

A

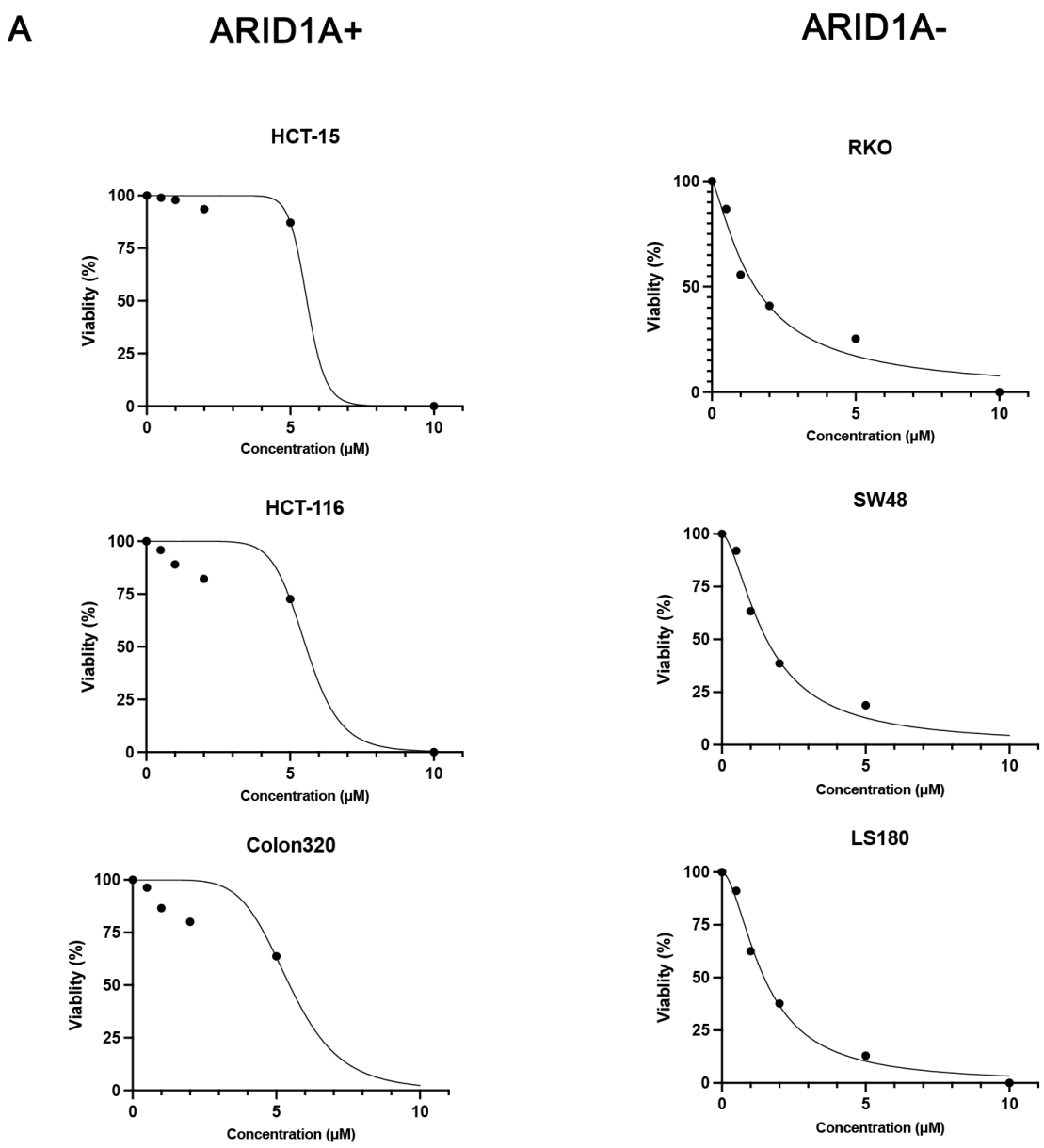
ARID1A+
ARID1A-
HCT-15
RKO
HCT-116
SW48
Colon320
LS180
Viablity (%)
Concentration (μM)
100
75
50
25
0
5
10

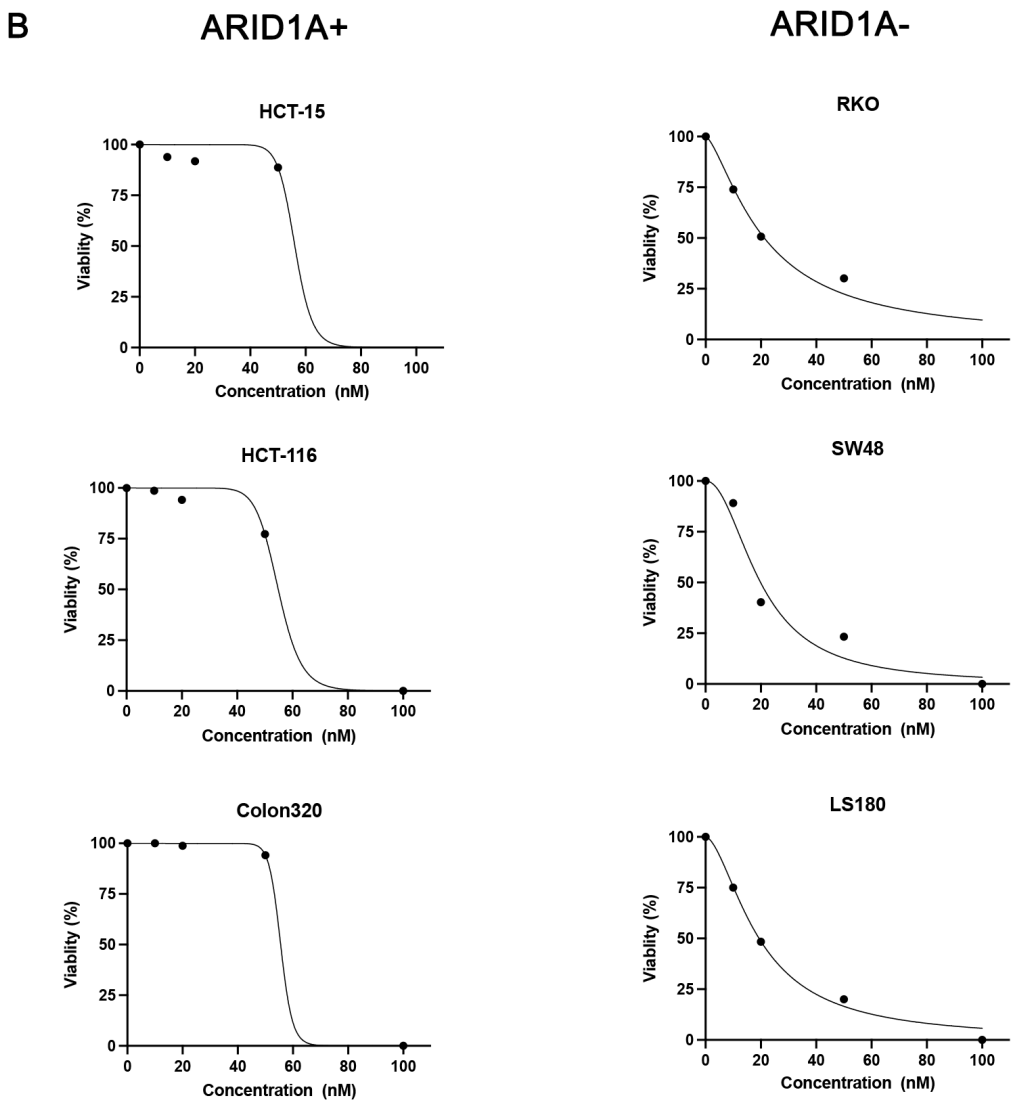

Figure 4.7 The IC50 of ARID1A+ and ARID1A- CRC cell lines to ATRi were calculated using the colony formation assay. A: IC50 of ATRi (VE821) in ARID1A+ and ARID1A- CRC cell lines; B: IC50 of ATRi (VE822) in ARID1A+ and ARID1A- CRC cell lines; Dose-response curves and IC50 were calculated with GraphPad Prism software; Representative results of 5 independent experiments are shown.

Table 7: IC50 values of ATR inhibitors in $ARID1A^+$ and $ARID1A^-$ colon cancer cell lines

	ARID1A +			ARID1A -			P[1]
	HCT15	HCT116	Colon320	SW48	RKO	LS180	
VE822 (nM)	60.95±22.3	56.76±16.7	59.54±18.3	19.0±1.5	23.0±1.3	20.0±2.3	<0.05
VE821 (μM)	6.3±1.3	5.75±2.2	5.3±1.7	1.1±0.3	1.3±0.18	1.4±0.3	<0.05

P[1]: ANOVA was used to calculate the statistical significance between groups, N=5.

Next, the effect of ATRi on radiation sensitivity was determined after the irradiation with 2 Gy. Both ATR inhibitors decreased more efficiently the viability of $ARID1A^-$ CRC cells after irradiation, compared with $ARID1A^+$ CRC cell lines (Figure 4.8)

A

ARID1A+

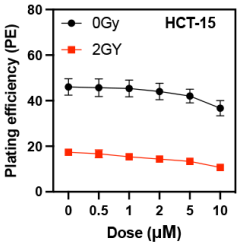

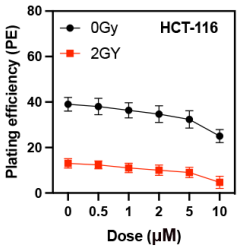

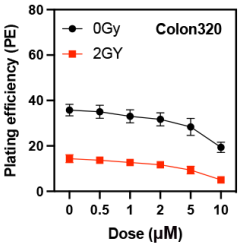

ARID1A-

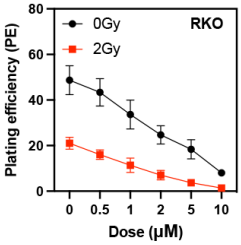

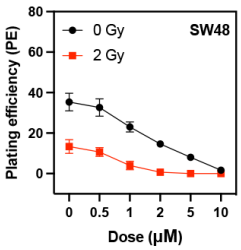

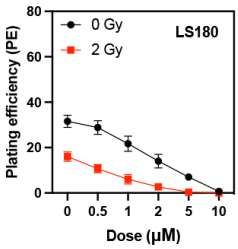

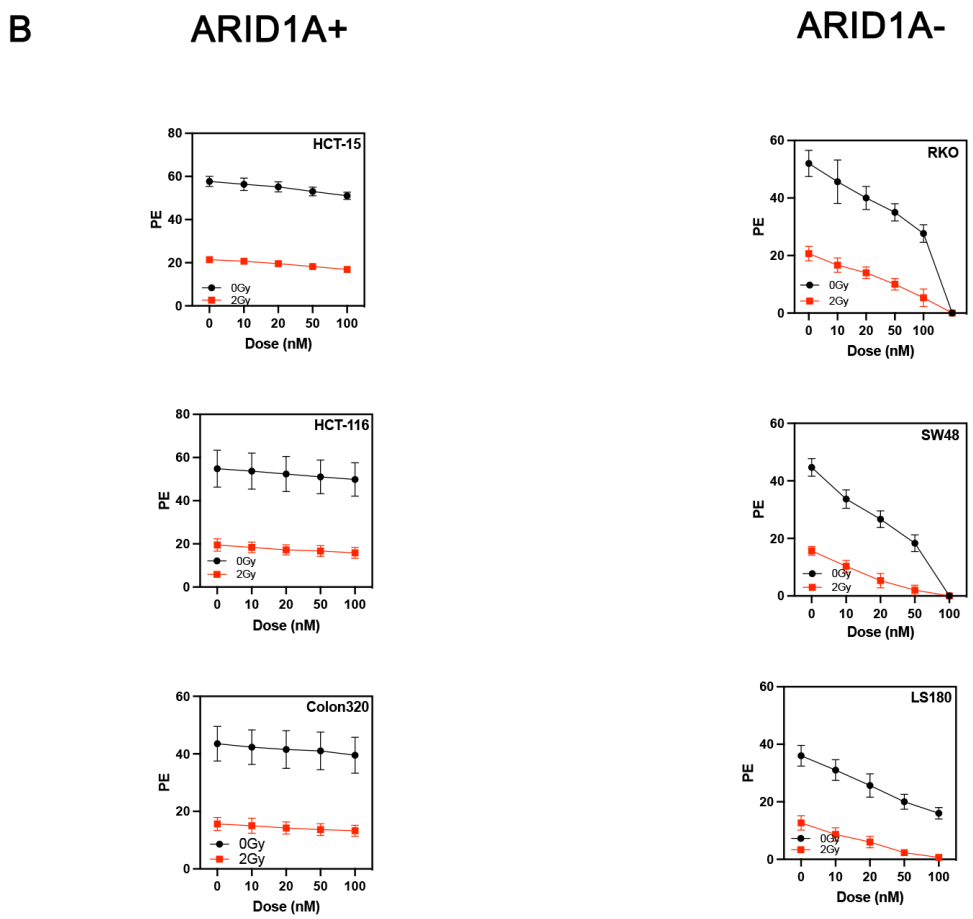

Figure 4.8 ARID1A/ ATRi synthetic lethality with 2Gy radiation; A: ATRi (VE821) results of ARID1A$^+$ and ARID1A$^-$ CRC cell lines; B: ATRi (VE822) results of ARID1A$^+$ and ARID1A$^-$ CRC cell lines. Representative results of 5 independent experiments are shown.

The IC50 concentration of VE821 (1 μM) and VE822 (20 nM) obtained in ARID1A$^-$ cells was used to compare the viability to better compare the synthetic lethal effect of ARID1A$^-$ and ATR inhibitor in both groups of CRC cell lines. Both ATR inhibitors increased the radiosensitivity in ARID1A$^-$ cell lines (P<0.05) (Table 8).

Table 8: The radiosensitivity of ATR inhibitor on ARID1A+/ ARID1A- colon cancer cell lines.

		ARID1A +			ARID1A -			
		HCT15	HCT116	Colon320	RKO	SW48	LS180	P[1]
Control	SF2	0.39 ± 0.019	0.38±0.021	0.4±0.042	0.36 ±0.018	0.35±0.019	0.35±0.058	>0.05
VE821 (1 μM)	SF2	0.35±0.012	0.34±0.023	0.38±0.021	0.28±0.032	0.20±0.045	0.28±0.033	<0.01
VE822 (20 nM)	SF2	0.34±0.055	0.35±0.031	0.37±0.018	0.25±0.017	0.13±0.016	0.22±0.011	<0.001

SF2: survival fraction in 2Gy. P[1]: ANOVA was used to calculate the statistical significance between groups, N=5.

Table 9: The radiosensitivity of ATR inhibitors, PARP inhibitors and AURKA inhibitor on ARID1A+ and ARID1A- colon cancer cell lines

	ARID1A +			ARID1A -			
	HCT15	HCT116	Colon320	RKO	SW48	LS180	P_i
Control SF2	0.39 ± 0.019	0.38±0.021	0.4±0.042	0.36 ±0.018	0.35±0.019	0.35±0.058	>0.05
ARID1B KD SF2	0.36 ± 0.027	0.36±0.03	0.37±0.045	0.30 ±0.016	0.26±0.013	0.30±0.011	<0.05
ATRi							
VE821 (1 μM) SF2	0.35±0.012	0.34±0.023	0.38±0.021	0.28±0.032	0.20±0.045	0.28±0.033	<0.01
VE822 (20 nM) SF2	0.34±0.055	0.35±0.031	0.37±0.018	0.25±0.017	0.13±0.016	0.22±0.011	<0.001
PARPi							
Olaprib (1 μM) SF2	0.37±0.018	0.35±0.02	0.41±0.017	0.27±0.011	0.25±0.033	0.28±0.031	<0.05
AZD2561 (1 nM) SF2	0.38±0.022	0.35±0.09	0.31±0.038	0.26±0.032	0.24±0.018	0.27±0.022	<0.05
AURKAi							
Alisertib (20 nM) SF2	0.38±0.031	0.37±0.02	0.31±0.034	0.26±0.02	0.22±0.013	0.25±0.07	<0.05

SF2: survival fraction in 2Gy. P_i: ANOVA was used to calculate the statistical significance between $ARID1A^+$ and $ARID1A^-$ groups.

Among these inhibitors, the ATRi VE822 was more effective in sensitizing $ARID1A^-$ CRC cell lines and thus were used for further experiments (Table 9). $ARID1A^+$ and $ARID1A^-$ cell lines were pre-treated for 1 h with 20 nM VE822 and irradiated with 0 Gy, 2 Gy, 4 Gy and 6 Gy. The radiosensitising effect of VE822, as quantitated by the dose modifying factor (DMF), was highly significant (P<0,0001) for $ARID1A^-$ cells but not for ARID1A competent cell lines (Figure 4.9 and Table 10).

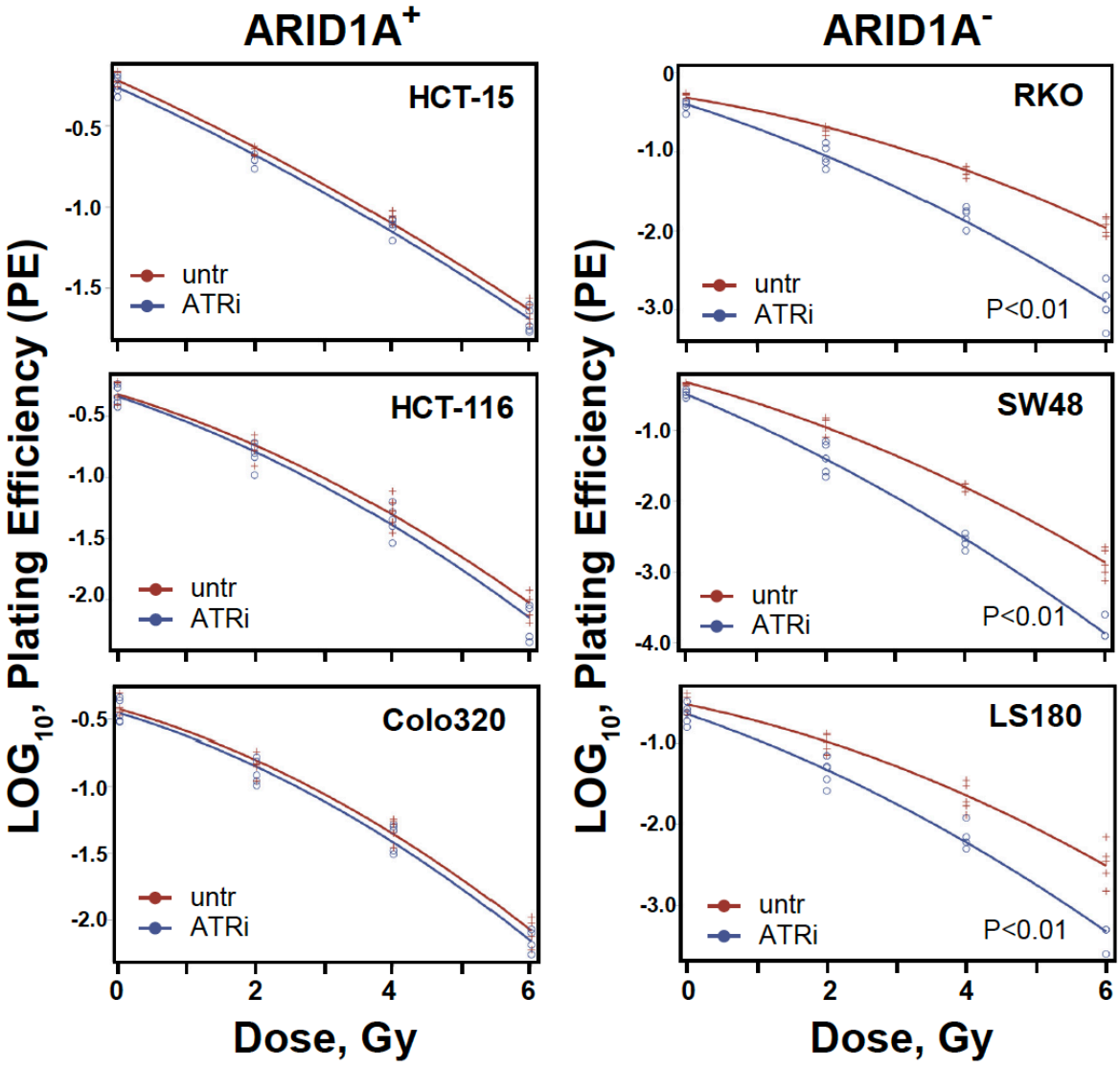

Figure 4.9 Effect of ATRi on radiosensitivity. Effect of ATRi (VE822) on radiosensitivity. ARID1A+ and ARID1A- cell lines were pre-treated for 1 h with 20 nM VE822 and irradiated with 0 Gy, 2 Gy, 4 Gy and 6 Gy. Plating efficiency of sham treated (untr) and VE822 treated (ATRi) cells were plotted as log10 for ARID1A+ and ARID1A- cell lines. Results of 3 independent experiments are shown for CRC cell lines.

Table 10: Radiosensitizing effect of ATRi (VE822) for ARID1A^{+} and ARID1A^{-} colon cancer cell lines from the clonogenic assay.

Cell line	Dose modifying factor (DMF)	P
HCT15 (ARID1A^{-})	0.995 (95% CI:0.959-1.032)	0.78
HCT116 (ARID1A^{-})	0.962 (95% CI:0.894-1.036)	0.30
Colon320 (ARID1A^{-})	0.981(95% CI:0.924-1.041)	0.51
SW48 (ARID1A)	0.726 (95% CI:0.669-0.790)	<0.0001
RKO(ARID1A)	0.721 (95% CI:0.664-0.783)	<0.0001
LS180 (ARID1A)	0.766 (95% CI:0.691-0.849)	<0.0001

Colony data were analyzed using a linear-quadratic model describing the dependence of the logarithm of cellular survival on dose. The interaction between ATRi and the radiation dose response was described as a slope modifying effect of the linear term of the linear-quadratic model. ANOVA was used to calculate the statistical significance between groups, N=5.

In addition, ARID1A^{+} cell lines were also exposed to a concentration of 90 nM V822, but the slope of the linear term of the survival curves did not change ($p>0.4$ for all three ARID1A^{+} cell lines)

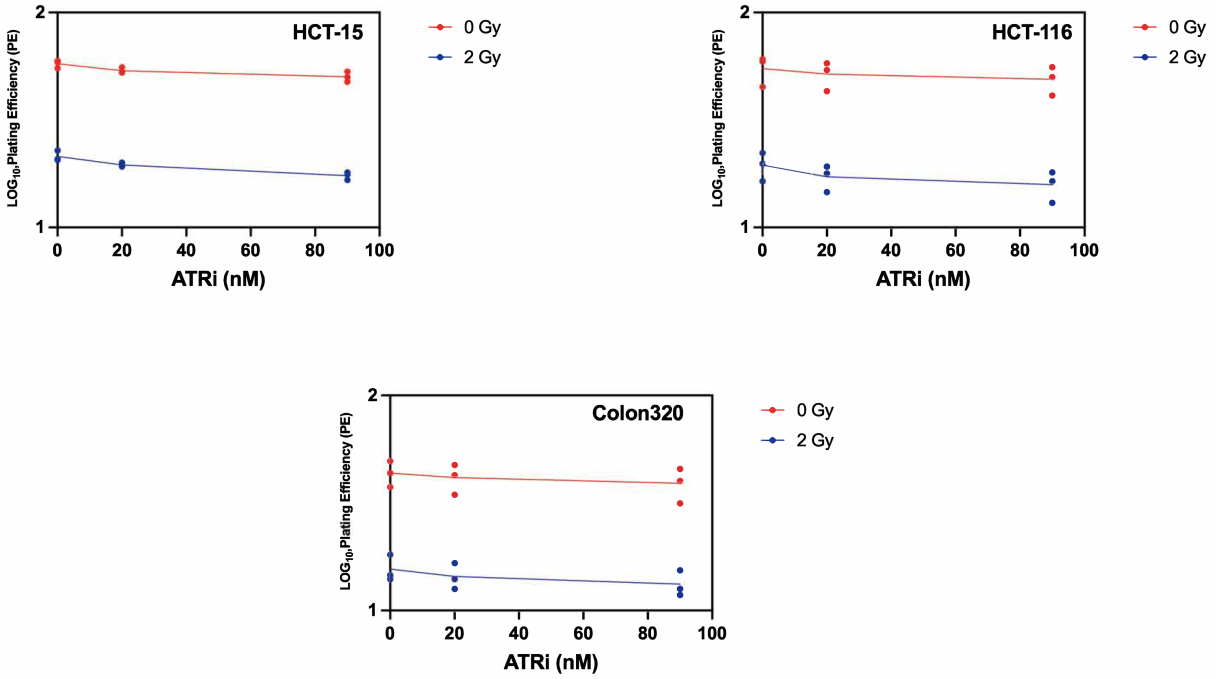

Figure 4.10: Effect of ATR inhibitor (VE822) in ARID1A- cell. Plating efficiency of sham treated (untr) and different concentration of VE822 treated (ATRi) cells were plotted as log10 for ARID1A^{+} cell lines. Results of 3 independent experiments are shown for CRC cell lines.

Because of the mutually exclusive nature of subunits ARID1A and ARID1B, when ARID1A is missing, ARID1B can substitute for ARID1A in SWI/SNF complexes in maintaining DNA accessibility to various nuclear proteins[95]. It was of interest to evaluate

whether inhibition of ATR with VE822 and VE821 increased the radiosensitization effect of ARID1B$^-$ cells. In the present study, colon cancer cells were transfected with siRNA targeting ARID1B for 48 h and treated with either VE822 or VE821 1 h before 2Gy irradiation. The results confirmed the previous results[96], such as the knock-down of ARID1B significantly sensitized ARID1A$^-$ (P<0.01) but not ARID1A$^+$ CRC cell lines. In addition, the combined treatment ATRi with ARID1B knock-down further increased the radiosensitization effect in ARID1A$^-$ CRC cell lines (Figure 4.11). Results also show that VE822 has better radiosensitivity in ARID1A$^-$ CRC cell lines. Overall, these results showed that ARID1A$^-$ CRC cell lines were more sensitive to the single as well as the combined treatment with siARID1B and ATRi.

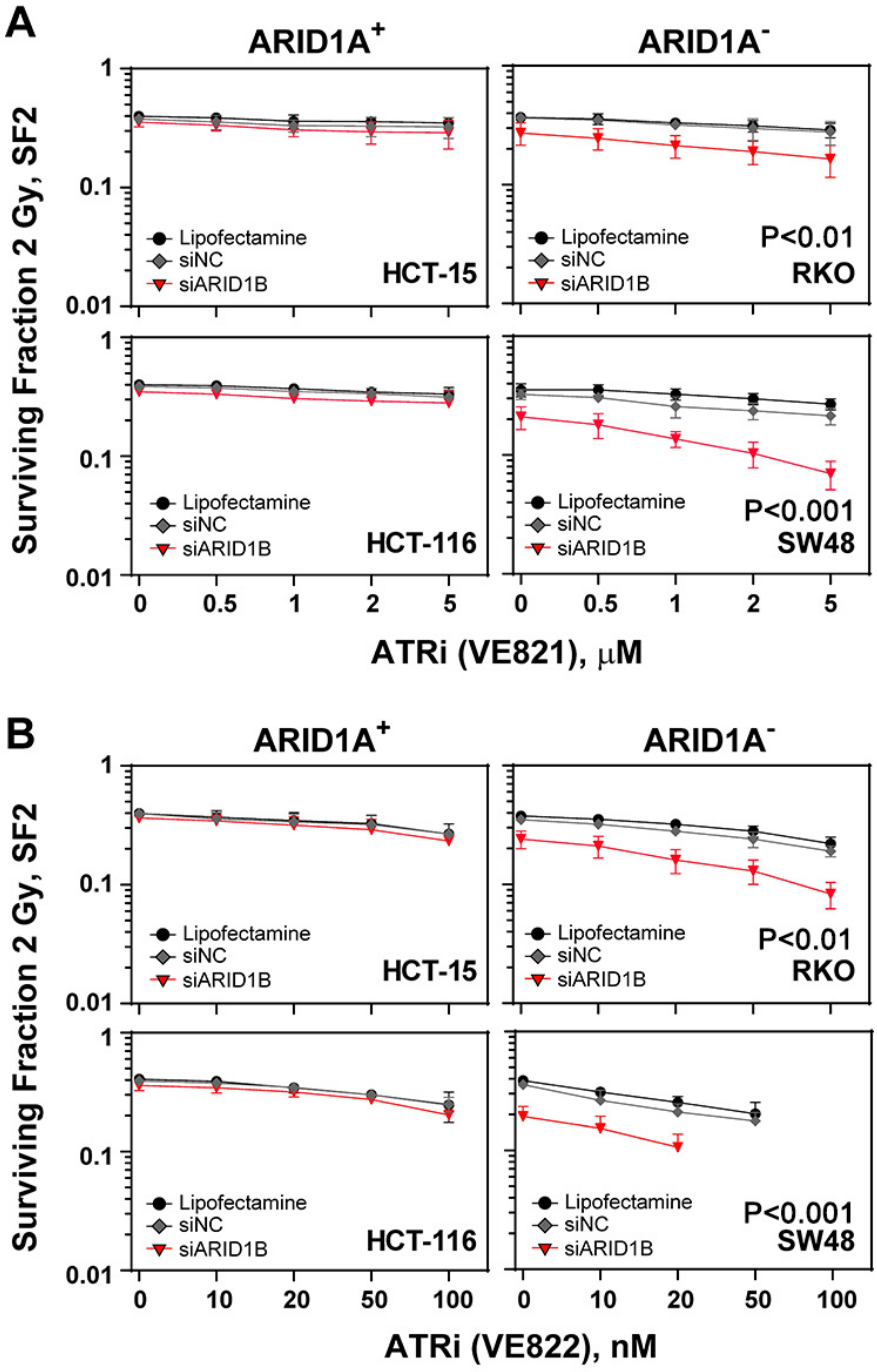

Figure 4.11: Effect of ARID1B/ARID1A on radiosensitivity. Survival curves for ARID1B depleted and non-targeted siControl transfected cells are shown together with residual values of the observed surviving fractions. Surviving fraction: Natural logarithm of the surviving fraction normalized to the mean of the sham irradiated controls, exposed to control- or ARIDIB-siRNA. Representative results of 5 independent experiments are shown. P values indicate the results from the ANOVA F-test for the radiation response-modifying effect ofARID1B-knockdown.

Since the cell lines were not isogenic and thus have different gene expression profiles, it is unclear how these heterogeneities among different cell lines influence the observed results and if this only depends on the ARID1A status. Therefore, the effect of ATRi after the knock-down of ARID1A expression was evaluated in two different ARID1A^{+} CRC cell lines (HCT15 and HCT116) to assess the effect of different genetic background on the treatment response (Figure 4.12). The treatment of ARID1A^{+} cell lines with 20 nM V822 after transfection with control siRNA had no effect on the viability after irradiation. In comparison, ARID1A knock-down led to a significant ($P<0.01$) reduction of the viability in both ARID1A^{+} CRC cells. In addition, knock-down of ARID1A combined with VE822 further enhanced the radiosensitivity of ARID1A^{+} CRC cells ($P<0.001$). These results were consistent with our previous observations that ARID1A^{-} CRC cell lines are more sensitive to ATR inhibitors and indicated that the radiosensitising effect after ATRi treatment mainly relied on the ARID1A status of the cell lines.

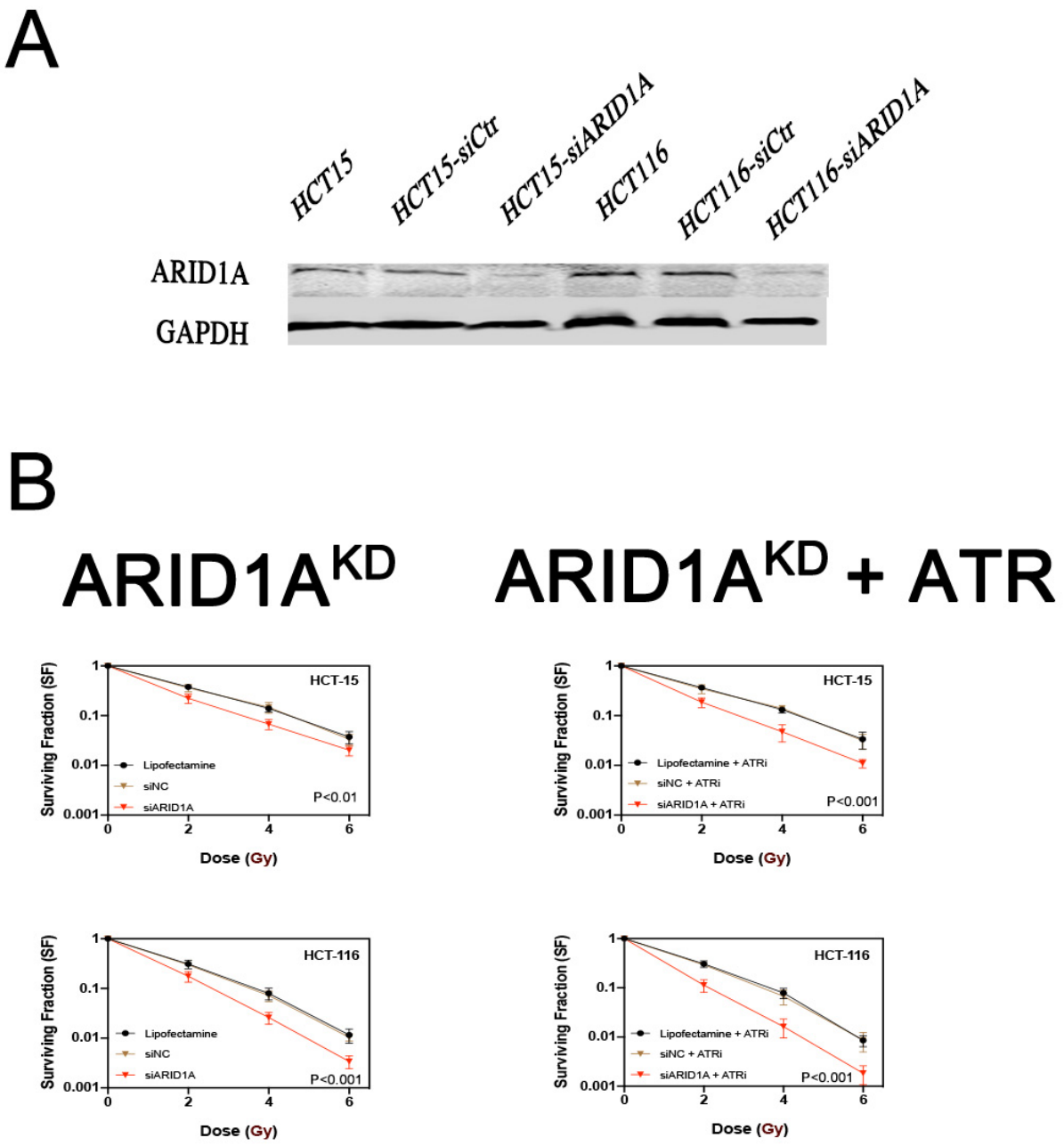

Figure 4.12 Effect of ARID1A knockdown in ARID1A^{-} cell plus ATR inhibitor (VE822) on radiosensitivity. A: Western blot results of ARID1Aknockdown by siRNA. B: The effect of ARID1A knockdown in ARID1A^{-} CRC cell lines and the effect of ARID1A knockdown plus ATR inhibitor (VE822) in ARID1A^{-}CRC cell lines. Representative results of 5 independent experiments are shown. Statistically significant differences compared with corresponding control cells, P values indicate the results from the ANOVA F-test.

4.3 Cell cycle specific radiosensitization of CRC cell lines by ATRi

The present results show that inhibition of ATR increased the radiosensitising effect especially in ARID1A deficient CRC cell lines. Therefore, the evaluation of the mechanism into the inhibitor induced synthetic lethality effects after ARID1A loss is necessary.

ATR is an important mediator of the intra-S-phase and G2/M cell cycle checkpoint. Thus, the effect of cell cycle distribution on the synthetic lethality effect of ATRi in the background of ARID1A deficiency was evaluated. Aphidicoline was used to synchronize the cell lines at an early S phase or mid S phase of the cell cycle. Cells in the early S- and in mid S-phase of the cell cycle were treated with the ATR inhibitor VE822 and its effect on radiosensitization was assessed. $ARID1A^-$ and $ARID1A^+$ cells were firstly treated with aphidicoline for 20 h, then the medium supplemented with the drug was replaced with fresh medium and cell cycle distribution was measured at different time points (0 h, 2 h, 4 h, 6 h, 8 h and 24 h) after the washout of aphidicoline. Cell cycle analysis at 0 h showed that approximately 70% of the cells were mainly in early S phase, while approximately 65% were in mid S stage phase at 6 h after washout (Figure 4.13).

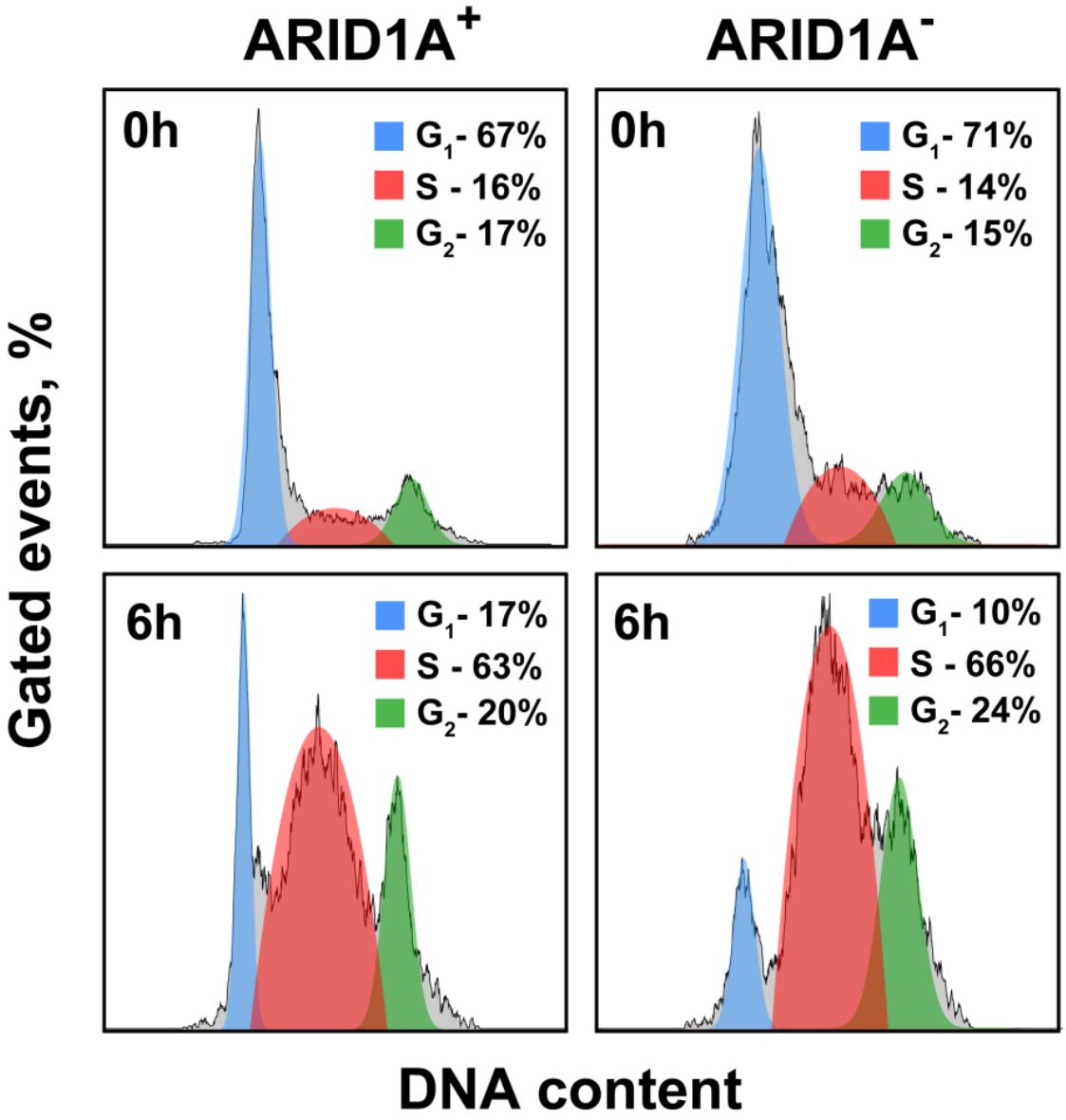

Figure 4.13: Cell cycle synchronization by Aphdicoline. ARID1A+ and ARID1A- colon cancer cells were synchronized by 20 h incubation with aphidicolin. After aphidicolin removal, cells were collected at different time thereafter (from 0 to 24 h). DNA content was measured by flow cytometry by tracing the fluorescence intensity of the cells. Treatment with aphidicolin for 20 h synchronizes cells at early S-phase stage of the cell cycle and at mid S-phase at 6 h after release from the aphidicolin block.

Cells were divided into two groups to test whether the radiosensitising effect of the ATRi VE822 was higher on cells in early S- or in mid S-phase: cells were treated in the early S phase (Group 1) or mid S phase (Group 2). The effect on radiation sensitivity in these two different groups was measured by colony formation assay. ARID1A$^-$ and ARID1A$^+$ CRC cell lines were firstly treated with aphidicoline and then the medium supplemented with the drug was replaced with fresh medium at 0 h and 6 h after the treatment with aphidicoline. Cells were then seeded into 6 well plates and treated with ATRi VE822 for 1 h, irradiated with 0 Gy or 4 Gy and colony formation was determined at approximately 2-3 weeks.

As a result, treatment with ATRi significantly reduced the surviving fraction of ARID1A$^-$ but not of ARID1A$^+$ cell lines at both early as well as in mid S-phase irradiated cells (Figure 4.14). The respective dose modifying factor for radiosensitization by ATRi are depicted in Table 11. The data show a tendency towards higher DMF in mid S-phase cells.

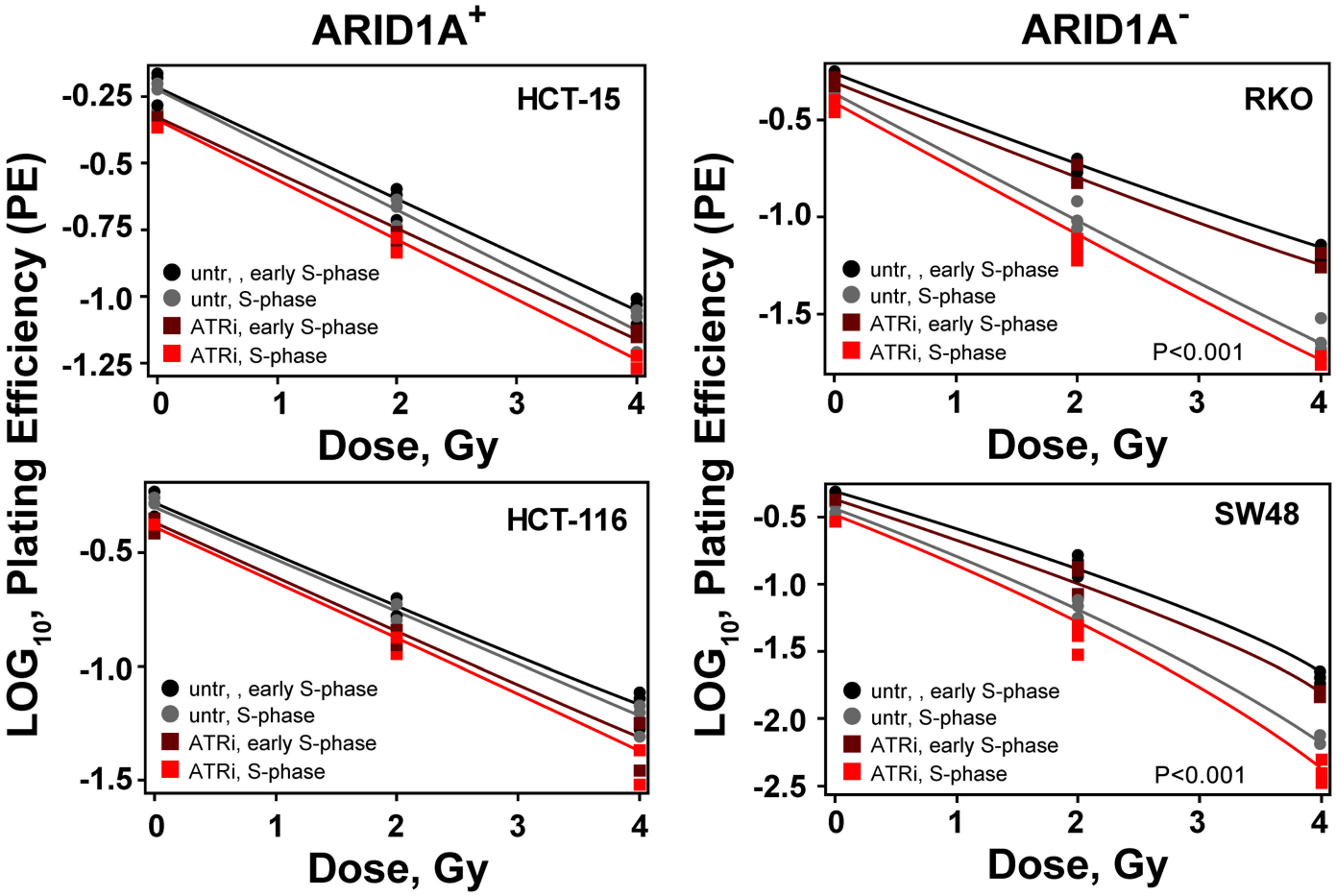

Figure 4.14: Cell cycle effect of ATRi/ARID1A. Synchronized cells in early S phase and mid S phase were pre-treated for 1 h with VE822 and irradiated thereafter with 0 Gy, 2 Gy and 4 Gy. Plating efficiency of sham treated (untr) and VE822 treated (ATRi) cells were plotted as log10 for ARID1A^{+} and ARID1A^{-} cell lines. Representative results of 3 independent experiments are shown. Statistically significant differences compared with corresponding control cells, P values indicate the results from the ANOVA F-test.

Table 11: The radiosensitising effect of ATRi in ARID1A$^-$colon cancer cell lines in early S and S phase quantified by the dose modifying factor (DMF)

Cell line	Cell cycle phase	Dose modifying factor (DM) due to ATRi	P[1]-value for the ATRi effect	P[1] for dependence of DM on cell cycle position
HCT15	Early S phase	0.969 (95% CI:0.891-1.055)	0.44	0.88
HCT15	Mid S phase	0.968 (95% CI:0.928-1.010)	0.12	
HCT116	Early S phase	0.988 (95% CI:0.903-1.081)	0.78	0.29
HCT116	Mid S phase	0.976 (95% CI:0.863-1.104)	0.68	
SW48	Early S phase	0.828 (95% CI:0.770-0.891)	<0.0001	0.09
SW48	Mid S phase	0.740 (95% CI:0.660-0.830)	<0.0001	
RKO	Early S phase	0.827 (95% CI:0.765-0.894)	0.0002	0.44
RKO	Mid S phase	0.780 (95% CI:0.736-0.826)	<0.0001	

[1]P: Colony data were analyzed using a linear-quadratic model describing the dependence of the logarithm of cellular survival. ANOVA was used to calculate the statistical significance between groups, N=3.

Above results indicated that ATRi had better effect on cells in mid S phase. To further investigate the effect of ATRi on the activation of cell cycle checkpoint after irradiation, we examined the cell cycle distribution by flow cytometer. ARID1A$^-$ and ARID1A$^+$ CRC cells were treated ATRi mainly in early S phase (Group 1) or mid S phase (Group 2). ARID1A$^-$ and ARID1A$^+$ CRC cell lines were firstly treated with aphidicoline and then the medium containing the drug was replaced with medium containing ATRi at 0 h (Group 1) and 6 h (Group2) after the treatment with aphidicoline. Cells were treated with ATRi VE822 for 1 h, irradiated with

0 Gy or 4 Gy and collected for cell cycle analysis. A significant increase of cells at G2/M phase was observed in ARID1A$^-$ CRC cell lines whether it was group 1 or group 2, suggesting that ATRi plus ARID1A$^-$cells weakened S phase checkpoint activation (Figure 4.15).

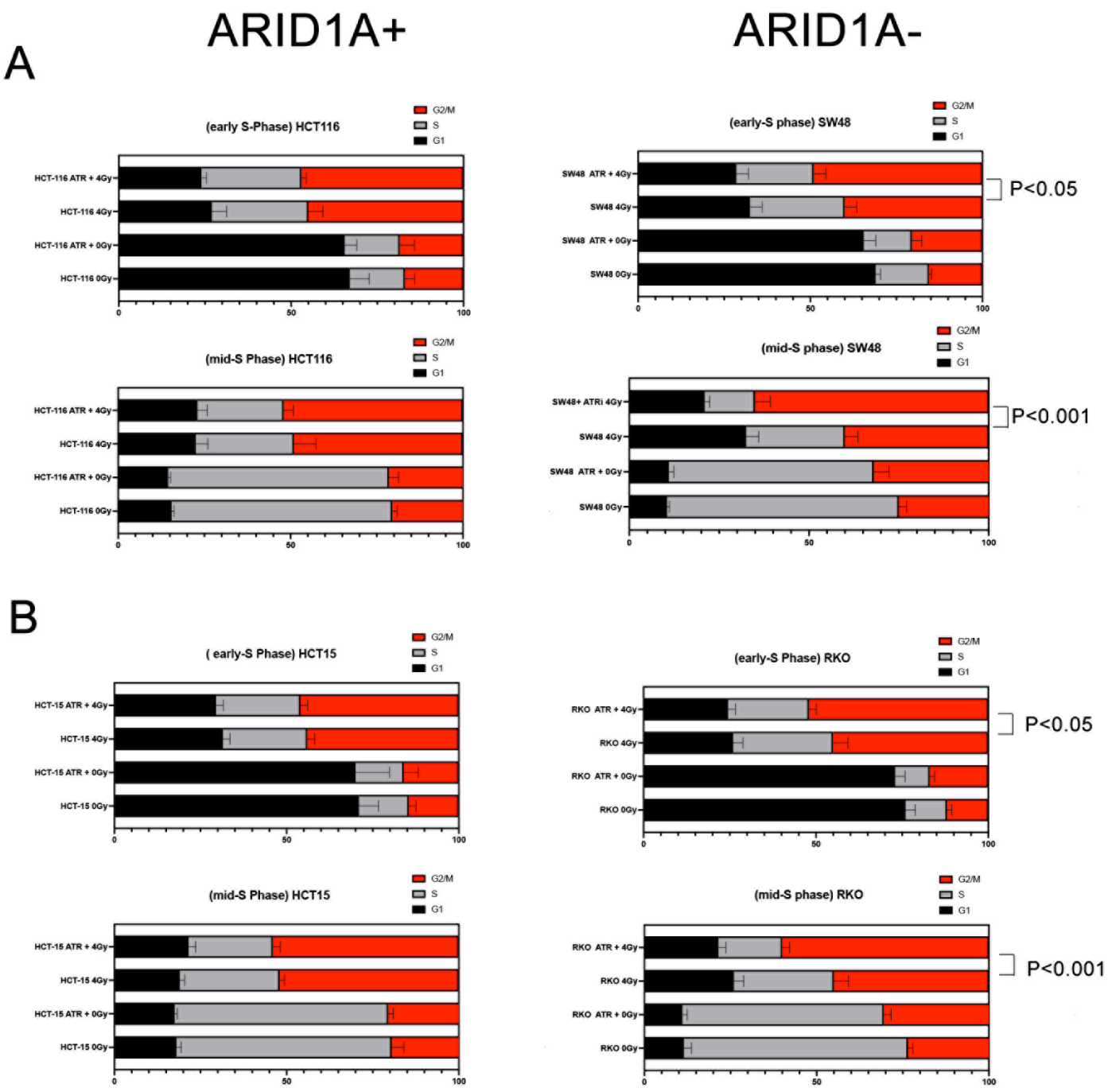

Figure 4.15: Cell cycle redistribution of ATRi/ARID1A.

A: HCT15 (ARID1A^{-}) and SW48 (ARID1A^{-}) CRC cells; B: HCT-116 (ARID1A^{-}) and RKO (ARID1A^{-}) CRC cells; Synchronized cells in early S phase and mid S phase were pre-treated for 1 h with VE822 and irradiated thereafter with 0 Gy and 4 Gy. Representative results of 3 independent experiments are shown. Statistically significant differences compared with corresponding control cells, P values indicate the results from the ANOVA.

ATR is a principal mediator of the G2/M cell cycle checkpoint that prevents the premature entry of cells into mitosis[97]. Thus, ATR inhibition could abrogate the G2/M cell cycle checkpoint and increase the sensitivity of cancer cells. The transition of cells from the G2 phase into mitosis was measured by the level of phosphorylated histone H3 (Ser-10) as a marker for mitosis to investigate the effect of ATR inhibition on the cell cycle checkpoint after irradiation. Wild type and mutant ARID1A CRC cell lines, as well as siRNA mediated ARID1A silenced cells were used. Cells were treated with the ATR inhibitor VE822 for 1 h and then irradiated with 4 Gy. The fraction of phospho-histone H3 staining cells was measured at different time points (4 h, 8 h, and 24 h) after the exposure to 4 Gy. The results showed that radiation significantly reduced the fraction of mitotic cells at approximately 4 h after irradiation because of radiation induced G2 arrest. Cells continuously release thereafter from the G2 arrest and enter mitosis. Interestingly, no apparent difference in the percentage of mitosis was observed between ATRi and non-treated ARID1A wild type cell line HCT116 (Figure 4.16). In contrast, the treatment with ATRi inhibitor resulted in a significantly increased percentage of mitotic cells at 4 h, 8 h and 24 h after the exposure to 4 Gy in the ARID1A deficient cell line SW48. This effect was confirmed after silencing of ARID1A by siRNA in the wild-type cell line HCT116, showing the same pattern as ARID1A deficient cell line SW48 with a remarkable increase in the mitotic percentage after irradiation.

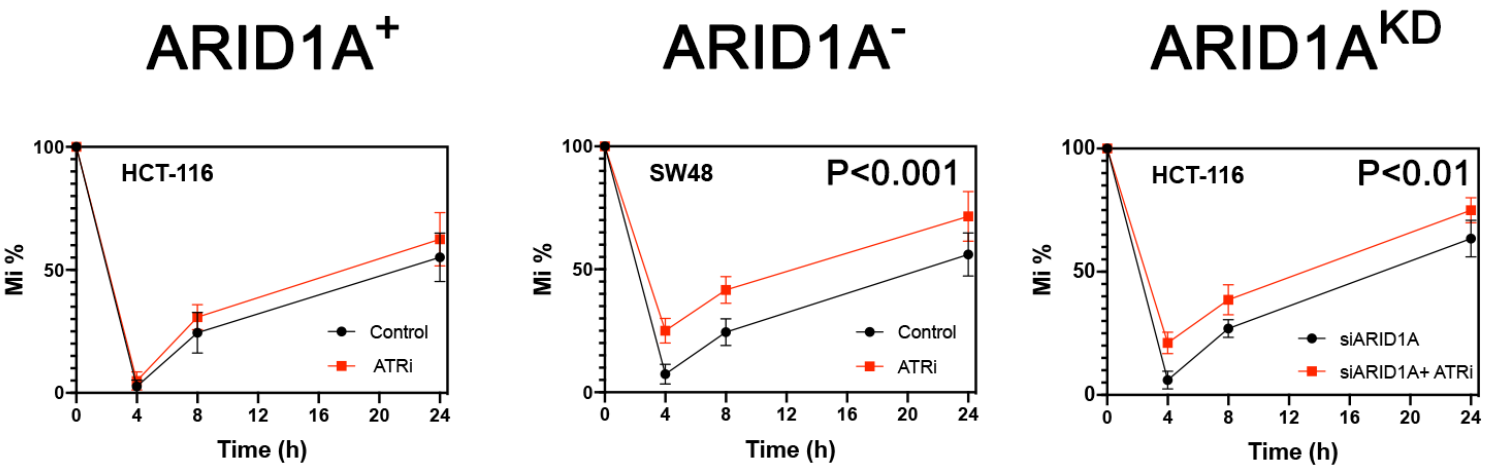

Figure 4.16: ATRi/ARID1A synthetic lethality on phospho-Histone H3 expression. MI= H3 in radiation / H3 in no-radiation * 100%. Representative results of 3 independent experiments are shown. Statistically significant differences compared with corresponding control cells, P values indicate the results from the ANOVA F-test.

4.4 Impact of ATRi /ARID1A- on DSB repair

ARID1A participates in the early phase of DSB repair through its rapid localization to the DSB sites, clearing the local nucleosome occupancy, and physically facilitating the recruitment of DNA repair enzymes and other modulators to the vicinity of DSBs**.** Therefore, loss of ARID1A may disturb the balance of HR/NHEJ DNA repair efficacy and may render cells susceptible to a specific genotoxic treatment. In addition, the inhibition of ATR activity not only blocks the cell cycle checkpoint activation but also impairs DNA repair. Therefore, the molecular mechanisms underlying the synthetic lethality effect of ATRi /ARID1A were

evaluated by measuring DSB repair signaling in the form of RAD51 focus formation as a marker of homologous recombination repair (HRR) and γH2AX associated with non-homologous end-joining (NHEJ).

γH2AX focus formation in both ARID1A^{+} and ARID1A^{-} cells were firstly examined in the G2-phase. Cells were pulse labelled for 30 mins with EdU, irradiated with different doses and fixed at different times. Repair foci were measured in the EdU negative cell population on the G2/M phase, which represented cells irradiated at the G2 phase of the cell cycle (Figure 4.17).

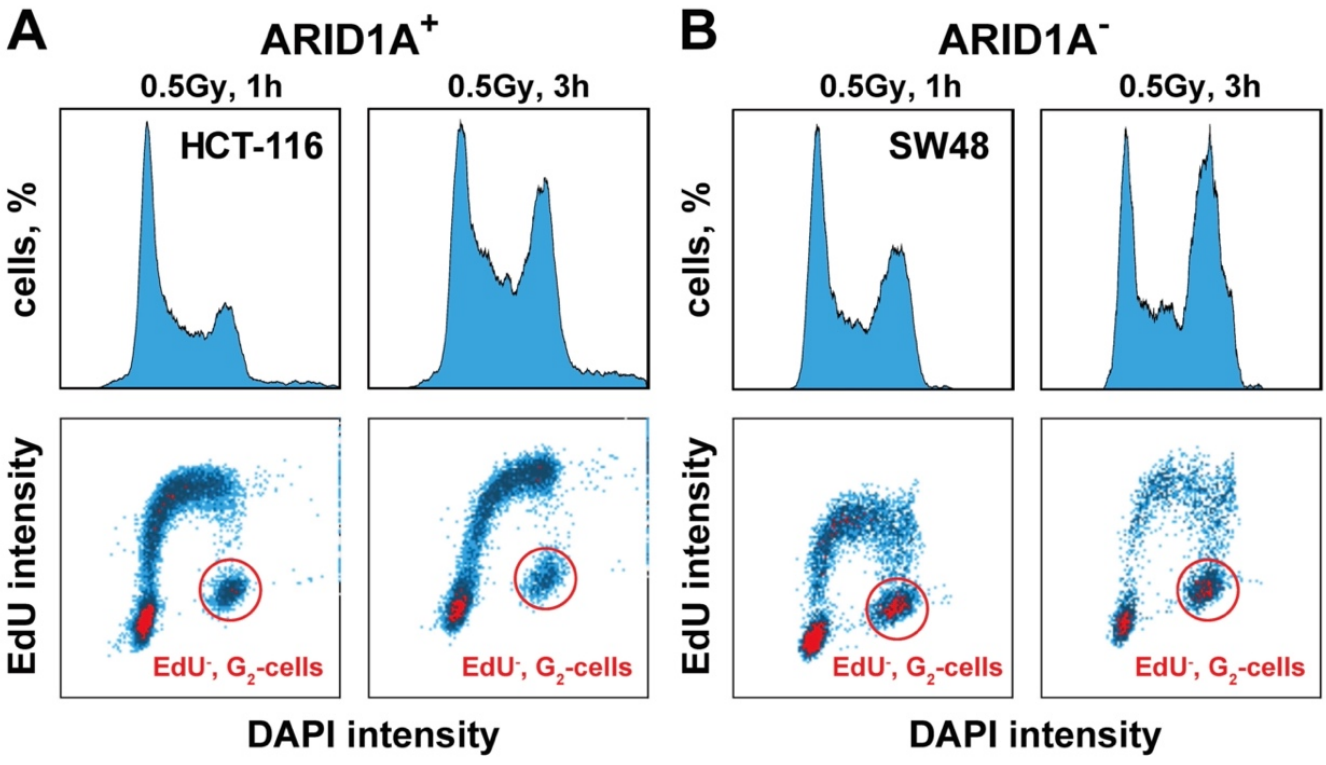

Figure 4.17 Foci formation in the G2-phase based on EdU staining. A: ARID1A^{+} CRC cells EdU staining; B: ARID1A^{-} CRC cells. Histogram and dot plots of data obtained by quantitative image-based cytometry analysis (QIBC) of ARID1A^{+} and ARID1A^{-} CRC cells.

The number of radiation induced γH2AX foci as a measure for overall repair increases with time after irradiation and reached its peak at about 1 h (tmax). The results showed that VE822 did not affect initial radiation induced γH2AX foci formation at t_{max} (Figure. 4.18) and its decay with time (Figure. 4.19) in the G2/M phase of ARID1A^{+} (HCT116, HCT15, Colo320D) and ARID1A^{-} (SW48, RKO) cell lines. However, in the ARID1A^{-}cell line LS180, a slight but significant decrease in foci formation at t_{max} was observed (Figure 4.20).

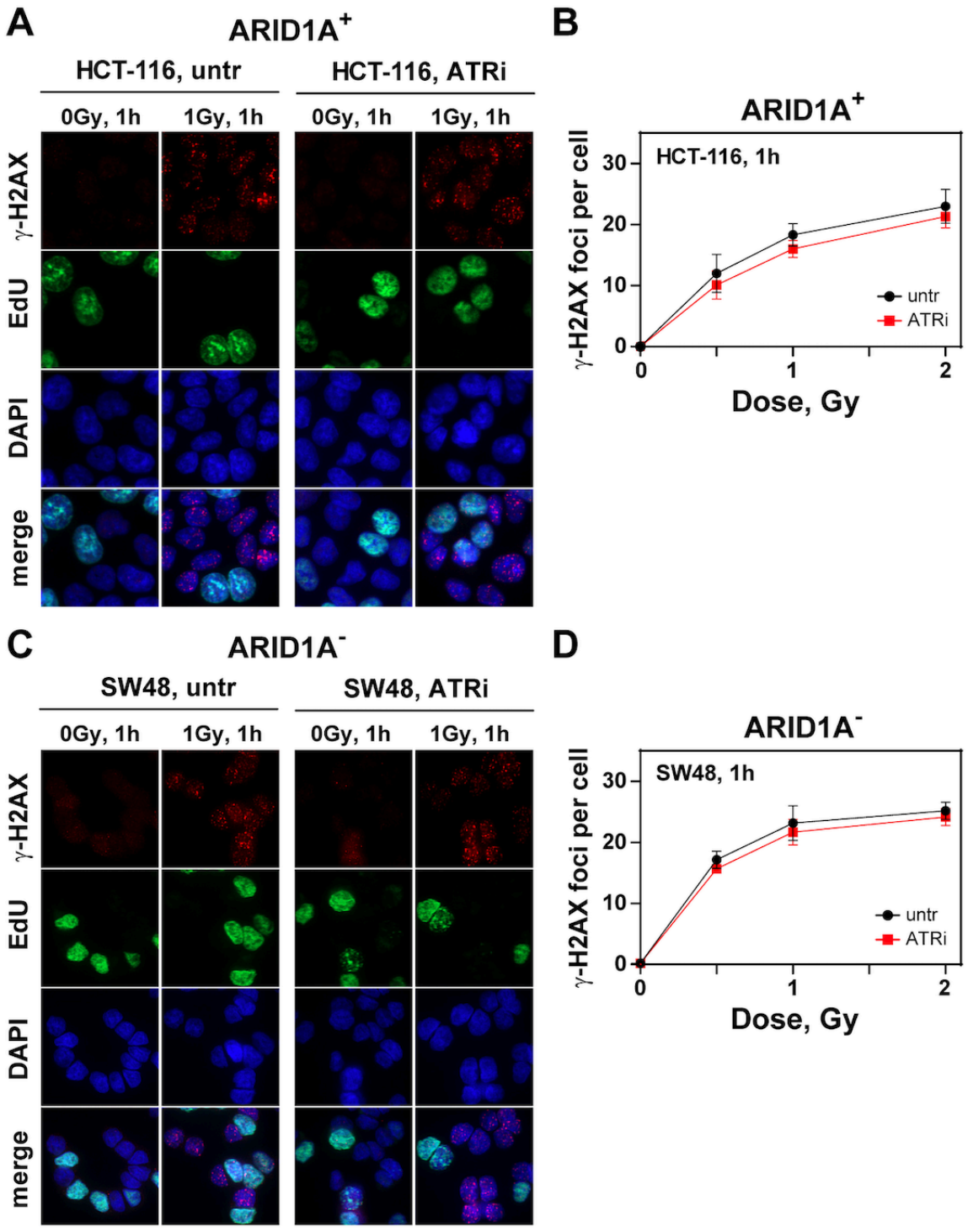

Figure 4.18: Effect of ATRi on γH2AX foci formation in G2-phase CRC cell lines. Maximum intensity projection (MIP) images of γH2AX foci (red) at tmax (1h) in G2-phase ARID1A$^+$ (**A, B**) and ARID1A$^-$ (**C, D**) cells without (untr) and with 20 nM VE822 (ATRi) in EdU$^-$ (green) cells after exposure to the indicated IR doses. Cells were counterstained with DAPI (blue). The respective numbers of γH2AX foci at tmax as a function of IR dose are shown in **B** (ARID1A$^+$ cells) and **D** (ARID1A$^-$ cells). Results of 3 independent experiments are shown for CRC cell lines.

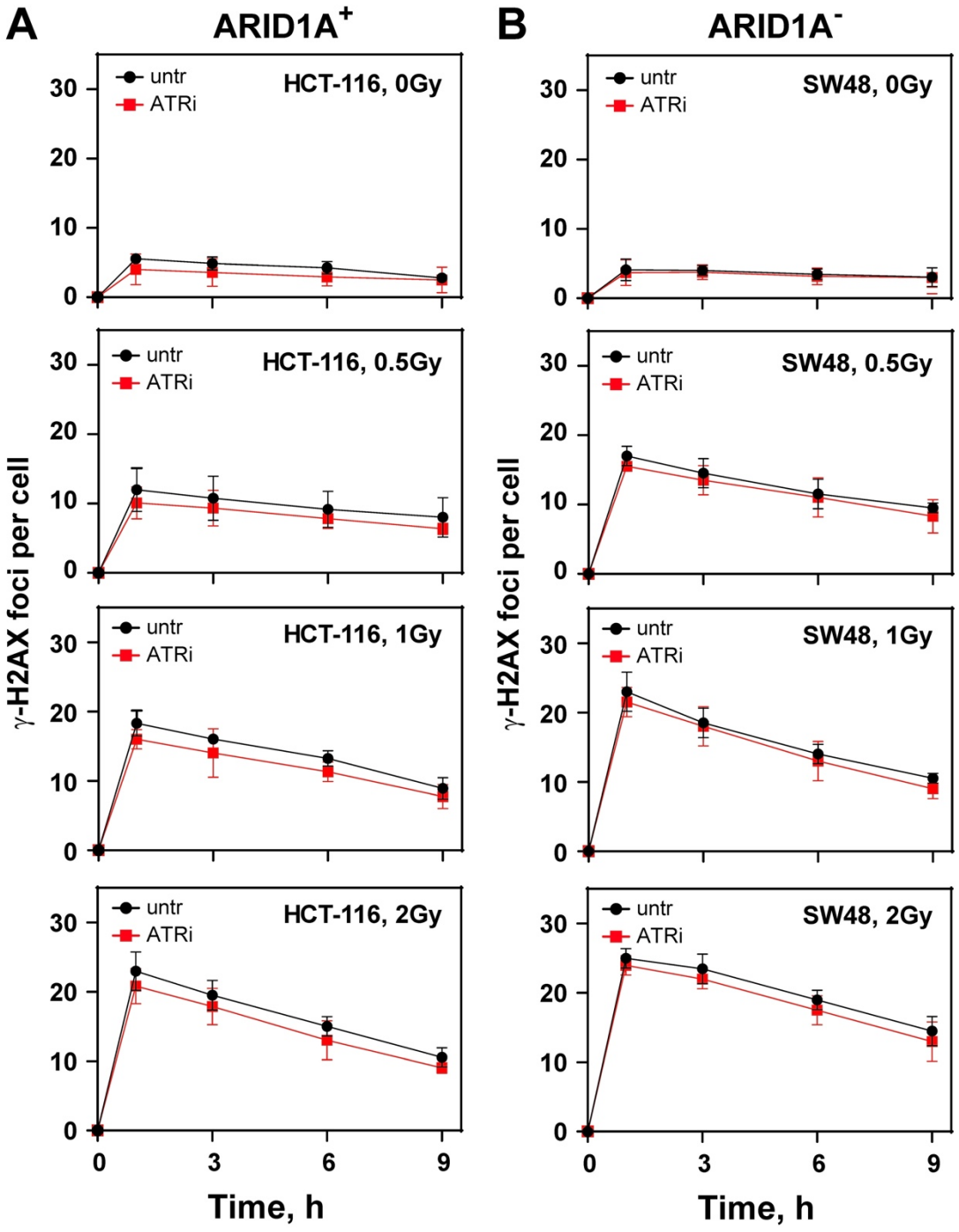

Figure 4.19: Kinetics of γH2AX foci formation and decay in G_2-cells in ARID1A$^+$ and ARID1A$^-$ CRC cells exposed to 0 Gy, 0.5 Gy, 1.0 Gy and 2.0 Gy. A: Kinetics of γH2AX foci formation and decay in ARID1A$^+$ cells. B: Kinetics of γH2AX foci formation and decay in ARID1A$^-$ cells. Results of 3 independent experiments are shown for CRC cell lines.

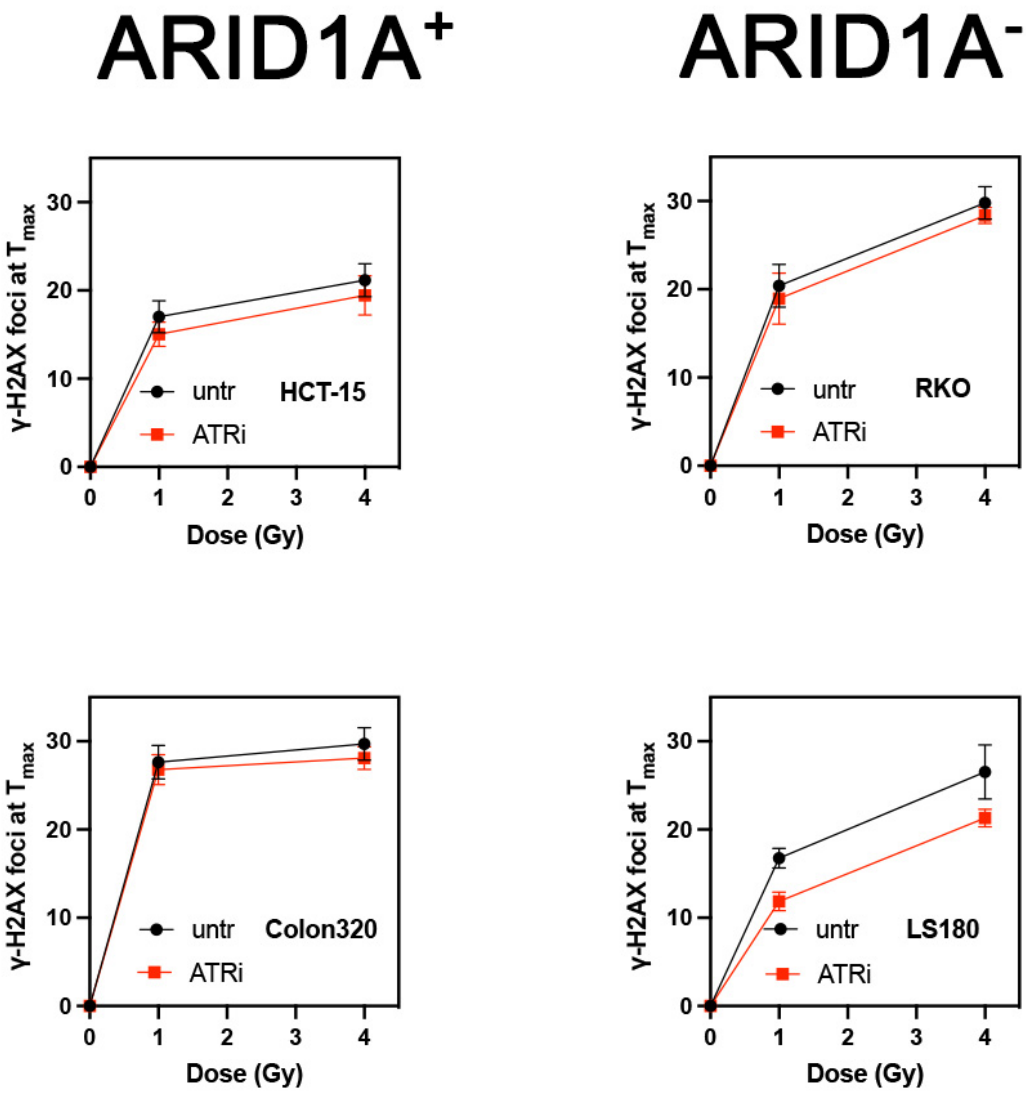

Figure 4.20: Effect of ATRi on γH2AX foci formation in G2-phase CRC cell lines. The respective numbers of γH2AX foci at tmax (1h) in G2-phase ARID1A$^+$ and ARID1A$^-$ cells without (untr) and with 20 nM VE822 (ATRi) after exposure to the indicated IR doses. Results of 3 independent experiments are shown for CRC cell lines.

In comparison, radiation induced RAD51 foci as a measure for HR reached its peak at about 6 h (t_{max}) after irradiation. Irradiation with increasing radiation doses shows no significant difference between VE822 and sham treated ARID1A+ cell line HCT116 in the initial RAD51 foci formation at t_{max} (Figure 4.21A) and its decay with time (Figure 4.22A). In comparison, VE822 significantly ($p<0.01$) decreased the initial number of IR induced RAD51 foci especially in the ARID1A- cell line SW48 (Figure 4.21B and Figure 4.22B). Figure 4.18B clearly shows a significant ($P <0.001$) decrease of RAD51 foci in the presence of ATR inhibitor at t_{max} in ARID1A- cell line SW48 ($P<0.01$). We also confirmed above results from other ARID1A+ (HCT15, Colo320) and ARID1A- (RKO, LS180) CRC cell lines (Figure 4.23).

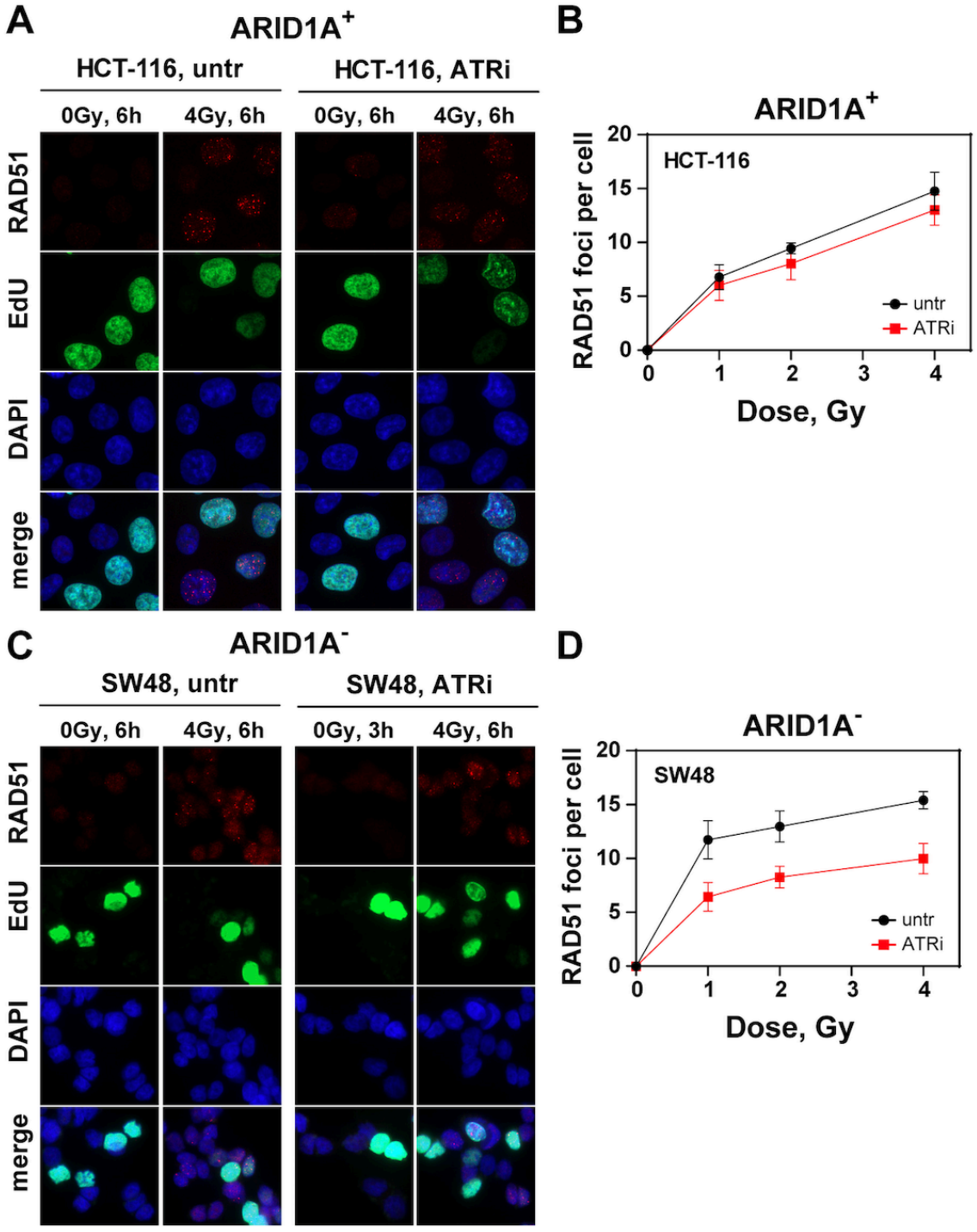

Figure 4.21: Effect of ATRi on RAD51 foci formation in G2-phase CRC cells. Maximum intensity projection (MIP) images of RAD51 foci (red) at tmax (6h) in G2-phase ARID1A+ (**A, B**) and ARID1A- (**C, D**) cells without (untr) and with 20 nM VE822 (ATRi) in EdU- (green) cells after exposure to the indicated IR doses. Cells were counterstained with DAPI (blue). The respective numbers of Rad51 foci at tmax as a function of IR dose are shown in **B** (ARID1A+ cells) and **D** (ARID1A- cells). Results of 3 independent experiments are shown for CRC cell lines.

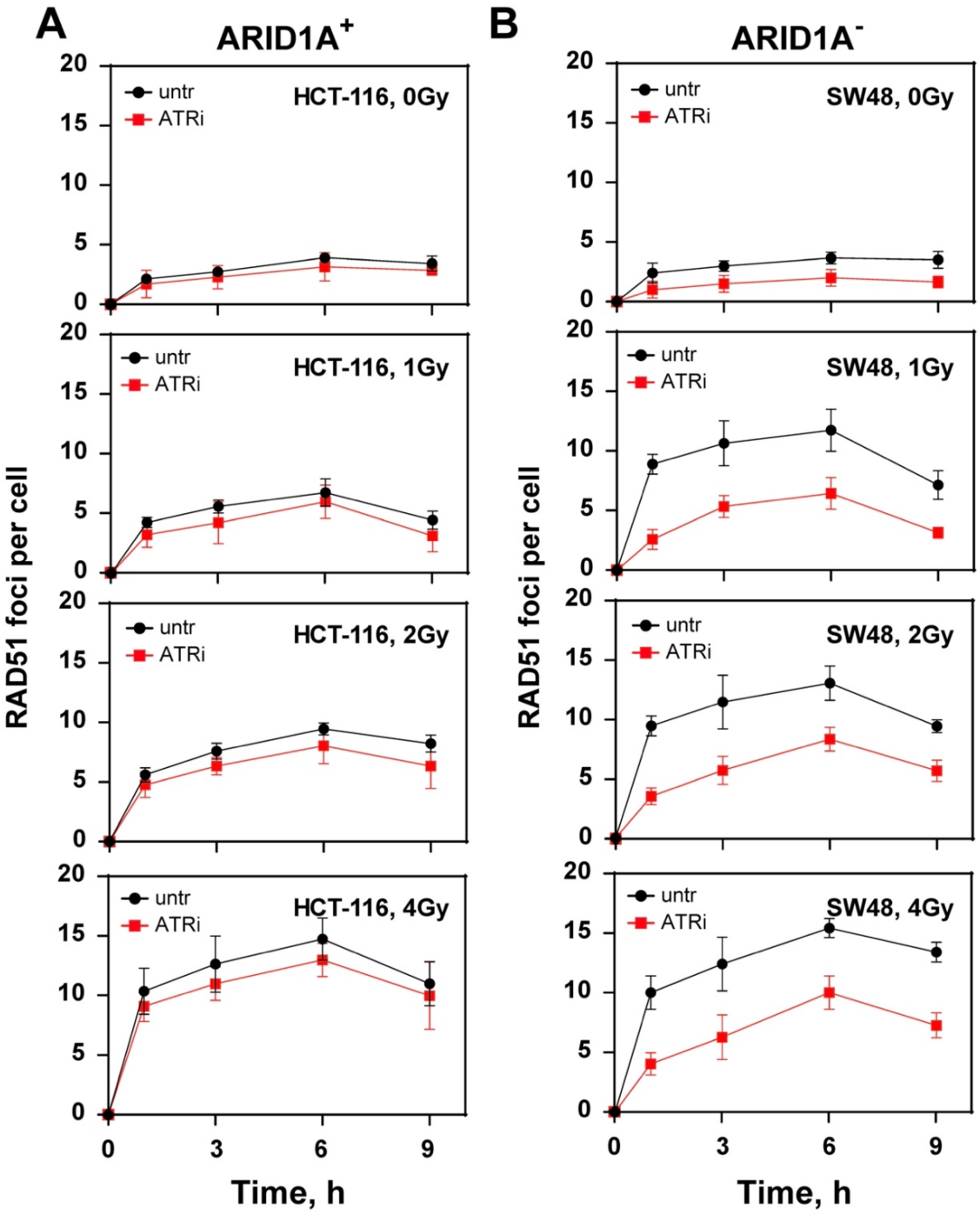

Figure 4.22: Kinetics of RAD51 foci formation and decay in G2-cells in ARID1A$^+$ and ARID1A$^-$ CRC cells exposed to 0 Gy, 0.5 Gy, 1.0 Gy and 2.0 Gy. A: Kinetics of RAD51 foci formation and decay in ARID1A$^+$ cells. B: Kinetics of RAD51 foci formation and decay in ARID1A$^-$ cells. Results of 3 independent experiments are shown for CRC cell lines.

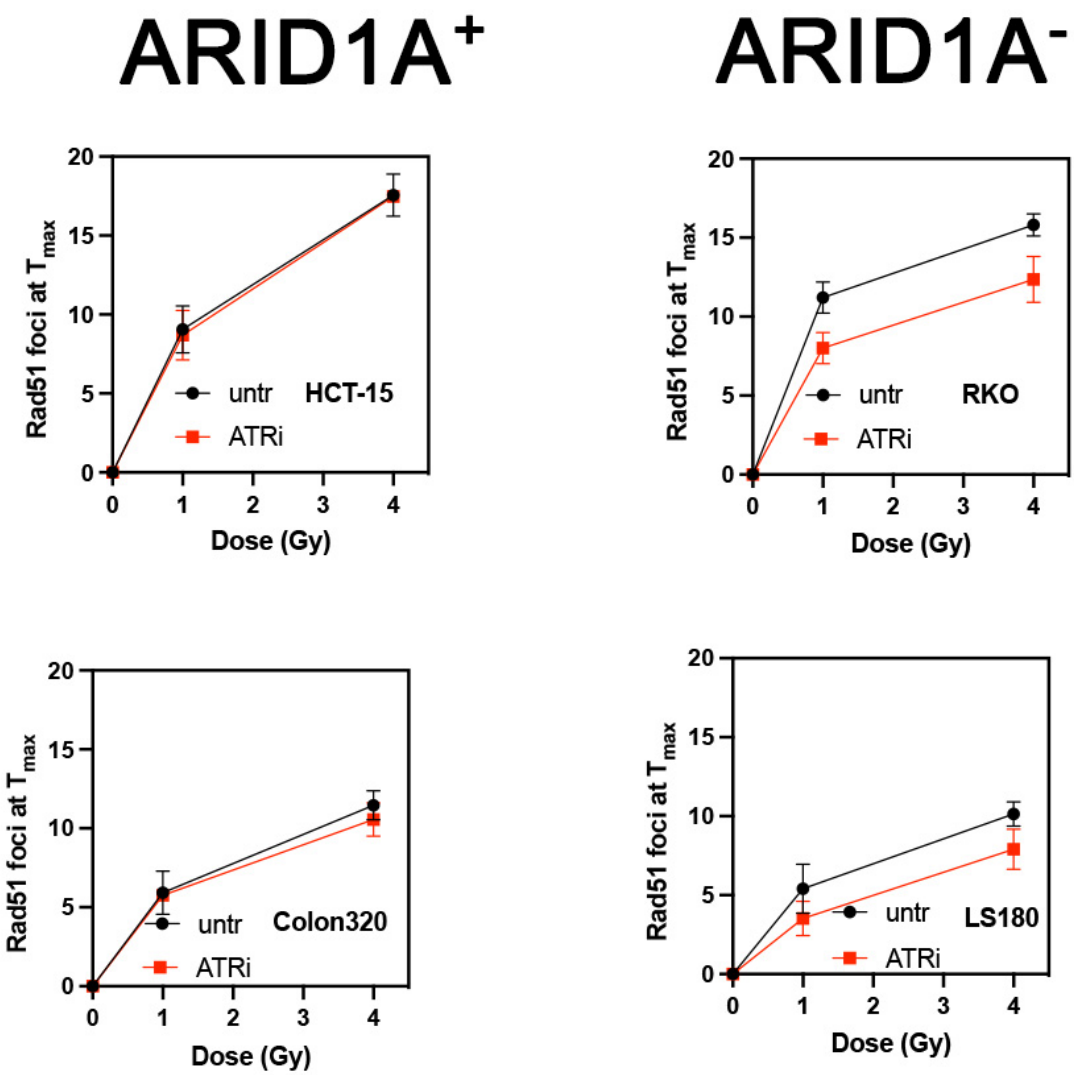

Figure 4.23: Effect of ATRi on RAD51 foci formation in G2-phase CRC cell lines. The respective numbers of RAD51 foci at tmax (6h) in G2-phase ARID1A^{+} and ARID1A^{-} cells without (untr) and with 20 nM VE822 (ATRi) after exposure to the indicated IR doses. Results of 3 independent experiments are shown for CRC cell lines.

To determine whether this effect on HR could be reproduced with an HR specific reporter assay, DR-GFP-U2OS and DR-GFP-A549 cell lines were used as a model system for HR repair. The reporter expresses GFP upon repair by HR of an I-SceI induced DSB as outlined under materials and methods. At first, ARID1A expression was knocked-down in these 2 cell lines with siRNA (Figure. 4.24A). Next, cells were treated with or without VE822. The data show, that ARID1A knock-down reduced the number of GFP^+ cells and thus HR by 50.4 ± 8.3%. In comparison, ARID1A knock down plus ATR inhibitor has the lowest fraction of GFP^+ cells at 5.4 ± 1.7% (Figure. 4.24B).

To further elucidate the impact of ATRi /ARID1A on the single strand annealing repair pathway, SA-GFP-U2OS cells which report for single strand annealing (SSA) efficiency [98] was used in our experiment. After knocked-down ARID1A expression in SA-GFP-U2OS cells (Figure 4.24A), cells were treated with or without VE822. The results show that ARID1A knock-down (94 ± 3.3%) and ARID1A knock down plus ATR inhibitor (88 ± 4.1%) did not significantly reduce SSA (Figure 4.24C). To test if ARID1A knockdown affects another well described alternative repair pathway to NHEJ (alt-NHEJ), the well-established EJ2-GFP reporter for alt-NHEJ[99] was used. The results show that ARID1A knockdown impaired alt-NHEJ (65 ± 9.3%). In addition, ARID1A knock down plus ATR inhibitor enhanced this effect (40 ± 5.3%) (Figure 4.24D).

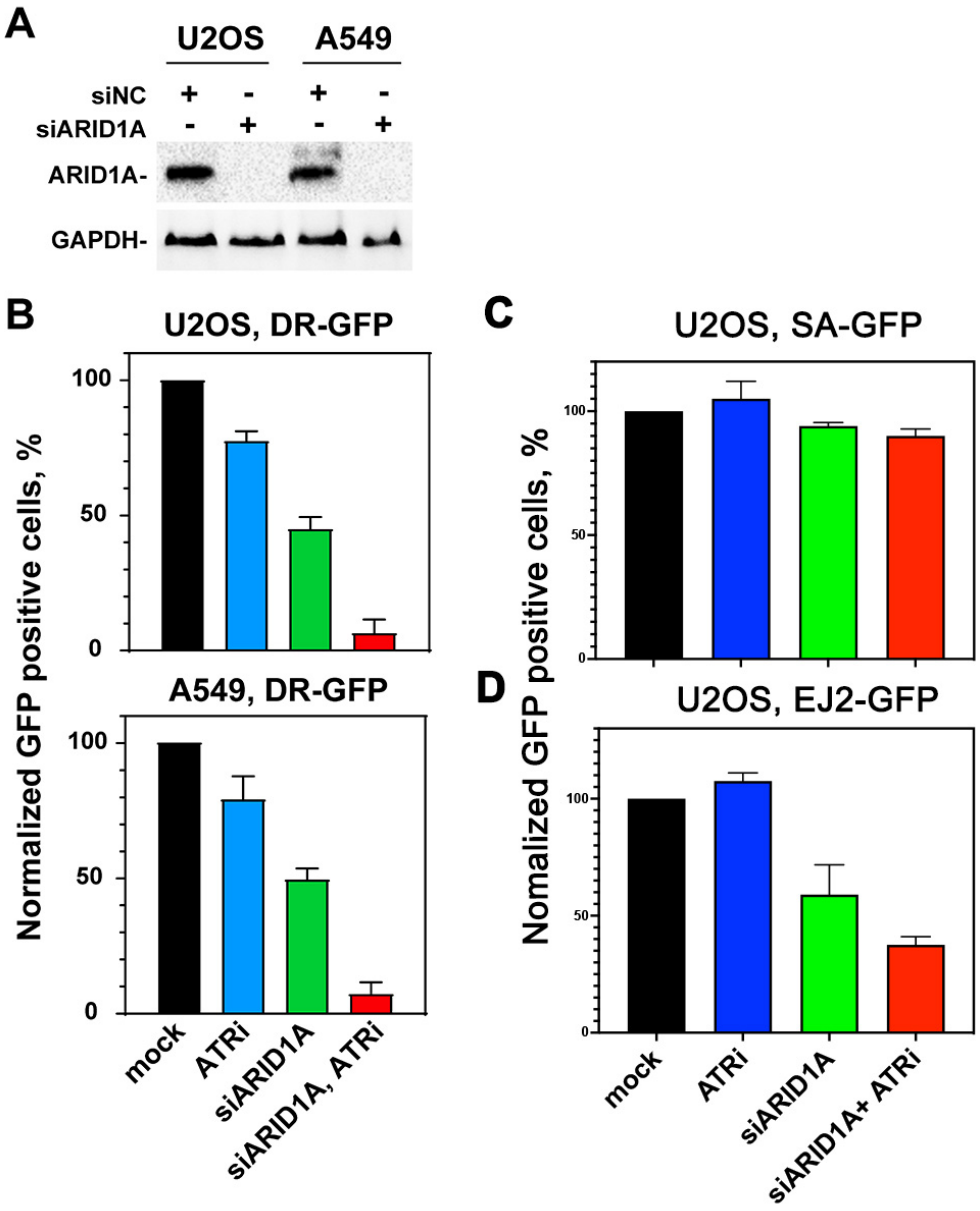

Figure 4.24: Knockdown of ARID1A decreases HRR in U2OS/DR-GFP and A549/DR-GFP reporter cells. A: Western blot results of ARID1A knockdown in U2OS/DR-GFP and A549/DR-GFP reporter cells; B: Relative expression in U2OS/DR-GFP and A549/DR-GFP reporter cells； C: Relative expression in U2OS/SA-GFP reporter cells; D: Relative expression in U2OS/EJ2-GFP reporter cells. Results of 3 independent experiments are shown for CRC cell lines.

We also tested different concentration of VE822 in DR-GFP reporter cell line with or without ARID1A knock down. The results show (Figure 4.25) that treatment with 20 nM VE822 of DR-GFP-U2OS reporter cell line with ARID1A knock down halved HR repair (45.1 ± 9.1%). This result confirmed that VE822 could significantly potentiate the effect on HR repair after knocked-down of ARID1A.

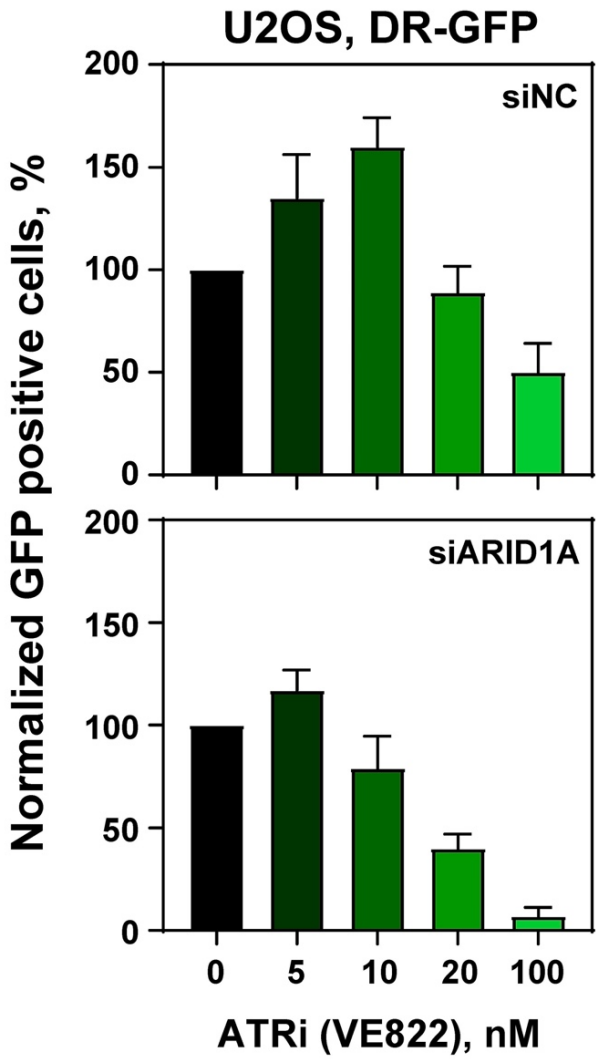

Figure 4.25: ATRi effect on HRR in ARID1A+ U2OS/DR-GFP reporter cells and ARID1AKD U2OS/DR-GFP reporter cells. ATRi: VE822, concentration from 5nM to 100nM. U2O2/DR-GFP cells were firstly transfected with siRNA for knock-down of ARID1A expression, and then U2O2/DR-GFP positive cells are measured 24h after I-SceI transfection in untreated cells, as well as in cells treated with VE822 from 0 to 100 nM. Results shown are normalized to those of untreated controls . Results of 3 independent experiments are shown for CRC cell lines.

4.5 ARID1A expression and characteristics in CRC primary tumors

ARID1A expression in tumor specimens from a total of 46 CRC patients was evaluated. Patient clinicopathologic characteristics are summarized in Table 12.

Table 12: Clinicopathologic characteristics and ARID1A expression in patient samples of colorectal cancer.

Characteristics	ARID1A Expression		
	Negative (n=5)	Positive (n=41)	P
Age			>0.05
≤50	3	18	
>50	2	23	
Gender			>0.05
Male	3	34	
Female	2	7	
Tumor location			>0.05
Right Colon	2	10	
Left colon	0	2	
Rectal	3	29	
TNM stage (AJCC)			>0.05

I	0	14	
II	1	10	
III	4	17	
Pathologic differentiation			<0.05
Poor	3	2	
Moderate	2	10	
Well	0	29	
Tumor size (cm)			>0.05
≤5	1	9	
>5	4	32	
Lymphatic penetration			<0.05
Negative	2	36	
Positive	3	5	

AJCC: American Joint Committee on Cancer; TNM: Tumor-node- metastasis; ARID1A: AT-rich interactive domain 1A.

Five of 46 tumors (10.8%) showed low or no expression of ARID1A in tumor cell nuclei. Loss of ARID1A expression was not associated with gender, age, tumor location, TNM stage, or tumor size. However, a statistically significant difference was found between ARID1A expression and pathologic differentiation and lymphatic penetration

($P<0.05$). The lack of ARID1A expression is relevant to poor pathologic differentiation and higher lymphatic penetration.

4.6 ATRi /ARID1A interaction in primary tumors of CRC patients

The sensitization effect of ATRi on CRC with and without ARID1A expression was further evaluated in an *ex vivo* experimental setting. Cells from primary tumors with and without ARID1A expression were tested in an ATP-based tumor chemosensitivity assay (ATP-TCA) (Figure 4.26A). Among the 46 CRC specimens, 43 completed the ATP-TCA test, and 3 were discarded due to the low cell number or weak colon cancer marker CK20 (Figure 4.26B). The evaluable rate of the ATP-TCA method for CRC specimens was 93.4%.

All the 43 cases (4 negative CRC specimens and 39 positive CRC specimens) were used to generate a dose-response curve of ATRi using the ATP-TCA method (Figure 4.26C). The results clearly demonstrated that ARID1A negative cells were significantly (p value) more sensitive to ATRi compared with ARID1A positive cells, with an IC50 value of 19.83 ± 7.83 nM for the ARID1A negative cells and 98.8 ± 45.4 nM for the ARID1A positive cells.

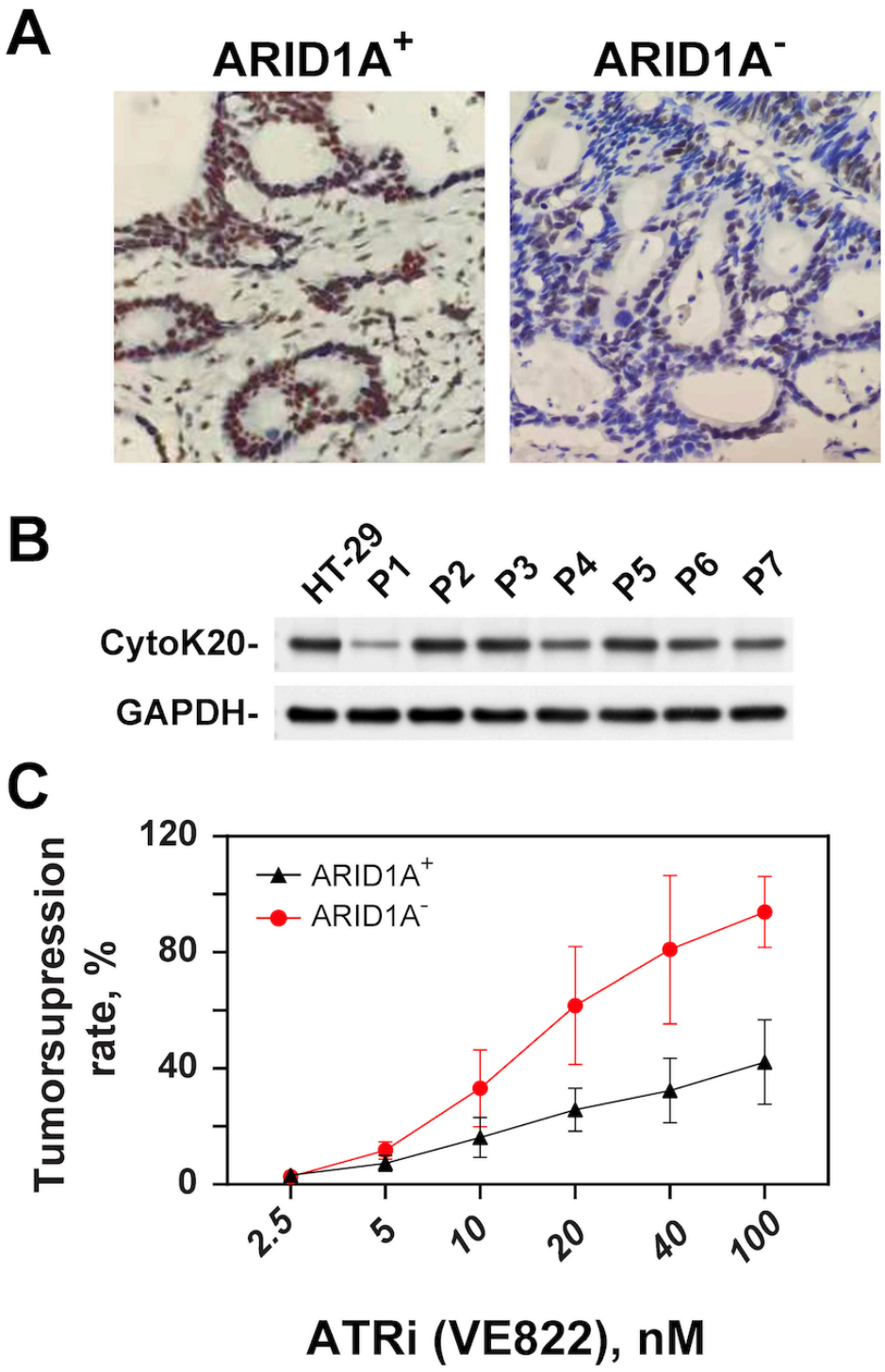

Figure 4.26: Effect of ATRi on ex vivo explants from CRC patients. A: Example of IHC staining of ARID1A expression from clinical CRC tumor cells with and without ARID1A expression. **B:** Western blot of CK20 expression from primary CRC cells; GAPDH was used as an internal control. **C:** ATP-Tumor Chemosensitivity Assay for the effect of the ATR inhibitor VE822 on *ex-vivo* cells from CRC patients. ATP activity was measured after treatment of *ex-vivo* cells with concentration ranged from 0, 2.5 up to 100 nM in cells from CRC patients with (+) and without (-) ARID1A expression.

5. Discussion

5.1 ARID1A directed synthetic lethal in SWI/SNF complex

Among the SWI/SNF complex subunits, ARID1A has the highest frequency of mutations in cancer and is related to poor prognosis and tumor activity. It is also involved in DNA repair, a molecular function that plays a significant role in the resistance to radiation and chemotherapy. Thus, research mainly focused on the development of cancer therapeutics related to the mutational status of ARID1A. Up to now, the research on ARID1A$^-$ cancer has identified some vulnerabilities [91; 100]. Many of them based on the concept of synthetic lethality, where the simultaneous perturbation of two genes results in cellular death. Like other epigenetic complexes, paralog pairs are recognized as vulnerabilities. According to Helming et al [103], ARID1B is not only the closely connected paralog of ARID1A, but it is also a synthetic target in ARID1A negative cells. Nevertheless, the mechanistic basis of synthetic lethality between ARID1A and ARID1B is unclear. Our previous work provided one possible mechanism, such as the depletion of ARID1B in ARID1A negative CRC cell lines significantly reduces the homologous recombination repair[102]. Kelso et al.[27] reported that ARID1B knockdown in ARID1A negative cells results in further up- or down-regulation of accessibility at ARID1A-dependent unique sites. Regions sensitive to ARID1A or ARID1B loss are predominantly found at enhancers and distal regulatory sites, where ARID1A and ARID1B are required for the maintenance of active enhancer histone marks. Additionally, ARID1A and ARID1B are critical for the binding of AP-1 family members at the enhancers, consistent with the reduced nucleosome spacing around AP-1 motifs after the loss of ARID1A and ARID1B. These alterations are highly correlated with changes in gene expression after the loss of one or

both ARID proteins and significant changes are found in the expression of genes encoding signaling intermediates in cell growth and adhesion, including MET. The use of similar techniques in a naturally occurring ARID1A negative ovarian cancer cell line leads to the discovery that knockdown of ARID1B results in the loss of accessibility and active histone marks around AP-1 motifs at enhancers, suggesting a common mechanistic function for ARID proteins among cancer types. Although ARID1B targeted treatment has some effect in ARID1A negative cancer cells, some challenges exist in the design of an ARID1B-targeted therapy. Specifically, ARID1B does not include small molecule-binding domain, thus, the targeting of a protein-protein or protein-DNA domain is necessary.

5.2 Effect ATRi/ ARID1A synthetic lethality on colon cancer cell lines

Several studies showed that ARID1A-directed synthetic lethality can be achieved through diverse molecular mechanisms[74], including the targeting of DNA damage response, PI3K/AKT signaling in ARID1A$^-$ cancers. Shen et al. 2015[80] revealed that ARID1A plays a role in regulating the DNA damage checkpoint of DNA DSBs and a loss of ARID1A leads to an increased dependence on Ataxia Telangiectasia and Rad3 Related (ATR) kinase[82]. Firstly, different inhibitors involved in the DNA damage response such as ATR, PARP and AURKA were used. As results, ATR inhibitors, PARP inhibitors and AURKA inhibitor sensitized ARID1A$^-$ CRC cell lines more effectively than ARID1A$^+$ CRC cell lines. These results

reconfirm that ATR, PARP and AURKA inhibitors exerted synthetic lethality effects in ARID1A$^-$ colon cancer cell lines.

Among these inhibitors, ATR inhibitors were the most effective in ARID1A$^-$ CRC cell lines. Results from the literature also suggested that ATR inhibitors can be a synthetic lethal partner of ARID1A deficiency [77; 79]. ATR refers to a significant element in the cellular DNA damage response and is activated by the single-stranded DNA that is induced during replicative stress. Deficiency of ARID1A results in defects of cell cycle progression and topoisomerase 2A, leading to a strengthened dependence on ATR checkpoint activities[79]. Suppression of ATR in ARID1A-mutant cancer cells induces genomic instability and consequent programmed cell death [79]. Hence, ATR inhibitors may represent a potential synthetic lethal strategy to target cancer cells with mutant or low expressed ARID1A.

The results of the present work showed that the combination of radiation with ATR inhibitor therapy was highly effective in eradicating ARID1A$^-$ CRC cancer cells. Both ATR inhibitors (VE821 and VE822) significantly increased the radiation sensitivity in ARID1A$^-$ CRC cells, while no sensitizing effect was observed ARID1A$^+$ CRC cells. Of particular importance, ATR inhibitor plus ARID1B knockdown further increased the radiosensitivity in ARID1A$^-$ CRC cells. In addition, ARID1A was down-regulated by siRNA in ARID1A$^+$ colon cancer cell lines (HCT15 and HCT116) to evaluate the effect of ATRi in the same genetic background. Our results showed that ARID1A knockdown led to a significant reduction in the

viability of both ARID1A$^+$ CRC cells after siRNA mediated knock-down of ARID1A, suggesting the necessity of ARID1A deficiency to obtain the sensitizing effect of ATRi.

Therefore, our data suggest that ATRi has a potential synthetic lethality effect with respect to the radiation sensitivity of ARID1A$^-$ CRC cells. This effect tends to be higher in S-phase enriched cell populations, indicating a higher sensitizing effect on cells with higher proliferation capacity, i.e. in tumor cells compared to normal cells, which should increase the therapeutic window. The rather marginal increase in the radiation sensitivity of cells in the middle S phase compared to cells in the early S could possibly be increased by comparing cells in the early G1 phase versus middle S phase.

5.3 ATRi/ ARID1A impact on DNA damage repair in colon cancer

The effect of ATR inhibitor on the formation of DSB repair foci in ARID1A$^+$ and ARID1A$^-$ CRC cell lines was evaluated to further investigate the mechanisms of radiation sensitization of ARID1A$^-$ cell lines. RAD51 focus formation as a marker of HRR and γH2AX associated with overall repair was examined especially in G2-phase at different times after the exposure to different doses of irradiation. The results showed that the ATR inhibitor VE-822 significantly decreased RAD51 focus formation in ARID1A$^-$ CRC cells, but not in ARID1A$^+$ cell lines, suggesting that VE-822 mediated radiosensitization was mainly associated with the inhibition of HRR. In contrast, ATR inhibitor did not influence γH2AX foci in ARID1A$^-$ as well as in ARID1A$^+$ CRC cell lines.

In addition the well-established DR-GFP reporter assay[101] was used to specifically measure the effect of ARID1A deficiency on HRR to strengthen the above results with Rad51. The data showed that knockdown of ARID1A also resulted in reduced HRR. Shen et al. [77] suggest that ARID1A recruits BAF to DSBs through the interaction with ATR and promotes DNA end resection at DSB. BAF complexes are implicated in DSB repair by regulating DNA end-resection and RAD51 loading on the damaged sites. The consequences of ARID1A deficiency in this setting are a homologous recombination defect and increased sensitivity to ATR inhibitors. In addition, Tsai et al. [102] showed that ARID1A deletion increases transcription-replication conflicts and R-loop associated genome instability. The dysregulation of replication and transcriptional programs is associated with altered targeting of TOP2A to R-loop prone regions. Taken together, these different studies suggested that HRR can be affected by ARID1A knockdown, especially after the exposure to an ATR inhibitor.

Our observation that ATRi did not equally reduce the different repair pathways that play a role in S/G2 phases of the cell cycle and where end-resection is implicated in the repair pathways, may either derive from the concentration used or the duration of the treatment with ATRi. Especially, the resection capacity of the cells upon long-term versus acute ATR inhibition may be different. In this respect, it has been shown that distinct modes of ATRi treatment, i.e. acute and chronic treatment, lead to different outcomes as to how DNA lesions are repaired[103]. ATR inhibition was previously reported to impair RAD51 localization to IR-induced foci, which requires ATR-mediated phosphorylation of PALB2 and its subsequent interaction with BRCA1[104]. Since resection is only mildly affected upon acute ATR

inhibition, cells treated acutely with ATR inhibitors should still be proficient in utilizing Single Strand Annealing (SSA), a homology-directed repair pathway dependent on RAD52, but independent of RAD51. Consistent with this prediction, it was found that acute VE-821 treatment of U2OS cells impaired PARPi-induced RAD51 foci, as a measure for HR, but did not alter RAD52 foci, as a measure for SSA[103]. Therefore, the concentration and time we used in the present study seems to be differentially effective on the repair pathways, which are active in S/G2 phases of the cell cycle and may thus partially explain the differential effect of ATRi on the different repair pathways.

5.4 ATRi/ ARID1A significantly decreased maintenance of radiation induced G2 checkpoint in colon cancer

Multiple studies indicated the tumor-suppressor role of ATR inhibitor and ARID1A in the transcriptional regulation of cell-cycle progression [79; 105]. Our study showed that ARID1A$^-$ cells treated with ATRi resulted in a significant increase of cells at G2/M phase as well as number of mitotic cells after irradiation exposure. Williamson et al. [79] suggested that the loss of ARID1A causes a reduced rate of S-phase progression and increases the utilization of the second growth G2/ M cell cycle checkpoint. Caumanns et al. [74] demonstrated that ARID1A loss in HCT116 cells resulted in the accumulation of cells in G2/M phase of the cell cycle. In comparison, our present results further revealed the evidence that ATR inhibition forced ARID1A$^-$ cells with DNA damage in G2 phase to rapidly progress into the M phase with DNA

repair that was severely incomplete. Interestingly, Vávrová et al. [105] and Kim et al. [106] demonstrated a significant increase in the proportion of HL-60 cells and HER2-positive breast cancer cells in the S phase after the treatment with an ATR inhibitor. These results indicate that the inhibition of ATR delays the progression of cells through the S and G2 phases of the cell cycle. However, the present study showed that ATR inhibitor decreased the maintenance of the G2 checkpoint and increased the persistent DNA damage, thereby sensitizing ARID1A$^-$ CRC cells to ionizing irradiation. Mechanistically, the role of ARID1A in the ATR-mediated DNA damage checkpoint plays a dominant role in determining cell cycle progression after DNA damage[92]. It is likely that impaired DSB repair and cell cycle checkpoint activity may allow ARID1A-deficient cells to transmit damaged (unrepaired) DNA to the next cell cycle, which could potentially lead to genomic instability.

5.5 ATRi/ ARID1A synthetic lethality in clinical colon cancer patients

Although currently a lot of evidence showing the advantages of ATR inhibitors in the treatment of ARID1A$^-$ tumor cells is available, clinical verification is lacking. This reason led us to investigate the efficacy of ATR inhibitors in an *ex-vivo* setting using primary tumor cells from CRC patients with and without ARID1A expression. Our results showed that no ARID1A protein expression was detectable in 5 out of 46 cases of CRC (10.8%). No significant correlation was found between the loss of ARID1A negative expression and gender, age, tumor location, TNM stage, or tumor size. However, a statistically significant association was found

between ARID1A negative expression and poor pathologic differentiation and lymphatic penetration, suggesting that ARID1A may play an important role in the progression of CRC. Lee, et al. [107] also showed that ARID1A loss is associated with poor tumor differentiation, lymphovascular invasion, and microsatellite instability. In addition, Wei et al. [70] showed that ARID1A protein expression is a prognostic factor for a better overall survival in stage IV CRC. Hence, the above pieces of evidence showed that ARID1A mutations may be potential candidates for new targeted therapeutic approaches in CRC patients.

The ATP-based tumor chemosensitivity assay (ATP–TCA) was developed in the early 1990s, and proved to be a useful tool for cell-based research and drug development work [108]. The ATP-TCA assay is more effective compared with previous comparable methods in terms of standardization, evaluability, tumor cell number required, reproducibility and accuracy [109]. It is possible to test cells from needle biopsies and malignant effusions as well as solid tumor biopsies from as low as 1500 cells[110]. The present study used ATP-TCA directed ATR inhibitor therapy on *ex-vivo* material from a total of 43 untreated colon cancer patients. The ATP-TCA assay showed that the ATR inhibitor VE-822 had a significantly higher sensitivity by a factor of approximately 5 in ARID1A negative compared to ARID1A positive cells from CRC.

In conclusion, the present study showed for the first time the impact of ATR inhibitor on $ARID1A^-$ in CRC cells. ARID1A deficiency regulated DNA repair especially HRR, which was the obviously the main mechanism for the observed increase in radiation sensitivity after ATR

inhibition. Collectively, our results provided mechanistic insights into the synthetic lethality and radiation sensitization of ARID1A defective CRC cells caused by ATR inhibitors and provided new therapeutic approaches for patients with ARID1A$^-$ tumors.

6. Summary

ARID1A is frequently mutated in CRC cells. Thus, it is of fundamental clinical importance to understand its molecular functions and determine whether ARID1A deficiency can be used in CRC therapy. Usually, the loss of ARID1A compromises DNA damage repair, and induced DNA damage burdens may increase the reliance on PARP or ATR-dependent DNA repair pathways of cancer cells to maintain genome integrity and render these cells susceptible to ATR inhibitors (ATRi) and PARP inhibitors (PARPi). The present study evaluated the effect of IR in combination with ATRi, PARPi and Aurora Kinases A/B inhibitor in colon carcinoma cell lines with ARID1A$^-$ and ARID1A$^+$. Besides, recent studies from our laboratory showed that its homolog ARID1B is synthetically lethal with ARID1A$^-$. Thus, the effect of IR in combination with these inhibitors on the sensitivity after ARID1B knockdown was assessed in ARID1A$^-$and ARID1A$^+$ CRC cell lines.

In the present work CRC cell lines with ARID1A$^+$ (HCT15, HCT116, Colon320) and ARID1A$^-$ (RKO, SW48, LS180) were used and treated with ATRi, PARPi and Aurora Kinases A/B inhibitor and the consequence on radiation sensitivity was measured by clonogenic survival. In addition, the effect of ARID1B knock-down with siRNA in combination with ATRi on radiation sensitivity was further assessed. The effect on DSB repair signaling as a molecular endpoint for non-homologous and homologous repair was measured by immunofluorescence staining of γ-H2AX and RAD51-foci, respectively. In addition, a plasmid based direct-repeat green fluorescent protein (DR-GFP) repair system

was used to evaluate its effect specifically on the homologous recombination repair (HRR) of DNA double-strand breaks (DSBs). The concept of selective vulnerability of ARID1A deficient CRC cells to ATRi was also evaluated in an *ex-vivo* system in cells from untreated CRC patients with $ARID1A^-$ and $ARID1A^+$ genotypes using the ATP-tumor chemosensitivity assay (ATP-TCA).

The results showed and confirmed that CRC cell lines with mt ARID1A were selectively sensitized to IR after the silencing of ARID1B by siRNA ($P< 0.01$). Moreover, our results reconfirm that ATR, PARP and AURKA inhibitors had synthetic lethality in $ARID1A^-$ colon cancer. Among these inhibitors, ATR inhibitors were more effective in $ARID1A^-$ CRC cell lines, which showed reduced viability compared to the viability of $ARID1A^+$ ($P<0.01$) also after the combined treatment with ATRi and *IR* ($P<0.001$). Therefore, ATR inhibitors were used for further experiments. Downregulation of ARID1B in addition to ATRi in $ARID1A^-$ CRC cell lines further increased the radiosensitization effect compared with $ARID1A^+$ CRC cell lines ($P <0.01$). Mechanistically, the treatment with ATRi in ARID1A deficient cells significantly decreased the maintenance of radiation induced G2 checkpoint ($P <0.01$), decreased the number of RAD51 foci induced by radiation in $ARID1A^-$ CRC cell lines compared with $ARID1A^+$ CRC cell lines ($P <0.01$) and thus negatively affect HRR. DR-GFP homologous recombination reporter system confirmed that knock-down of ARID1A selectively decreased HRR in $ARID1A^-$ cell lines. *Ex-vivo* experiments using the ATP-TCA assay showed that ATRi exerted the highest sensitizing effect in ARID1A negative cells of CRC patients.

In conclusion, the present results provide clues for a pre-clinical and clinical mechanism of action of ARID1A defects as a biomarker for ATR inhibitor response as a single agent or as a synthetic lethal approach in combination with ionizing radiation for CRC with ARID1A^{-}.

7. Zusammenfassung

ARID1A ist in CRC-Zellen häufig mutiert. Daher ist es von grundlegender klinischer Bedeutung, seine molekularen Funktionen zu verstehen und festzustellen, ob ein ARID1A-Mangel in der Therapie von Patienten mit Kolonkarzinomen (CRC, colo rectal cancer) eingesetzt werden kann. Normalerweise beeinträchtigt der Verlust von ARID1A die Reparatur von DNA-Schäden und induzierte DNA-Schäden in diesen Zellen können die Abhängigkeit von PARP- oder ATR-abhängigen DNA-Reparaturwegen von Krebszellen erhöhen, um die Genomintegrität aufrechtzuerhalten, und machen diese Zellen anfällig für ATR-Inhibitoren (ATRi) und PARP-Inhibitoren (PARPi). Die vorliegende Studie bewertete die Wirkung von ionisierenden Strahlen (IR) in Kombination mit ATRi, PARPi und Aurora-Kinasen-A/B-Inhibitor in Kolonkarzinom-Zelllinien mit ARID1A$^-$ und ARID1A$^+$. Zudem haben neuere Studien aus unserem Labor gezeigt, dass der Ausfall des homologen Partners ARID1B synthetisch letal mit ARID1A$^-$ ist. Daher wurde die Wirkung von IR in Kombination mit diesen Inhibitoren auf die Empfindlichkeit nach Reduzierung der Expression von ARID1B in ARID1A$^-$ und ARID1A$^+$ CRC$^-$ Zelllinien untersucht.

In der vorliegenden Arbeit wurden CRC-Zelllinien mit ARID1A+ (HCT15, HCT116, Colon320) und ARID1A- (RKO, SW48, LS180) verwendet, diese mit ATRi, PARPi und Aurora Kinases A/B-Inhibitoren behandelt und die Auswirkung auf die Strahlenempfindlichkeit mittels klonogenem Überleben gemessen. Darüber hinaus wurde die Wirkung von ARID1B-Knockdown mit siRNA in Kombination mit ATRi auf die Strahlenempfindlichkeit weiter untersucht. Die Wirkung auf die DSB-Reparatur als

molekularer Endpunkt wurde durch Immunfluoreszenzfärbung von γH2AX- und RAD51-Foci als Signale für die nicht-homologe und homologe Rekombinationsreparatur gemessen. Zudem wurde ein plasmidbasiertes Reparatursystem (direct-repeat green fluorescent protein, DR-GFP) verwendet um die Wirkung spezifisch auf die homologe Rekombinationsreparatur (HRR) von DNA Doppelstrangbrüchen (DSBs) zu evaluieren. Das Konzept der selektiven Vulnerabilität von ARID1A-defizienten CRC-Zellen gegenüber ATRi wurde auch in einem *ex-vivo* System in Zellen von unbehandelten CRC-Patienten mit ARID1A- und ARID1A+-Genotypen unter Verwendung des ATP-Tumor-Chemosensitivitätsassays (ATP-TCA) bewertet.

Die Ergebnisse zeigten und bestätigten, dass CRC-Zelllinien mit mt ARID1A nach der Reduzierung der Expression von ARID1B durch siRNA selektiv für IR sensibilisiert wurden ($P < 0,01$). Darüber hinaus bestätigen unsere Ergebnisse erneut, dass ATR-, PARP- und AURKA-Inhibitoren bei $ARID1A^-$ CRC eine synthetische Letalität aufwiesen. Unter diesen Inhibitoren waren ATR-Inhibitoren wirksamer in $ARID1A^-$ CRC-Zelllinien, die auch nach der kombinierten Behandlung mit ATRi und IR ($P < 0,001$) eine reduzierte Lebensfähigkeit im Vergleich zu $ARID1A^+$ ($P < 0,01$) zeigten. Daher wurden ATR-Inhibitoren für weitere Experimente verwendet. Die Herunterregulierung von ARID1B zusätzlich zu ATRi in $ARID1A^-$ CRC-Zelllinien verstärkte die sensibilisierende Wirkung im Vergleich zu $ARID1A^+$ CRC-Zelllinien weiter ($p < 0,01$). Mechanistisch verringerte die Behandlung mit ATRi in ARID1A-defizienten Zellen signifikant die Aufrechterhaltung des strahlungsinduzierten G2-Checkpoints ($P <0,01$), verringerte die Anzahl der durch Strahlung induzierten RAD51-Reparaturfoci in $ARID1A^-$ im Vergleich zu $ARID1A^+$ CRC-Zelllinien ($P <0,01$) und

verringerte somit die homologe Rekombinationsreparatur. Das DR-GFP-homologe Rekombinations-Reportersystem bestätigte, dass die Herunterregulation der Expression von ARID1A die HRR in ARID1A$^-$ Zelllinien selektiv senkte. *Ex-vivo* Experimente unter Verwendung des ATP-TCA Tests zeigten, dass ATRi die höchste sensibilisierende Wirkung in ARID1A negativen Zellen von CRC Patienten ausübte.

Zusammenfassend liefern unsere Ergebnisse einen Hinweis auf den vorklinischen und klinischen Wirkungsmechanismus von ARID1A-Defekten als Biomarker für die ATR-Inhibitor-Reaktion als Einzelwirkstoff oder als synthetischer letaler Ansatz in Kombination mit ionisierender Strahlung für CRC mit einem ARID1A$^-$ Status.

8. Acknowledgements

First of all, my profound appreciation goes to my supervisor, Prof. Dr. Martin Stuschke. I would like to thank you very much for giving me this great opportunity to be a member of his team and to work on my PhD thesis at the Department of Radiotherapy in University hospital Essen. Also, I would like to thank Dr. Ali Sak for all the support during the last years, whether scientifically or personally, as well as for the critical reading of this thesis and the valuable suggestions on structure and interpretation.

Special thanks go to the "Deutsche Forschungsgemeinschaft" for the financial support of my thesis and for allowing me to be a member of the DFG graduate training program 1739 "Molecular determinants of the cellular radiation response and their potential for response modulation". To all the participants of the GRK1739, graduate students, PIs and coordinators, thank you for teaching and advising, and all the helpful suggestions and critical comments during the meetings.

I wish to express profound gratitude to Prof. Dr. George Iliakis for agreeing to be my mentor and the second reviewer for this thesis.

I am also very grateful to Dr. Emil Mladenov for his support and valuable discussions during my research work.

I would like to thank all members of my lab and especially Michael Groneberg for his continued support throughout the years not only on scientific but also on personal matters.

Finally, but profoundly, heartily thanks to my family and friends for their love, support for my success during the whole period of my studies.

9. References

[1] A.R. Marley, and H. Nan, Epidemiology of colorectal cancer. International journal of molecular epidemiology and genetics 7 (2016) 105.

[2] L.H. Biller, and D. Schrag, Diagnosis and treatment of metastatic colorectal cancer: a review. Jama 325 (2021) 669-685.

[3] R. Cardoso, A. Zhu, F. Guo, T. Heisser, M. Hoffmeister, and H. Brenner, Incidence and Mortality of Proximal and Distal Colorectal Cancer in Germany: Trends in the Era of Screening Colonoscopy. Deutsches Ärzteblatt International 118 (2021) 281.

[4] G. Soltani, A. Poursheikhani, M. Yassi, A. Hayatbakhsh, M. Kerachian, and M.A. Kerachian, Obesity, diabetes and the risk of colorectal adenoma and cancer. BMC endocrine disorders 19 (2019) 1-10.

[5] I.R. Novelli, B.A. Araújo, L.F. Grandisoli, E.C. Furtado, E.K. Aguchiku, M.C. Bertocco, T.P. Sudbrak, I.C.d. Araújo, A.C. Bosko, and N.R. Damasceno, Nutritional counseling protocol for colorectal cancer patients after surgery improves outcome. Nutrition and Cancer 73 (2021) 2278-2286.

[6] A. Malki, R.A. ElRuz, I. Gupta, A. Allouch, S. Vranic, and A.-E. Al Moustafa, Molecular mechanisms of colon cancer progression and metastasis: Recent insights and advancements. International journal of molecular sciences 22 (2021) 130.

[7] L.D. Murillo Baidal, Características clínicas tempranas y el manejo diagnóstico y terapéutico en pacientes con cáncer colorrectal. Estudio a realizar en el Hospital Dr. Abel Gilbert Pontón; enero 2015 a diciembre 2016, Universidad de Guayaquil. Facultad de Ciencias Médicas. Carrera de Medicina, 2018.

[8] R.M. Byrne, and V.L. Tsikitis, Colorectal polyposis and inherited colorectal cancer syndromes. Annals of gastroenterology 31 (2018) 24.

[9] Y.-H. Xie, Y.-X. Chen, and J.-Y. Fang, Comprehensive review of targeted therapy for colorectal cancer. Signal transduction and targeted therapy 5 (2020) 1-30.

[10] P.L. Bedard, D.M. Hyman, M.S. Davids, and L.L. Siu, Small molecules, big impact: 20 years of targeted therapy in oncology. The Lancet 395 (2020) 1078-1088.

[11] H.-S. Lee, Z. Lin, S. Chae, Y.-S. Yoo, B.-G. Kim, Y. Lee, J.L. Johnson, Y.-S. Kim, L.C. Cantley, and C.-W. Lee, The chromatin remodeler RSF1 controls centromeric histone modifications to coordinate chromosome segregation. Nature communications 9 (2018) 1-13.

[12] L. Mariño-Ramírez, M.G. Kann, B.A. Shoemaker, and D. Landsman, Histone structure and nucleosome stability. Expert review of proteomics 2 (2005) 719-729.

[13] L. Ho, and G.R. Crabtree, Chromatin remodelling during development. Nature 463 (2010) 474-484.

[14] A.F. Hohmann, and C.R. Vakoc, A rationale to target the SWI/SNF complex for cancer therapy. Trends in Genetics 30 (2014) 356-363.

[15] S. He, Z. Wu, Y. Tian, Z. Yu, J. Yu, X. Wang, J. Li, B. Liu, and Y. Xu, Structure of nucleosome-bound human BAF complex. Science 367 (2020) 875-881.

[16] M. Wanior, A. Krämer, S. Knapp, and A.C. Joerger, Exploiting vulnerabilities of SWI/SNF chromatin remodelling complexes for cancer therapy. Oncogene 40 (2021) 3637-3654.
[17] A. Alpsoy, and E.C. Dykhuizen, Glioma tumor suppressor candidate region gene 1 (GLTSCR1) and its paralog GLTSCR1-like form SWI/SNF chromatin remodeling subcomplexes. Journal of Biological Chemistry 293 (2018) 3892-3903.
[18] N. Mashtalir, A.R. D'Avino, B.C. Michel, J. Luo, J. Pan, J.E. Otto, H.J. Zullow, Z.M. McKenzie, R.L. Kubiak, and R.S. Pierre, Modular organization and assembly of SWI/SNF family chromatin remodeling complexes. Cell 175 (2018) 1272-1288. e20.
[19] B.H. Alver, K.H. Kim, P. Lu, X. Wang, H.E. Manchester, W. Wang, J.R. Haswell, P.J. Park, and C.W. Roberts, The SWI/SNF chromatin remodelling complex is required for maintenance of lineage specific enhancers. Nature communications 8 (2017) 1-10.
[20] J.M. Alexander, S.K. Hota, D. He, S. Thomas, L. Ho, L.A. Pennacchio, and B.G. Bruneau, Brg1 modulates enhancer activation in mesoderm lineage commitment. Development 142 (2015) 1418-1430.
[21] X. Wang, R.S. Lee, B.H. Alver, J.R. Haswell, S. Wang, J. Mieczkowski, Y. Drier, S.M. Gillespie, T.C. Archer, and J.N. Wu, SMARCB1-mediated SWI/SNF complex function is essential for enhancer regulation. Nature genetics 49 (2017) 289-295.
[22] L.F. Langer, J.M. Ward, and T.K. Archer, Tumor suppressor SMARCB1 suppresses super-enhancers to govern hESC lineage determination. Elife 8 (2019) e45672.
[23] X. Sima, J. He, J. Peng, Y. Xu, F. Zhang, and L. Deng, The genetic alteration spectrum of the SWI/SNF complex: the oncogenic roles of BRD9 and ACTL6A. PLoS One 14 (2019) e0222305.
[24] T.W. Kelso, D.K. Porter, M.L. Amaral, M.N. Shokhirev, C. Benner, and D.C. Hargreaves, Chromatin accessibility underlies synthetic lethality of SWI/SNF subunits in ARID1A-mutant cancers. Elife 6 (2017) e30506.
[25] G.R. Hoffman, R. Rahal, F. Buxton, K. Xiang, G. McAllister, E. Frias, L. Bagdasarian, J. Huber, A. Lindeman, and D. Chen, Functional epigenetics approach identifies BRM/SMARCA2 as a critical synthetic lethal target in BRG1-deficient cancers. Proceedings of the National Academy of Sciences 111 (2014) 3128-3133.
[26] N. Mashtalir, H. Suzuki, D.P. Farrell, A. Sankar, J. Luo, M. Filipovski, A.R. D'Avino, R.S. Pierre, A.M. Valencia, and T. Onikubo, A structural model of the endogenous human BAF complex informs disease mechanisms. Cell 183 (2020) 802-817. e24.
[27] I. Versteege, N. Sévenet, J. Lange, M.-F. Rousseau-Merck, P. Ambros, R. Handgretinger, A. Aurias, and O. Delattre, Truncating mutations of hSNF5/INI1 in aggressive paediatric cancer. Nature 394 (1998) 203-206.
[28] R.T. Nakayama, J.L. Pulice, A.M. Valencia, M.J. McBride, Z.M. McKenzie, M.A. Gillespie, W.L. Ku, M. Teng, K. Cui, and R.T. Williams, SMARCB1 is required for widespread BAF complex–mediated activation of enhancers and bivalent promoters. Nature genetics 49 (2017) 1613-1623.

[29] B.G. Wilson, X. Wang, X. Shen, E.S. McKenna, M.E. Lemieux, Y.-J. Cho, E.C. Koellhoffer, S.L. Pomeroy, S.H. Orkin, and C.W. Roberts, Epigenetic antagonism between polycomb and SWI/SNF complexes during oncogenic transformation. Cancer cell 18 (2010) 316-328.
[30] J. Clark, P.J. Rocques, A.J. Crew, S. Gill, J. Shipley, A.M.-L. Chan, B.A. Gusterson, and C.S. Cooper, Identification of novel genes, SYT and SSX, involved in the t (X; 18)(p11. 2; q11. 2) translocation found in human synovial sarcoma. Nature genetics 7 (1994) 502-508.
[31] K. Kohashi, and Y. Oda, Oncogenic roles of SMARCB 1/INI 1 and its deficient tumors. Cancer science 108 (2017) 547-552.
[32] C. Hodges, J.G. Kirkland, and G.R. Crabtree, The many roles of BAF (mSWI/SNF) and PBAF complexes in cancer. Cold Spring Harbor perspectives in medicine 6 (2016) a026930.
[33] D.N. Reisman, J. Sciarrotta, W. Wang, W.K. Funkhouser, and B.E. Weissman, Loss of BRG1/BRM in human lung cancer cell lines and primary lung cancers: correlation with poor prognosis. Cancer research 63 (2003) 560-566.
[34] B.Z. Stanton, C. Hodges, J.P. Calarco, S.M. Braun, W.L. Ku, C. Kadoch, K. Zhao, and G.R. Crabtree, Smarca4 ATPase mutations disrupt direct eviction of PRC1 from chromatin. Nature genetics 49 (2017) 282-288.
[35] S. Glaros, G. Cirrincione, C. Muchardt, C. Kleer, C. Michael, and D. Reisman, The reversible epigenetic silencing of BRM: implications for clinical targeted therapy. Oncogene 26 (2007) 7058-7066.
[36] E.N. Pavlidou, and V. Balis, Diagnostic significance and prognostic role of the ARID1A gene in cancer outcomes. World Academy of Sciences Journal 2 (2020) 49-64.
[37] J. Bai, P. Mei, C. Zhang, F. Chen, C. Li, Z. Pan, H. Liu, and J. Zheng, BRG1 is a prognostic marker and potential therapeutic target in human breast cancer. PloS one 8 (2013) e59772.
[38] L. Zhang, C. Wang, S. Yu, C. Jia, J. Yan, Z. Lu, and J. Chen, Loss of ARID1A expression correlates with tumor differentiation and tumor progression stage in pancreatic ductal adenocarcinoma. Technology in Cancer Research & Treatment 17 (2018) 1533034618754475.
[39] R.L. Chandler, J.S. Damrauer, J.R. Raab, J.C. Schisler, M.D. Wilkerson, J.P. Didion, J. Starmer, D. Serber, D. Yee, and J. Xiong, Coexistent ARID1A–PIK3CA mutations promote ovarian clear-cell tumorigenesis through pro-tumorigenic inflammatory cytokine signalling. Nature communications 6 (2015) 1-14.
[40] E.P. Samartzis, K. Gutsche, K.J. Dedes, D. Fink, M. Stucki, and P. Imesch, Loss of ARID1A expression sensitizes cancer cells to PI3K-and AKT-inhibition. Oncotarget 5 (2014) 5295.
[41] J. Hoyer, A.B. Ekici, S. Endele, B. Popp, C. Zweier, A. Wiesener, E. Wohlleber, A. Dufke, E. Rossier, and C. Petsch, Haploinsufficiency of ARID1B, a member of the

SWI/SNF-a chromatin-remodeling complex, is a frequent cause of intellectual disability. The American Journal of Human Genetics 90 (2012) 565-572.
[42] G.W. Santen, E. Aten, Y. Sun, R. Almomani, C. Gilissen, M. Nielsen, S.G. Kant, I.N. Snoeck, E.A. Peeters, and Y. Hilhorst-Hofstee, Mutations in SWI/SNF chromatin remodeling complex gene ARID1B cause Coffin-Siris syndrome. Nature genetics 44 (2012) 379-380.
[43] M. Li, H. Zhao, X. Zhang, L.D. Wood, R.A. Anders, M.A. Choti, T.M. Pawlik, H.D. Daniel, R. Kannangai, and G.J.A. Offerhaus, Inactivating mutations of the chromatin remodeling gene ARID2 in hepatocellular carcinoma. Nature genetics 43 (2011) 828-829.
[44] G. Manceau, E. Letouzé, C. Guichard, A. Didelot, A. Cazes, H. Corté, E. Fabre, K. Pallier, S. Imbeaud, and F. Le Pimpec-Barthes, Recurrent inactivating mutations of ARID2 in non-small cell lung carcinoma. International journal of cancer 132 (2013) 2217-2221.
[45] A. Oba, S. Shimada, Y. Akiyama, T. Nishikawaji, K. Mogushi, H. Ito, S. Matsumura, A. Aihara, Y. Mitsunori, and D. Ban, ARID2 modulates DNA damage response in human hepatocellular carcinoma cells. Journal of hepatology 66 (2017) 942-951.
[46] C.S. Lee, I.H. Song, A. Lee, J. Kang, Y.S. Lee, I.K. Lee, Y.S. Song, and S.H. Lee, Enhancing the landscape of colorectal cancer using targeted deep sequencing. Scientific reports 11 (2021) 1-26.
[47] A.R. Sepulveda, S.R. Hamilton, C.J. Allegra, W. Grody, A.M. Cushman-Vokoun, W.K. Funkhouser, S.E. Kopetz, C. Lieu, N.M. Lindor, and B.D. Minsky, Molecular biomarkers for the evaluation of colorectal cancer: guideline from the American Society for Clinical Pathology, College of American Pathologists, Association for Molecular Pathology, and American Society of Clinical Oncology. American journal of clinical pathology 147 (2017) 221-260.
[48] Z.C. Deans, J.L. Costa, I. Cree, E. Dequeker, A. Edsjö, S. Henderson, M. Hummel, M.J. Ligtenberg, M. Loddo, and J.C. Machado, Integration of next-generation sequencing in clinical diagnostic molecular pathology laboratories for analysis of solid tumours; an expert opinion on behalf of IQN Path ASBL. Virchows Archiv 470 (2017) 5-20.
[49] N.C. Nicolaides, N. Papadopoulos, B. Liu, Y.-F. Weit, K.C. Carter, S.M. Ruben, C.A. Rosen, W.A. Haseltine, R.D. Fleischmann, and C.M. Fraser, Mutations of two P/WS homologues in hereditary nonpolyposis colon cancer. Nature 371 (1994) 75-80.
[50] S. Velho, C. Oliveira, A. Ferreira, A.C. Ferreira, G. Suriano, S. Schwartz Jr, A. Duval, F. Carneiro, J.C. Machado, and R. Hamelin, The prevalence of PIK3CA mutations in gastric and colon cancer. European journal of cancer 41 (2005) 1649-1654.
[51] W. Bleeker, V. Hayes, A. Karrenbeld, R. Hofstra, J. Hermans, C. Buys, and J.T.M. Plukker, Impact of KRAS and TP53 mutations on survival in patients with left- and right-sided Dukes' C colon cancer. The American journal of gastroenterology 95 (2000) 2953-2957.

[52] W.S. Samowitz, M.L. Slattery, C. Sweeney, J. Herrick, R.K. Wolff, and H. Albertsen, APC mutations and other genetic and epigenetic changes in colon cancer. Molecular Cancer Research 5 (2007) 165-170.
[53] R. Tokunaga, J. Xiu, R.M. Goldberg, P.A. Philip, A. Seeber, F. Battaglin, H. Arai, J.H. Lo, A. Puccini, and M. Naseem, Gene mutations of SWI/SNF complex and molecular profile in colorectal cancer, American Society of Clinical Oncology, 2019.
[54] C.B. Bridges, The origin of variations in sexual and sex-limited characters. The American Naturalist 56 (1922) 51-63.
[55] T. Dobzhansky, Genetics of natural populations. XIII. Recombination and variability in populations of Drosophila pseudoobscura. Genetics 31 (1946) 269.
[56] A. Ashworth, C.J. Lord, and J.S. Reis-Filho, Genetic interactions in cancer progression and treatment. Cell 145 (2011) 30-38.
[57] L.H. Hartwell, P. Szankasi, C.J. Roberts, A.W. Murray, and S.H. Friend, Integrating genetic approaches into the discovery of anticancer drugs. Science 278 (1997) 1064-1068.
[58] G. Rancati, J. Moffat, A. Typas, and N. Pavelka, Emerging and evolving concepts in gene essentiality. Nature Reviews Genetics 19 (2018) 34-49.
[59] A. Ashworth, and C.J. Lord, Synthetic lethal therapies for cancer: what's next after PARP inhibitors? Nature reviews Clinical oncology 15 (2018) 564-576.
[60] K.C. Helming, X. Wang, and C.W. Roberts, Vulnerabilities of mutant SWI/SNF complexes in cancer. Cancer cell 26 (2014) 309-317.
[61] S. Schick, A.F. Rendeiro, K. Runggatscher, A. Ringler, B. Boidol, M. Hinkel, P. Májek, L. Vulliard, T. Penz, and K. Parapatics, Systematic characterization of BAF mutations provides insights into intracomplex synthetic lethalities in human cancers. Nature genetics 51 (2019) 1399-1410.
[62] B.G. Wilson, K.C. Helming, X. Wang, Y. Kim, F. Vazquez, Z. Jagani, W.C. Hahn, and C.W. Roberts, Residual complexes containing SMARCA2 (BRM) underlie the oncogenic drive of SMARCA4 (BRG1) mutation. Molecular and cellular biology 34 (2014) 1136-1144.
[63] W.G. Kaelin, Synthetic lethality: a framework for the development of wiser cancer therapeutics. Genome medicine 1 (2009) 1-6.
[64] K.C. Helming, X. Wang, B.G. Wilson, F. Vazquez, J.R. Haswell, H.E. Manchester, Y. Kim, G.V. Kryukov, M. Ghandi, and A.J. Aguirre, ARID1B is a specific vulnerability in ARID1A-mutant cancers. Nature medicine 20 (2014) 251-254.
[65] S.V. Frye, The art of the chemical probe. Nature chemical biology 6 (2010) 159-161.
[66] C.H. Arrowsmith, J.E. Audia, C. Austin, J. Baell, J. Bennett, J. Blagg, C. Bountra, P.E. Brennan, P.J. Brown, and M.E. Bunnage, The promise and peril of chemical probes. Nature chemical biology 11 (2015) 536-541.
[67] V. Dötsch, J. Mathias, V.M. Li, J. Böttcher, D. Rauh, T.V. Hughes, C. Tse, B.D. Marsden, J.L. Baryza, and A. IJzerman, Donated chemical probes for open science. eLife (2018).

[68] J.N. Wu, and C.W. Roberts, ARID1A mutations in cancer: another epigenetic tumor suppressor? Cancer discovery 3 (2013) 35-43.
[69] M. Erfani, S.V. Hosseini, M. Mokhtari, M. Zamani, K. Tahmasebi, M.A. Naini, A. Taghavi, J.M. Carethers, M. Koi, and H. Brim, Altered ARID1A expression in colorectal cancer. BMC cancer 20 (2020) 1-13.
[70] X.-L. Wei, D.-S. Wang, S.-Y. Xi, W.-J. Wu, D.-L. Chen, Z.-L. Zeng, R.-Y. Wang, Y.-X. Huang, Y. Jin, and F. Wang, Clinicopathologic and prognostic relevance of ARID1A protein loss in colorectal cancer. World Journal of Gastroenterology: WJG 20 (2014) 18404.
[71] T. Jiang, X. Chen, C. Su, S. Ren, and C. Zhou, Pan-cancer analysis of ARID1A alterations as biomarkers for immunotherapy outcomes. Journal of Cancer 11 (2020) 776.
[72] Z. Wang, K. Chen, Y. Jia, J.-C. Chuang, X. Sun, Y.-H. Lin, C. Celen, L. Li, F. Huang, and X. Liu, Dual ARID1A/ARID1B loss leads to rapid carcinogenesis and disruptive redistribution of BAF complexes. Nature cancer 1 (2020) 909-922.
[73] R.C. Centore, G.J. Sandoval, L.M.M. Soares, C. Kadoch, and H.M. Chan, Mammalian SWI/SNF chromatin remodeling complexes: emerging mechanisms and therapeutic strategies. Trends in Genetics 36 (2020) 936-950.
[74] J.J. Caumanns, G.B.A. Wisman, K. Berns, A.G. van der Zee, and S. de Jong, ARID1A mutant ovarian clear cell carcinoma: A clear target for synthetic lethal strategies. Biochimica et Biophysica Acta (BBA)-Reviews on Cancer 1870 (2018) 176-184.
[75] J.H. Park, E.J. Park, H.S. Lee, S.J. Kim, S.K. Hur, A.N. Imbalzano, and J. Kwon, Mammalian SWI/SNF complexes facilitate DNA double-strand break repair by promoting γ-H2AX induction. The EMBO journal 25 (2006) 3986-3997.
[76] R. Watanabe, A. Ui, S.-i. Kanno, H. Ogiwara, T. Nagase, T. Kohno, and A. Yasui, SWI/SNF factors required for cellular resistance to DNA damage include ARID1A and ARID1B and show interdependent protein stability. Cancer research 74 (2014) 2465-2475.
[77] J. Shen, Y. Peng, L. Wei, W. Zhang, L. Yang, L. Lan, P. Kapoor, Z. Ju, Q. Mo, and I.-M. Shih, ARID1A deficiency impairs the DNA damage checkpoint and sensitizes cells to PARP inhibitors. Cancer discovery 5 (2015) 752-767.
[78] J. Davidson, Z. Shen, X. Gong, and J.R. Pollack, SWI/SNF aberrations sensitize pancreatic cancer cells to DNA crosslinking agents. Oncotarget 9 (2018) 9608.
[79] C.T. Williamson, R. Miller, H.N. Pemberton, S.E. Jones, J. Campbell, A. Konde, N. Badham, R. Rafiq, R. Brough, and A. Gulati, ATR inhibitors as a synthetic lethal therapy for tumours deficient in ARID1A. Nature communications 7 (2016) 1-13.
[80] T.A. Yap, B. O'Carrigan, M.S. Penney, J.S. Lim, J.S. Brown, M.J. de Miguel Luken, N. Tunariu, R. Perez-Lopez, D.N. Rodrigues, and R. Riisnaes, Phase I trial of first-in-class ATR inhibitor M6620 (VX-970) as monotherapy or in combination with carboplatin in patients with advanced solid tumors. Journal of Clinical Oncology 38 (2020) 3195.

[81] L. Gorecki, M. Andrs, M. Rezacova, and J. Korabecny, Discovery of ATR kinase inhibitor berzosertib (VX-970, M6620): Clinical candidate for cancer therapy. Pharmacology & therapeutics 210 (2020) 107518.
[82] C. Wu, J. Lyu, E.J. Yang, Y. Liu, B. Zhang, and J.S. Shim, Targeting AURKA-CDC25C axis to induce synthetic lethality in ARID1A-deficient colorectal cancer cells. Nature communications 9 (2018) 1-14.
[83] H. Zhou, J. Kuang, L. Zhong, W.-l. Kuo, J. Gray, A. Sahin, B. Brinkley, and S. Sen, Tumour amplified kinase STK15/BTAK induces centrosome amplification, aneuploidy and transformation. Nature genetics 20 (1998) 189-193.
[84] L. Macůrek, A. Lindqvist, D. Lim, M.A. Lampson, R. Klompmaker, R. Freire, C. Clouin, S.S. Taylor, M.B. Yaffe, and R.H. Medema, Polo-like kinase-1 is activated by aurora A to promote checkpoint recovery. Nature 455 (2008) 119-123.
[85] F. Toyoshima-Morimoto, E. Taniguchi, and E. Nishida, Plk1 promotes nuclear translocation of human Cdc25C during prophase. EMBO reports 3 (2002) 341-348.
[86] T.-P. Chuang, J.-Y. Wang, S.-W. Jao, C.-C. Wu, J.-H. Chen, K.-H. Hsiao, C.-Y. Lin, S.-H. Chen, S.-Y. Su, and Y.-J. Chen, Over-expression of AURKA, SKA3 and DSN1 contributes to colorectal adenoma to carcinoma progression. Oncotarget 7 (2016) 45803.
[87] Y.-M. Jeng, S.-Y. Peng, C.-Y. Lin, and H.-C. Hsu, Overexpression and amplification of Aurora-A in hepatocellular carcinoma. Clinical Cancer Research 10 (2004) 2065-2071.
[88] D. Li, J. Zhu, P.F. Firozi, J.L. Abbruzzese, D.B. Evans, K. Cleary, H. Friess, and S. Sen, Overexpression of oncogenic STK15/BTAK/Aurora A kinase in human pancreatic cancer. Clinical cancer research 9 (2003) 991-997.
[89] C.M. Kurbacher, O.M. Grecu, U. Stier, T.J. Gilster, M.-M. Janát, M. Untch, G. Konecny, H.W. Bruckner, and I.A. Cree, ATP chemosensitivity testing in ovarian and breast cancer: early clinical trials. Chemosensitivity Testing in Oncology (2003) 221-230.
[90] B.G. Bitler, N. Fatkhutdinov, and R. Zhang, Potential therapeutic targets in ARID1A-mutated cancers. Expert opinion on therapeutic targets 19 (2015) 1419-1422.
[91] B.G. Bitler, K.M. Aird, A. Garipov, H. Li, M. Amatangelo, A.V. Kossenkov, D.C. Schultz, Q. Liu, I.-M. Shih, and J.R. Conejo-Garcia, Synthetic lethality by targeting EZH2 methyltransferase activity in ARID1A-mutated cancers. Nature medicine 21 (2015) 231-238.
[92] J. Shen, Y. Peng, L. Wei, W. Zhang, L. Yang, L. Lan, P. Kapoor, Z. Ju, Q. Mo, and I.-M. Shih, ARID1A Deficiency Impairs the DNA Damage Checkpoint and Sensitizes Cells to PARP InhibitorsTargeting ARID1A Deficiency with PARP Inhibitors. Cancer discovery 5 (2015) 752-767.
[93] Y. Park, M.H. Chui, Y. Suryo Rahmanto, Z.-C. Yu, R.A. Shamanna, M.A. Bellani, S. Gaillard, A. Ayhan, A. Viswanathan, and M.M. Seidman, Loss of ARID1A in Tumor Cells Renders Selective Vulnerability to Combined Ionizing Radiation and PARP

Inhibitor TherapyIonizing Radiation Primes ARID1A-Mutated Tumors for PARPi. Clinical Cancer Research 25 (2019) 5584-5594.
[94] M. Furqan, A. Fayyaz, F. Firdous, H. Raza, A. Bilal, R.S.Z. Saleem, S. Shahzad-ul-Hussan, D. Wang, F.S. Youssef, and N.M. Al Musayeib, Identification and Characterization of Natural and Semisynthetic Quinones as Aurora Kinase Inhibitors. Journal of Natural Products (2022).
[95] J. Mandal, P. Mandal, T.-L. Wang, and I.-M. Shih, Treating ARID1A mutated cancers by harnessing synthetic lethality and DNA damage response. Journal of biomedical science 29 (2022) 1-15.
[96] B. Niedermaier, A. Sak, E. Zernickel, S. Xu, M. Groneberg, and M. Stuschke, Targeting ARID1A-mutant colorectal cancer: depletion of ARID1B increases radiosensitivity and modulates DNA damage response. Scientific Reports 9 (2019) 1-9.
[97] A.M. Weber, and A.J. Ryan, ATM and ATR as therapeutic targets in cancer. Pharmacology & therapeutics 149 (2015) 124-138.
[98] A. Gunn, and J.M. Stark, I-SceI-based assays to examine distinct repair outcomes of mammalian chromosomal double strand breaks, DNA repair protocols, Springer, 2012, pp. 379-391.
[99] M.K. Kenny, U. Schlegel, H. Furneaux, and J. Hurwitz, The role of human single-stranded DNA binding protein and its individual subunits in simian virus 40 DNA replication. Journal of Biological Chemistry 265 (1990) 7693-7700.
[100] T. Takeda, K. Banno, R. Okawa, M. Yanokura, M. Iijima, H. Irie-Kunitomi, K. Nakamura, M. Iida, M. Adachi, and K. Umene, ARID1A gene mutation in ovarian and endometrial cancers. Oncology reports 35 (2016) 607-613.
[101] E. Mladenov, C. Staudt, A. Soni, T. Murmann-Konda, M. Siemann-Loekes, and G. Iliakis, Strong suppression of gene conversion with increasing DNA double-strand break load delimited by 53BP1 and RAD52. Nucleic acids research 48 (2020) 1905-1924.
[102] S. Tsai, L.-A. Fournier, E.Y.-c. Chang, J.P. Wells, S.W. Minaker, Y.D. Zhu, A.Y.-H. Wang, Y. Wang, D.G. Huntsman, and P.C. Stirling, ARID1A regulates R-loop associated DNA replication stress. PLoS Genetics 17 (2021) e1009238.
[103] D. Dibitetto, J.R. Sims, C.F. Ascenção, K. Feng, D. Kim, S. Oberly, R. Freire, and M.B. Smolka, Intrinsic ATR signaling shapes DNA end resection and suppresses toxic DNA-PKcs signaling. NAR cancer 2 (2020) zcaa006.
[104] R. Buisson, J. Niraj, A. Rodrigue, C.K. Ho, J. Kreuzer, T.K. Foo, E.J.-L. Hardy, G. Dellaire, W. Haas, and B. Xia, Coupling of homologous recombination and the checkpoint by ATR. Molecular cell 65 (2017) 336-346.
[105] J. Vávrová, L. Zárybnická, E. Lukášová, M. Řezáčová, E. Novotná, Z. Šinkorová, A. Tichý, J. Pejchal, and K. Ďurišová, Inhibition of ATR kinase with the selective inhibitor VE-821 results in radiosensitization of cells of promyelocytic leukaemia (HL-60). Radiation and environmental biophysics 52 (2013) 471-479.

[106] H.J. Kim, A. Min, S.A. Im, H. Jang, K.H. Lee, A. Lau, M. Lee, S. Kim, Y. Yang, and J. Kim, Anti-tumor activity of the ATR inhibitor AZD6738 in HER2 positive breast cancer cells. International journal of cancer 140 (2017) 109-119.
[107] L.H. Lee, E. Sadot, S. Ivelja, E. Vakiani, J.F. Hechtman, C.J. Sevinsky, D.S. Klimstra, F. Ginty, and J. Shia, ARID1A expression in early stage colorectal adenocarcinoma: an exploration of its prognostic significance. Human pathology 53 (2016) 97-104.
[108] S. Glaysher, and I.A. Cree, Cell sensitivity assays: the ATP-based tumor chemosensitivity assay, Cancer Cell Culture, Springer, 2011, pp. 247-257.
[109] S. Sharma, M.H. Neale, F. Di Nicolantonio, L.A. Knight, P.A. Whitehouse, S.J. Mercer, B.R. Higgins, A. Lamont, R. Osborne, and A.C. Hindley, Outcome of ATP-based tumor chemosensitivity assay directed chemotherapy in heavily pre-treated recurrent ovarian carcinoma. BMC cancer 3 (2003) 1-10.
[110] R.D. Petty, L.A. Sutherland, E.M. Hunter, and I.A. Cree, Comparison of MTT and ATP-based assays for the measurement of viable cell number. Journal of bioluminescence and chemiluminescence 10 (1995) 29-34.

Declaration

Erklärung:

Hiermit erkläre ich, gem. § 6 Abs. (2) g) der Promotionsordnung der Fakultät für Biologie zur Erlangung der Dr. rer. nat., dass ich das Arbeitsgebiet, dem das Thema „Synthetic lethality concepts for colon cancer cell lines in the background of mutations in the SWI/SNF complex*"* zuzuordnen ist, in Forschung und Lehre vertrete und den Antrag von *Shan Xu* befürworte und die Betreuung auch im Falle eines Weggangs, wenn nicht wichtige Gründe dem entgegenstehen, weiterführen werde.

Essen, den _____ _____ _____

Name des Betreuers an der Universität Duisburg-Essen

Unterschrift

Erklärung:

Hiermit erkläre ich, gem. § 7 Abs. (2) d) + f) der Promotionsordnung der Fakultät für Biologie zur Erlangung des Dr. rer. nat., dass ich die vorliegende Dissertation selbständig verfasst und mich keiner anderen als der angegebenen Hilfsmittel bedient, bei der Abfassung der Dissertation nur die angegeben Hilfsmittel benutzt und alle wörtlich oder inhaltlich übernommenen Stellen als solche gekennzeichnet habe.

Essen, den_____ _____

Unterschrift des/r Doktoranden/in

Erklärung:

Hiermit erkläre ich, gem. § 7 Abs. (2) e) + g) der Promotionsordnung der Fakultät für Biologie zur Erlangung des Dr. rer. nat., dass ich keine anderen Promotionen bzw. Promotionsversuche in der Vergangenheit durchgeführt habe und dass diese Arbeit von keiner anderen Fakultät/Fachbereich abgelehnt worden ist.

Essen, den_____ _____

Unterschrift des/r Doktoranden/in

Der Lebenslauf ist aus Datenschutzrechtlichen Gründen in der Online-Version nicht enthalten

Publications

1. **Xu S,** Xia J, Ye S, et al. Preparation and characterization of electrospun poly(e-caprolactone)–pluronic–poly(e-caprolactone)-based polyurethane nanofibers [J]. *Journal of Applied Polymer Science, 2016, 33(27).*
2. **Xu S,** Zhan H, Fu S and Wu J. Progress of New Formulations of Paclitaxel. *Austin Oncol. 2016; 1(2):1009.*
3. **Xu S,** Tang Y Y, Yu Y X, et al. Novel composite drug delivery system as a novel radio sensitizer for the local treatment of cervical carcinoma[J]. *Drug delivery, 2017, 24(1): 1139-1147.*
4. Yu Y, **Xu S**, You H, et al. In vivo synergistic anti-tumor effect of paclitaxel nanoparticles combined with radiotherapy on human cervical carcinoma.[J]. *Drug Delivery, 2017:75-82.*
5. **Xu S,** Y Yu，J Rong，D Hu, et al. Expression of BRCA1 and ERCC1 as predictive clinical outcome after radiochemotherapy in patients with locoregionally moderate-advanced nasopharyngeal carcinoma [J].*Oncotarget, 2017.*
6. **Xu S,** Du X, Feng G, et al. Efficient inhibition of cervical cancer by dual drugs loaded in biodegradable thermosensitive hydrogel composites[J]. *Oncotarget, 2018, 9(1): 282.*
7. Yun Q, Wang S S, **Xu S,** et al. Use of 5-Fluorouracil Loaded Micelles and Cisplatin in Thermosensitive Chitosan Hydrogel as an Efficient Therapy against Colorectal Peritoneal Carcinomatosis.[J]. *Macromolecular Bioscience, 2016.*
8. Peng QX, Han YW, Zhang YL, **Xu S**, et al Apatinib inhibits VEGFR-2 and angiogenesis in an in vivo murine model of nasopharyngeal carcinoma.[J].*Oncotarget, 2017*
9. Chen L X, Ni X L, Zhang H, **Xu S**, et al. Preparation, characterization, in vitro and in vivo anti-tumor effect of thalidomide nanoparticles on lung cancer[J]. *International journal of nanomedicine, 2018, 13: 2463.*
10. Zhang H, Jiang Y, Ni X L, **Xu S**, et al. Glycyrrhetinic Acid-Modified Norcantharidin Nanoparticles for Active Targeted Therapy of Hepatocellular Carcinoma[J]. *Journal of biomedical nanotechnology, 2018, 14(1): 114-126.*
11. Yang H, Chen X, Lin S, **Xu S**, et al. Treatment outcomes after reduction of the target volume of intensity-modulated radiotherapy following induction chemotherapy in patients with locoregionally advanced nasopharyngeal carcinoma: A prospective, multi-center, randomized clinical trial[J]. *Radiotherapy and Oncology, 2018, 126(1): 37-42.*
12. Ni X L, Chen L X, Zhang H, **Xu S**, et al. In vitro and in vivo antitumor effect of gefitinib nanoparticles on human lung cancer[J]. *Drug delivery, 2017, 24(1): 1501-1512.*
13. **Shan XU,** Yanxin Y U, Yang J, et al. Antitumor effect of thermosensitive hydrogel co-loading paclitaxel and cisplatin on cervical cancer[J]. *Tumor, 2016.*
14. **Shan XU,** WU Jing- bo，FU Shao-zhi. Research progress of albumin-bound paclitaxel in treatment of metastatic breast cancer [J].*Chin J New Drugs Clin Rem, 2016.*

15. Shan XU, Zhang Y, Xiao-Bo D U. Association between higher expression of Y-box-binding protein-1 and poor prognosis in cervical cancer[J]. *Medical Journal of West China, 2012*.

16. Niedermaier B, Sak A, Zernickel E, **Shan Xu**, et al. Targeting ARID1A-mutant colorectal cancer: depletion of ARID1B increases radiosensitivity and modulates DNA damage response[J]. Scientific Reports, 2019, 9(1): 1-9.

17. Li Y, Lu K, Zhao B, **Shan Xu** et al. Depletion of insulin-like growth factor 1 receptor increases radiosensitivity in colorectal cancer[J]. Journal of Gastrointestinal Oncology, 2020.

18. Xu S, Sak A, Erol Y B. Network Meta-analysis of First-Line Systemic Treatment for Patients With Metastatic Colorectal Cancer[J]. Cancer Control, 2021.

19. Zong R, Chen X, **Xu S,** et al. IGF-1R depletion sensitizes colon cancer cell lines to radiotherapy[J]. Cancer Biomarkers, 2021.

20. Xu S, Shi B, Yuxian J, et al. Comparative Analysis of the Wounded in Patients and Deaths in a Hospital Following the Three Major Earthquakes in Western China[J]. Frontiers in Public Health, 2022.

21. Xu S, Sak A, Niedermaier B, et al. Selective vulnerability of ARID1A deficient colon cancer cells to combined radiation and ATR-inhibitor therapy[J]. Frontiers in oncology, 2022.

22. Shan XU, Lijun Zhang, Yuying Tang. Leg fixed box [P]. Sichuan CN205181523U,2016-04-27.